Spring 5-7-2016

Spatiotemporal Control of Staphylococcus aureus Biofilm Development

Derek E. Moormeier
University of Nebraska Medical Center

Spatiotemporal Control of *Staphylococcus aureus* Biofilm Development

by

Derek E. Moormeier

A DISSERTATION

Presented to the Faculty of the University of Nebraska Graduate College in

Partial Fulfillment of the Requirements for the Degree of Doctor of Philosophy

Pathology and Microbiology Graduate Program

Under the Supervision of Professor Kenneth W. Bayles

University of Nebraska Medical Center

Omaha, NE

February 2015

Supervisory Committee:

Paul D. Fey, Ph.D.

Marilynn A. Larson, Ph.D.

Jeffrey L. Bose, Ph.D.

Bradley E. Britigan, M.D.

Laurey Steinke, Ph.D.

Spatiotemporal Control of *Staphylococcus aureus* Biofilm Development

Derek E. Moormeier, Ph.D.

University of Nebraska Medical Center, 2015

Supervisor: Kenneth W. Bayles, Ph.D.

Chronic biofilm-related infections caused by the human pathogen *Staphylococcus aureus* often lead to significant increases in morbidity and mortality in both hospital- and community-associated settings. Typically, *S. aureus* biofilm development occurs in three stages: 1) attachment, 2) tower maturation, and 3) dispersal. Here, utilizing BioFlux1000 time-lapse microscopy we have expanded upon these fundamental stages of biofilm development and also unveiled and characterized two additional stages (multiplication and exodus).

The attachment and multiplication stages were shown to be protease sensitive but independent of most cell surface-associated proteins. Following multiplication, an exodus of the biofilm population that followed the transition of the biofilm to DNase I sensitivity was demonstrated. Furthermore, disruption of the gene encoding staphylococcal nuclease (*nuc*) abrogated this exodus event, causing hyper-proliferation of the biofilm and disrupting tower development. Prior to exodus, cells carrying a P*nuc*::*gfp* promoter fusion demonstrated Sae-dependent expression, but only in a subpopulation of cells. Additionally, we also determined that other Sae-regulated genes demonstrated unique Sae-dependent stochastic expression patterns. Collectively, these results suggest the presence of a Sae-controlled nuclease-mediated exodus of a biofilm subpopulation that is required for tower development as well as controlling the stochastic expression of Sae-regulated factors.

The *cidABC* and *lrgAB* operons have previously been shown to play specific roles in controlled cell death and release of extracellular DNA (eDNA) during biofilm maturation. Although the exact mechanisms controlling the *cid* and *lrg* operons have yet

to be completely elucidated, the expression of the operons is dependent on altered metabolic cues as a result of overflow metabolism. We hypothesized that the differential expression of the *cid* and *lrg* operons within a biofilm is a function of the metabolic heterogeneity found within different biofilm microenvironments. Time-lapse epifluorescent images indicate that expression of these operons is specific to distinct regions of a growing biofilm. Additionally, these results revealed the existence of different tower types, possibly reflecting their different functional roles in development. Altogether, nuclease-mediated eDNA degradation modulates the biofilm to produce two distinct towers that there are both spatially and temporally different between compared to the rest of the biofilm.

ACKNOWLEDGEMENTS

There are several individuals whom I have to acknowledge for their contributions in helping me survive and succeed in graduate school. It's because of all the following people that I have been able to gain confidence in myself as not only a scientist, but also as a person so that I could succeed in graduate school. I have learned something from each one of you and am greatly indebted to all of you for all that you have done for me.

First, I have to start by thanking my advisor Dr. Ken Bayles. He has provided me unwavering support and encouragement even in times of doubt on whether or not I could prosper at being a scientist. He has been a perfect role model as a principal investigator, a scientist, and an overall person. Being in his laboratory has provided numerous opportunities including the freedom to design and conduct my own experiments, and to present my data at several conferences both nationally and internationally. I truly could not have asked for a better person to have worked under for my graduate school career.

Second, I have to thank members of the Bayles laboratory both past and present. I have to first thank Dr. Ethan Mann for mentoring me during my undergraduate summer internship and sparking my interest in *Staphylococcus aureus* biofilms and for also laying much of the groundwork for my project by generating fluorescent reporter plasmids and charactering expression patterns for my AEM paper. I also have to especially thank Jennifer Endres for making sure the lab always ran smoothly and providing me endless help with both scientific and life issues as well as performing experiments and co-authoring a publication together. Todd Widhelm and Vijaya Kumar Yajjala, you are some of my best friends, and though we hardly worked on experiments together, you were always there to help me relax over a couple cold beers after work. I also have to give special thanks to all of the past and present post docs: Drs. Jeffrey Bose, Marat Sadykov, Vinai Thomas, Sujata Chaudari, and Jong-Sam Ahn who all gave unbelievable

science and life guidance. Jeff, you were always there to keep me focused and on task and teach me the ins-and-outs of how to clone and how to sell myself as a scientist. Marat, you are one of my first mentors in the lab and showed me tough love and forced me to perform my experiments the correct way. Vinai and Sujata, you were always there to walk me through long scientific discussions and provide insight on upcoming or potential experiments. Although we never worked closely on science in the lab, Sam, you were always there for life advice and a good laugh at coffee time. I also have to thank all of the past and present graduate students: Drs. McKenzie Lehman and Casey Gries, Christopher Wenstrom, Ian Windham, and Logan Bulock. McKenzie, you were always the go to person for graduate student advice and the perfect role model for what a graduate student should be, and I will never forget our endless talks about Creighton basketball and Nebraska football. Casey, you were always like an older brother who was there for graduate school, life, camping and hiking gear, bicycling gear, and craft beer advice, and I will always remember our heated fantasy football discussions. Although we were only in the lab together for a short time, Chris, you always provided great non-academic career and networking advice as well as the most outrageous comedic entertainment. Ian, you have been a staple in the lab and your heated science debates mixed with witty sarcasm always made the day interesting. Logan, you are the ‘Rookie’ of the lab and although Ian and I gave you a tough time, it has truly been fun mentoring you and introducing you to graduate school and fantasy football over the last year.

Thirdly, I have to thank all of the members of the Fey lab both past and present, you all have been extremely helpful and provided amazing feedback on my project in our combined lab meetings. I also have to specifically thank Dr. Paul Fey for his unparalleled advice throughout my graduate career; you have been like a second mentor to me.

Fourthly, I have to thank the all the members of my supervisory committee that I did not already mention. Your advice on my project and career path has always been extremely enlightening and beneficial.

I would also like to thank all of my collaborators from the Drs. Tammy Kielian group (UNMC), Kelly Rice (University of Florida), and the Alex Horswill group (University of Iowa) for all their help on making my project a success. And I also I have to give a shout out to my INBRE mentors at Wayne State College Drs. Doug Christensen and Shawn Pearcy for introducing me to research and providing guidance as I decided to go to graduate school.

Lastly, I have to thank all of my family and friends for their unrivaled support while getting my Ph.D. Mom and Dad, you have always supported me through every step of graduate school, and although you may not always understand what I am telling you about science-wise, you were always there to tell me I was doing a good job and that you were proud of me. My sisters, Hayley and Carisa, you guys were always there for sibling support on my graduate school decisions. My parents-in-law, Pat and Daryl, and sisters-in-law, Erin and Madison, you have been a second set of parents and sisters always providing endless support. And most importantly, I have to give all the thanks in the world to my beautiful wife Aleece. You had to put up with the late nights in the lab, the long nights writing, frustrating lab results, bad test grades, stressful presentations, a comprehensive exam, science conference traveling, and awkward science conversations. Without your love, support, and guidance, I know without a doubt I would not have been able to get through graduate school.

Table of Contents

LIST OF TABLES

LIST OF FIGURES

CHAPTER I:

INTRODUCTION - LITERATURE REVIEW

Staphylococcus aureus

Epidemiology

The highly virulent human pathogen, *Staphylococcus aureus*, is a facultative Gram-positive bacterium that can colonize several places on the human body including skin, throat, axilla, perirectal, groin and the nasopharynx (1-3). In fact, it is thought that *S. aureus* colonizes more than 30% of the human population's nares (4), and that colonization of the nares is increasingly becoming a risk factor for more serious infections. While *S. aureus* is considered a commensal organism, it is also considered an opportunistic pathogen because it can cause a plethora of both community and healthcare-associated infections ranging from skin and soft tissue infections to more serious life-threatening diseases such as bacteremia, infective endocarditis, osteomyelitis, necrotizing pneumonia, and septic arthritis under the right conditions (5). In fact, *S. aureus* is now the leading cause of infective endocarditis in the industrialized world (6), and a prominent cause of osteomyelitis (5). Collectively, in the United States alone, *S. aureus* is one of the leading causes of all community and healthcare-associated infections and has caused increased mortality rates and nearly doubles the hospitalization time when compared to normal hospital stays (7). As a result, the prevalence of these diseases has led to increased costs associated with *S. aureus* infections over the past decade, estimated to be near $450 million annually (8, 9). Thus, it is obvious why *S. aureus* has become one of the most notorious 'superbugs' not only in the United States, but all across the industrialized world.

Antibiotic Resistance

In order to cause so many different types of diseases, *S. aureus* has developed some unique virulence factors that aid in its survival and pathogenesis including toxin production, secreted enzyme production, host binding proteins, and biofilm formation. However, one of the most prominent capabilities is the ability of the organism to acquire antibiotic resistance. Starting in the 1940's, a plasmid-encoded penicillinase plasmid emerged, producing penicillin-resistant strains in several hospitals (10, 11). By the 1950's and 1960's as the penicillin-resistant strains continued to spread via the 80-81 phage-type, penicillin-resistant strains of *S. aureus* had become a pandemic (12), and it was not until the development of methicillin in the early 1960's that penicillin-strains were diminished greatly. However, the emergence of methicillin-resistant *S. aureus,* commonly known as MRSA, followed the wide-spread use of methicillin shortly thereafter (13). For decades following, MRSA strains have remained a prevalent cause of *S. aureus*-related infections, and in the 1990s, the emergence of community-acquired MRSA (CA-MRSA) strains has sparked an epidemic in the United States (14). Typically, disease manifestation of CA-MRSA strains appear to primarily cause skin and soft tissue infections in the form of abscess formation or cellulitis in 90% of the individuals with CA-MRSA infections (15, 16). In the last decades because CA-MRSA related infections remain such a persistent problem, the increased use of vancomycin, one of the last effective antibiotics against MRSA, has also led to the emergence of vancomycin-intermediate and vancomycin-resistant (VISA and VRSA) *S. aureus* strains (17, 18). Due to the constant rise in CA-MRSA related infections and the reoccurring emergence of different types of antibiotic resistance, it is becoming apparent that *S. aureus* is an astonishingly adaptable pathogen that we must continue to monitor and study.

Virulence Factors

Toxins

A major virulence factor that allows *S. aureus* to cause so many different types of diseases is its ability to produce toxins. Indeed, it is one of the most distinguishable capabilities that separate *S. aureus* from most other human pathogens. While several bacterial species can usually produce one or two types of toxins, *S. aureus* produces several categories of toxins that range in function from membrane damaging to interfering with the function of host cell receptors (19). Perhaps, the most well-known toxins are the receptor-mediated membrane damaging toxins that cause cytolysis of several host cell types by forming pores in the cell membrane. Within this group, the most well-known and well-studied is alpha-toxin (20), which can cause lysis of red blood cells and leukocytes (21) by interacting with the A Disintegrin And Metalloprotease 10 (ADAM10) receptor found on the host cell surfaces (22). Likewise, *S. aureus* also produces a similar group of host cell receptor-mediated pore forming toxins known as the bi-component toxin family consisting of the Panton-Valentine leukocidins (PVL), the leukocidins LukAB (LukGH) and LukDE, and the gamma-toxins (HlgA, HlgB, HlgC, gamma-hemolysin) (23-26). Like receptor-mediated pore forming toxins, a group of non-receptor-mediated membrane damaging toxins called the phenol soluble modullins (PSMs) has recently been discovered. This group of non-specific pore forming toxins consists of three groups of δ-toxin, PSMα, and PSMβ all of which have differing contributions to pathogenesis via non-specific cytolytic activity (27).

The second most well-known group of toxins produced by *S. aureus* is the toxins that interfere with specific receptor functions on host cells. This group is largely comprised of the superantigen group of toxins: enterotoxins and the toxic shock syndrome toxin (TSST), and the chemotaxis inhibitory protein of *S. aureus* (CHIPS),

which has been shown to function as an immune suppresser by blocking activation of the complement system (28). While the exact mechanism of how these toxins work remain largely undetermined, the approximately 20 enterotoxin and enterotoxin-like proteins produced by *S. aureus* have been shown to be involved in disturbing proper intestinal function and causing food borne illnesses such as vomiting and diarrhea (29). While it can also cause food borne illnesses, the superantigen TSST is primarily known for its function in causing toxic shock syndrome (30, 31). Like the other enterotoxins, it is also thought that TSST by-passes normal antigen presentation by binding MHC II proteins and initiating cytokine release (32).

Secreted Enzymes

Another major component included in the arsenal of virulence factors that are produced by *S. aureus* is the numerous secreted enzymes that enable degradation of host components or interfere with host molecular signaling. Although Staphylococci produce various types of secreted enzymes including proteases, coagulases, kinases, and nucleases, perhaps, the most studied are the ten secreted proteases because of their various roles in aiding pathogenesis. These ten proteases include seven serine proteases (SspA and SplABCDEF), two cysteine proteases (the Staphopains ScpA and SspB), and a metalloprotease (Aureolysin). In combination with the reports of affecting biofilm integrity *in vitro* (discussed below) (33), in some instances, the proteases have been shown to be important for causing infections. While the basic function of the proteases is to cleave both self and host proteins, the overall process in which the proteases affect biofilm maturation and pathogenesis remains unclear given the myriad of targets of each individual protease. One thought is that the proteases may degrade the host proteins for nutrient acquisition to aid in growth under proteinaceous-rich environments (34). However, a complete knock out of all ten proteases also showed an

increase in *S. aureus* extracellular virulence factor production and an increase in mortality in a systemic mouse model infection (34). Further complicating the understanding of protease contribution to pathogenesis is that in some cases individual proteases must be auto-activated (35, 36) or rely on a proteolytic cleavage cascade activation (37, 38). Nonetheless, it is apparent that the production of the secreted proteases plays a complex role in *S. aureus* pathogenesis that must continue to be evaluated.

Although not as well studied, other secreted enzymes also have important functions in pathogenesis in a number of different ways. For example, the two known coagulases, staphylocoagulase and van Willebrand factor (vWF), produced by staphylococci are important for forming clots in the blood plasma, inhibiting phagocytosis in abscess formation (39), and enhancing adhesion in catheter biofilm-associated infections (40). It is thought that the coagulases function by binding and activating prothrombin and converting fibrinogen to fibrin leading to the formation of the fibrin blood clots (41). And while these appear to be the main functions, staphylocoagulase has also been implicated in the formation of *S. aureus* biofilms grown under shear stress conditions (discussed in biofilm section) (42)

On the other hand, staphylokinase is thought to degrade fibrin clots generated during a *S. aureus* infection to maintain localization of the infection and allow bacterial invasion into deeper tissues (43, 44). It does so by activating plasminogen and converting it to plasmin, which may enhance lysis of surrounding host tissues allowing bacterial invasion. Additionally, it also aids in *S. aureus* infections by cleaving and inactivating the complement factor, C3b (45).

Lastly, while both *S. aureus* nucleases have continuously been shown to have a function in modulating biofilm formation (discussed below), the secreted nuclease (Nuc)

has also been shown to have a function in degrading neutrophil extracellular traps (NETs) during an *S. aureus* infection (46, 47). Further evidence for a nuclease as potential virulence factor is the recent data demonstrating a decreased bacterial load per organ in in mouse peritonitis model (48), although the exact mechanism contributing to this phenotype is not well understood.

Bacterial Biofilms

In contrast to laboratory conditions, bacteria are rarely grown in a planktonic state under nutrient rich conditions. Rather, they are almost exclusively living in nutrient-deficient environments in multicellular aggregations of cells called biofilms (49, 50). In order to form biofilms, bacteria must generate a self-produced extracellular matrix (ECM) composed of proteins, carbohydrates, and/or extracellular DNA (eDNA) (51). The ECM encases the cells in a sticky agglomeration that facilitates survival in hostile or extreme environments including adverse conditions of temperature, pH, therapeutic treatments, and/or immune cells within a host (52).

To allow survival in such harsh conditions, a fascinating ability of bacterial biofilms is the capability to allow single-celled organisms to assume multicellular group behavior mediated by complex regulatory networks that react to changes in the surrounding environmental or biofilm conditions (53). Indeed, multicellularity has been shown in several different bacterial species and provides the organism benefits that it would otherwise not typically have including division of labor into distinct cell types (54). A recent example of this is the non-pathogenic *Bacillus subtilis,* which distinctly differentiates into separate cell types. More specifically, *B. subtilis* has been shown to determine differential fates of cells involved in motility, matrix production, sporulation,

cell death, cannibalism and competence based on environmental conditions and correlating with spatiotemporal control within a developing biofilm (55, 56). Additionally, although not known for cell differentiation during biofilm formation, the soil predator *Myxococcus xanthus* has also been shown to coordinate unparalleled cell differentiation when ‘swarming’ and forming fruiting body structures when preying on other soil-dwelling organisms (57). In addition, individual cells within a biofilm have also been shown to differentiate and demonstrate genetic and physiologic heterogeneity based on differences in microscale chemical gradients, local environmental conditions, and stochastic gene expression (58). Although complex and varying across bacterial species, the conditions within the biofilm and regulatory processes are largely sensed and coordinated by two-component (59) and quorum sensing systems. In particular, the quorum sensing systems enable cells to communicate to each other to coordinate cell differentiation and gene expression based on self-produced cell density signals known as autoinducers (60). Overall, it is abundantly clear that biofilms that enable multicellularity processes that are dependent on a plethora of environmental sensing and quorum sensing mechanisms.

Typically, bacterial biofilm development is described in three successive stages: 1. attachment, 2. accumulation/maturation, and 3. detachment/dispersal (53, 61). During the initial attachment stage, planktonic cells adhere to a biotic or abiotic surface and proliferate into sticky aggregations called towers (also known as microcolonies). As these aggregations develop, bacterial cells produce an ECM that serves as a scaffold to determine three-dimensional architecture. Upon reaching a specific density, a mechanism is triggered to initiate ECM modulation to allow cells embedded within the biofilm ECM to detach and disperse to seed other environment to reinitiate biofilm development.

In recent years, bacterial biofilms produced by human pathogens have become particularly important to study due to their increase recalcitrance, to not only the host immune system and antimicrobial peptides (62), but to antibiotics and other therapeutic treatment (63, 64). Despite the prevalence of these biofilm-associated infections, the molecular mechanisms that control the steps of biofilm development are still being investigated.

Staphylococcal Biofilms

Like other human pathogens, *Staphylococcus aureus* has progressively become notorious for causing chronic nosocomial infections due to its ability to resist therapeutic treatment by forming biofilms on both indwelling medical devices including implanted artificial heart valves, pacemakers, catheters and joint prosthetics (65, 66). Indeed, nearly half of all nosocomial infections are associated with indwelling device infections (67). In addition, *S. aureus* has also developed the ability to form biofilms on host bone tissue and heart valves possibly leading to osteomyelitis and endocarditis infections, respectively (68). To cause such persistent infections, not only does the ECM of *S. aureus* biofilms provide a physical barrier to protect staphylococcal cells from antibiotic therapy and host immune system infiltration, but recent data also suggest that *S. aureus* biofilms actively skew the immune system limiting macrophage invasion *in vivo* and contributing to bacterial persistence (69-73). In addition, the metabolic state of the cell also enables persistence of bacterial cell in response to antibiotic treatment (74). Since antibiotics generally target metabolically active dividing cells, the formation of metabolically dormant cells known as persisters add another component to *S. aureus* biofilms abilities to resist antibiotic treatment independent of other encoded antibiotic resistance mechanisms (75). Thus, a continued understanding of the development of staphylococcal biofilms at the molecular level remains a high priority.

Stages of Staphylococcus aureus Biofilm Development

Attachment Stage

Like other bacterial biofilm development, *S. aureus* is thought to form biofilms in three sequential stages: 1. attachment, 2. accumulation/maturation, and 3. dispersal/detachment (76). During attachment, planktonic cells adhere to either abiotic or biotic surfaces. When attaching to biotic surfaces such as matrix components of the host tissue, *S. aureus* is thought to utilize a variety of different surface proteins specific for the host matrix substrates. A well-characterized group of surface anchored proteins known as the microbial surface components recognizing adhesive matrix molecules (MSCRAMMs) facilitate attachment to host matrix component such as fibronectin, fibrinogen, collagen, and cytokeratin (77). Specific examples of MSCRAMMs include the fibronectin-binding proteins (FnBPA and FnBPB) (78), the serine-aspartate repeat family proteins (SdrC, SdrD, and SdrE) (79, 80), the clumping factors (ClfA and ClfB) (81, 82), the collagen adhesin (83), and the bone sialo-binding protein (Bbp) (84). Additionally, while the primary purpose of MSCRAMMs is to bind host proteins and potentially initiate biofilm formation, it is also becoming more prevalent that these proteins also have additional functions which aid in pathogenesis including immune evasion (77).

S. aureus produces several surface proteins such as the MSCRAMMs that play a significant function in adhesion and initial accumulation to host matrix components, yet, more recent data suggests that these proteins play a less significant function in attachment to abiotic materials such as polystyrene or a glass. This is not a surprise considering the host matrix substrates important for MSCRAMM binding are absent when cells are binding to these types of abiotic surfaces. Recently, three different types of molecules have been implicated in binding to abiotic surfaces. First, a mutation in the Agr quorum sensing circuit, typically known for its function in biofilm dispersal by

regulating the PSMs (discussed below), was previously shown to inhibit attachment to polystyrene by preventing hydrophobic interactions between the cell and the polymer surface via limited production of the PSM δ-toxin (85). Second, like δ-toxin, the major autolysin AtlA has also been proposed to aid in cell attachment, (86, 87) although the multi-functionality of this protein makes it difficult to determine the exact mechanism of attachment. Lastly, there is some data to suggest that *S. aureus* teichoic aids also have a function attachment mediated by charge interactions with an abiotic surface (88).

Accumulation/Maturation Stage

During the accumulation/maturation stages of biofilm development, *S. aureus* begins to create the ECM composed of polysaccharide intercellular adhesin (PIA), eDNA, and/or proteins which allow cells within the biofilm to stick together and form three-dimensional structures. Possibly the most studied of these ECM components, PIA, produced by the *icaADBC* operon, has been shown numerous times to have a function in the accumulation and maturation of *S. aureus* biofilms (89-91). Yet, it appears to be strain- or condition-specific, given the number of strains that have also been shown to form PIA-independent biofilms (92-94). While PIA cannot be completely disregarded for its function in *S. aureus* biofilms, it appears that PIA-independent *S. aureus* biofilms may rely more on proteins and eDNA (95-97) than the closely related species *Staphylococcus epidermidis*.

Other components to consider as possible constituents of the ECM during early biofilm development are intracellular components. In support of this, a recent report demonstrates that *S. aureus* biofilms appear to recycle cytoplasmic proteins not typically characterized as biofilm-related proteins such as enolase and GAPDH which are somehow released into the extracellular milieu to attach to the surface of the cell (98). Although the mechanisms of how cytoplasmic proteins devoid of a signal peptide can be

transported into the extracellular milieu still remains unknown, the authors speculate that the accumulation of these moonlighting proteins in the ECM may be associated with mechanisms of autolysis-mediated release of eDNA. This may be a likely scenario considering eDNA release mediated via cell death and lysis by the *cidABC* and *lrgAB* operons and *atlA* has been shown to play a significant determinant in *S. aureus* biofilm structuring (discussed in detail below) (99-104). In conjunction with eDNA release, there are reports of proteins interacting with the eDNA within the ECM to provide the biofilm with structural support. Two recent examples include the moonlighting cytoplasmic proteins, enolase and GAPDH, binding to eDNA under low pH conditions (105) and the presence of eDNA to initiate PSM-mediated amyloid fiber production (106). In addition, there is data to suggest that cytoplasmic nucleoid-associated proteins (NAPs), typically used for chromosomal structuring, may also serve as a biofilm scaffold when released from the cell by binding eDNA (107). Likewise, other extracellular proteins such as beta-toxin (Hlb) (108) and the immunodominant surface antigen B (IsaB) (109) also have shown the ability to bind eDNA and potentially play a role in biofilm scaffolding.

Detachment/Dispersal Stage

During the last stage of biofilm development, the *S. aureus* cells switch from a biofilm state of growth to planktonic cells by detaching from the biofilm and dispersing to other sites to potentially start the biofilm process over. Normally, this process is thought to be controlled by the modulation or degradation of the ECM. Indeed, dispersal of *S. aureus* biofilms has been shown to be under the control of the Agr, quorum sensing network (85, 110) which controls several genes associated with ECM modulation. The first studies examining the contribution of the Agr system in *S. aureus* biofilm development demonstrated that *agr*-deficient strains developed more robust biofilms when compared to their wild-types counterparts (85) suggesting that the Agr system may

play a potential role in detachment of biofilms. Yet, it was not until flow-cell studies evaluating to role of Agr quorum sensing during *S. aureus* biofilm development that a more direct role was identified. More specifically, time-lapse microscopy identified that the P3 promoter was differentially expressed in a subpopulation of cells located primarily in the tower/microcolony portions of the biofilm. Additionally, P3 expression appeared to oscillate in waves over time coinciding with detached cells of the biofilm (110). While this initial report provided support that *agr* activity plays a role in dispersal of biofilms, the *agr*-regulated factors that mediate dispersal still remained unclear. It wasn't until later in which two independent studies provided evidence of contrasting modes of agr-mediated dispersal mechanisms. In one study, it was shown that the Agr system regulates expression of secreted proteases that degrade proteinaceous components of the ECM in order to disperse the biofilm. It was also demonstrated that there was a direct correlation of P3 activation via induction by AIP and dispersal of intact biofilms which they propose is due to increased protease activity (111). While this provides a connection with protease activity, Agr is not the only known regulator of the secreted proteases. In fact, other master regulators such as SarA, SigB, SaeRS, and Rot (33, 112-115) have all been shown to mediate protease activity and biofilm maturation.

An alternatively proposed *agr*-dependent dispersal mechanism is the production of the PSM peptides. These short amphipathic, α-helical peptides have been shown to be under the regulation of Agr system via direct binding of AgrA to the *psm* operon promoters, and under certain growth conditions, have been implicated in dispersing staphylococcal (116, 117). Indeed, *S. aureus* isogenic mutants in the either classes of PSMα or PSMβ or δ-toxin demonstrated more robust biofilm formation (117). Like the Yarwood et al. study, it was also shown that the induction of the Agr-system and the *psm* operon promoters correlates with waves of dispersal during late stages of biofilm

development (117). It is thought that when PSMs are produced that they act like surfactants disrupting covalent interactions within the biofilm matrix to mediate dispersal (27, 76). While the surfactant-like properties of the PSMs may indeed be the major player in biofilm dispersal, there is also contrasting evidence suggesting that under certain conditions that aggregation of the PSMs into nonsoluble amyloid-like fibers might abrogate biofilm dispersal and contribute to the integrity of the biofilm structure (118). Hence, the production of PSMs solely may not initiate dispersal, but rather the state in which the PSMs are assembled may contribute directly to the biofilm disassembly. Additionally, it is also apparent that the presence to of eDNA promotes the formation of these amyloid-like structures (106) suggesting a necessity for the production and interplay between ECM components to allow proper biofilm development.

Apparently separate from the Agr-mediated dispersal mechanisms, the production of two extracellular nucleases also have a function in biofilm detachment. eDNA is an important component of the ECM, and several studies have demonstrated that both the secreted nuclease (Nuc) and suface-attached nuclease (Nuc2) degrade eDNA initiating biofilm dispersal (100, 119-122). However, the studies in this dissertation demonstrate that nuclease-mediated detachment may be important form proper maturation under certain conditions, rather than an endpoint like Agr-mediated processes.

Mechanisms of cell death and lysis

The existence of pronounced death and lysis during bacterial biofilm development has led to the proposal that these relatively simple organisms have the capacity to control cell viability in a process analogous to apoptosis in more complex eukaryotic organisms (123, 124). A key function of these processes, referred to as bacterial programmed cell death (PCD), is likely to release genomic DNA into the biofilm

matrix, where it serves as an effective intercellular adherence molecule. The importance of extracellular DNA (eDNA) as a matrix molecule was originally demonstrated in *Pseudomonas aeruginosa* (125) and has since been shown to be important for biofilms produced by a wide range of bacterial species (99, 100, 125-129). Although some reports suggest the involvement of bacteriophage in DNA release during biofilm development (129-132), the presence of distinct regions of cell death and lysis indicates that this process is highly regulated (100, 126, 129, 133).

Insight into the molecular mechanisms controlling PCD has come from studies of the *S. aureus cidABC* and *lrgAB* operons, which were originally characterized as mediators of murein hydrolase activity and lysis (134-136). The mode of action of their gene products has been hypothesized to involve a mechanism analogous to the holin-/antiholin-mediated control of host cell lysis during bacteriophage infection (123, 137). A role for these operons during biofilm development was demonstrated by the observations that *cid* and *lrg* mutations affect biofilm formation, disrupting the normal architecture that is a characteristic of these multicellular communities (99, 100). Additionally, it was established that the *cid* mutant produced biofilm with reduced levels of matrix-associated eDNA, while the *lrg* mutant exhibited increased levels of this matrix component (100). Similar effects on biofilm development were also produced by *Pseudomonas aeruginosa* in which homologues of *cid* and *lrg* had been disrupted (138). These results suggest the existence of a careful balance between death effectors and inhibitors in normal biofilm, not unlike that proposed to control normal tissue homeostasis in more complex developmental organisms (124). Moreover, they support the notion that this mechanism is conserved in other bacterial species.

Recent evidence also suggests that Cid-/Lrg-like proteins are conserved much more broadly than was originally recognized. Recent studies of a putative *Arabidopsis*

CidAB/LrgAB homolog, designated AtLrgB, indicated that this gene is an important regulator of cell death in plants (139, 140). Disruption of the gene encoding AtLrgB produced plants with interveinal chlorotic and premature necrotic leaves, suggesting the involvement of this protein in leaf senescence. Furthermore, recent studies (141) also support the model that the mammalian Bcl-2 family of proteins functions in a manner analogous to holins and antiholins. Strikingly, these studies demonstrated that the death effector and inhibitor components of the Bcl-2 protein family can induce cell death and lysis in *Escherichia coli* similar to holins and antiholins, respectively. Indeed, replacement of the normal holin of bacteriophage lambda with derivatives of human Bax protein resulted in the formation of functional, plaque forming viral particles. These results suggest that the functions of the Cid and Lrg proteins span at least three Kingdoms of life.

It is clear that any model of controlled cell death and lysis during biofilm development must accommodate the observation that only a subpopulation of cells undergoes this process. Structured biofilms exhibit obvious spatial differences in cell viability and lysis, including localized dead cell and eDNA staining in towers and more homogeneous live cell populations in the basal biofilm (100, 126, 129, 133). This has led us to hypothesize that the differential expression of cell death and lysis within biofilm subpopulations is dictated by the heterogeneous expression of the *cid* and *lrg* operons within the biofilm (123, 124), possibly as a result of the metabolic heterogeneity commonly observed in them (142). The combined effects of metabolism are envisioned to result in an optimal balance of expression that is essential for normal biofilm development (124). Indeed, expression of the *S. aureus cidABC* and *lrgAB* operons has been shown to be tightly coordinated by regulators that sense and respond to basic metabolic processes. For example, *cidABC* expression is induced by the LysR-type

transcriptional regulator, CidR, under conditions of excess glucose and oxygen (overflow metabolism) (143-145), while *lrgAB* expression is stimulated by changes in membrane potential in a process that is dependent on the two-component regulatory system, LytSR (146). Although much is known about the regulatory signals important in *cidABC* and *lrgAB* expression, how these signals are integrated during biofilm development remains unknown.

BioFlux1000 microfluidic technology[1]

Given the propensity at which staphylococci develop biofilms and cause chronic infections, assays to aid in the understanding the molecular mechanisms in biofilm maturation are essential. Above all, biofilm assays designed to evaluate biofilm development in a real-time manner are of becoming particularly essential. The new gold standard for assessing developmental processes associated with biofilm formation are flow-cell systems that allow for the perfusion of media across bacterial cells attached to a synthetic surface, thus, providing a constant supply of nutrients under the pressure of a shear force. Today, several commercially available flow-cell systems from companies such as BioSurface Technologies, Corp., Stovall Life Science, Inc., and Fluxion Biosciences, Inc. are available for use in biofilm studies. In fact, a variety of flow-cell systems ranging from single to multi-channel designs are available in either reusable or disposable forms. While some flow-cell systems allow researchers to test the effects of various surfaces such as glass slides/coverslips, polycarbonate coupons, and plastic capillary tubing on biofilm development, others are designed to maximize versatile image acquisition using a high-throughput plate format. An example of this is the microfluidic system the BioFlux1000. The BioFlux1000 is comprised of an epifluorescence

---

Majority of this section has been published in Derek E. Moormeier and Kenneth W. Bayles. 2014. *Methods Mol Biol.*

microscope equipped with an automated temperature-controlled stage, a pneumatic compressor, a high-resolution camera, and specialized 24-well or 48-well plates equipped with microfluidic channels that connect two adjacent wells, one for sterile media and the other for effluent (Figure 1-1) (147). The microfluidic channels are seeded with bacteria and the sterile media is pneumatically perfused through the channels, resulting in biofilm growth. To assess biofilm development in each channel (up to 8 or 24 biofilms, depending on the plate being used), sequential images are automatically acquired using the high-resolution camera and compiled using BioFlux Montage image analysis software. Collectively, the automated image acquisition and the simultaneous growth of multiple biofilms enable an unprecedented comparison of biofilm development by bacterial strains containing different mutations. Additionally, the use of metabolic stains and/or fluorescent reporters allows for the localization of spatial and temporal patterns of metabolic activity and gene expression within the developing biofilm architecture (147, 148). Although the evaluation of the biofilm images is primarily qualitative, the BioFlux data analysis software contains some functions that enable areas of the two-dimensional images of light and/or fluorescence intensity to be quantified (147). In these studies, we took advantage of the BioFlux1000 capabilities to maximize evaluation of *S. aureus* biofilm in real time.

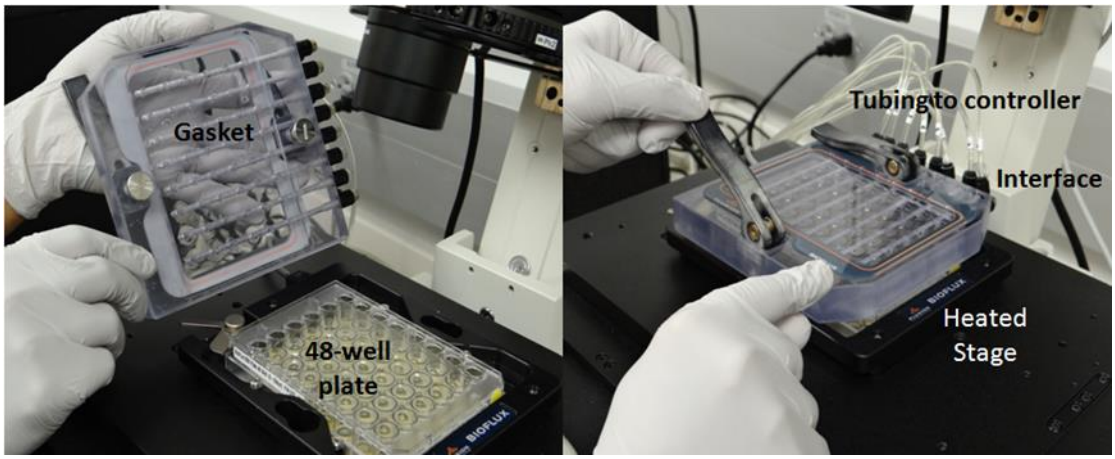

Figure 1-1 BioFlux1000 Interface, Gasket, Tubing, Stage, and 48-well plate setup

The BioFlux Interface locks the BioFlux plate to the heated stage and is connected to the BioFlux Controller via small tubing. The tubing allows media to be pneumatically pumped into the microfluidic channels of the BioFlux plate. It is important during every attachment of the BioFlux Interface to the BioFlux Plate to apply as little pressure as possible to the top of the Interface to prevent the plate from cracking.

Figure modified from Derek E. Moormeier and Kenneth Bayles. 2013. *Methods Mol Biol.*

CHAPTER II:

MATERIALS AND METHODS

Table 1. Bacterial strains and plasmids used in these studies

Bacterial Strains	Description	Reference
Escherichia coli		
DH5α	Host strain for construction of recombinant plasmids	(149)
S. aureus		
RN4220	Highly transformable strain; restriction-deficient	(150)
UAMS-1	Wild-type osteomyelitis clinical isolate	(151)
UAMS-1471	UAMS-1 Δ*nuc*	(112)
UAMS-155	UAMS-1 *agr*::tet	(152)
UAMS-1 hsdR-	UAMS-1 restriction-deficient	(153)
KB999	UAMS-1 *lytS*::*ermC*	(146)
KB1090	UAMS-1 *cidR*::*ermC*	(145)
*KB8037	UAMS-1 *icaA*:: *ΦNΣ*	This study
KB8000	UAMS-1 Δ*ackA::ermB,* Erm^r	(154)
KB8001	UAMS-1 Δ*pta*	(154)
USA300 LAC JE2	USA300 LAC derivative	(155)
JE2 *agrA:: ΦNΣ*	*bursa aurealis agrA* mutation in JE2	(155)
JE2 *nuc::ΦNΣ*	*bursa aurealis nuc* mutation in JE2	(155)
JE2 *atlA::ΦNΣ*	*bursa aurealis atlA* mutation in JE2	(155)
AH1263	USA300 CA-MRSA Erm^s LAC derivative	(97)
AH1558	AH1263 *saeQRS::spc*	(48)
AH1919	AH1263 Δ*aur* Δ*sspAB* Δ*scpA spl*::*erm* (protease KO)	(156)
AH2216	AH1263 Δ*saePQRS*	(157)
**CFS93	AH1263 Δ*saeP*	Horswill lab
**AH3499	AH1263 Δ*saeQ*	Horswill lab
AH3500	AH1263 Δ*saeS*	(157)
Plasmids		
pCR2.1	*E. coli* PCR cloning vector	Invitrogen
pJB38	Temperature sensitive allelic exchange plasmid	(158)
pBK123	Shuttle vector, pCN51ΔEM::CAT; Cm^R	(159)
pEM64	pBK123 derivative containing Cd-inducible GFPaav	This study
pEM80	*lrgAB* promoter::sGFP, Cm^R	This study
pEM81	*cidABC* promoter::sGFP, Cm^R	This study
pEM87	*ldh1* promoter::sGFP, Cm^R	This study
pCM11	Shuttle vector encoding sGFP	(160)
pKH4	Agr P3 promoter::sGFP	(161)
pDM4	*lrgAB* promoter::sDsRed, *cidABC* promoter::sGFP	This study

pSC14	*sarA* promoter::sDsRed, *cidABC* promoter::sGFP	Thomas lab
pDM17	*sarA* promoter::sDsRed, *nuc* promoter::sGFP	This study
pDM19	*coa* promoter::sDsRed, *nuc* promoter::sGFP	This study
pCM20	*nuc* promoter::sGFP	(119)
pCM27	*hla* promoter::sGFP	(157)
pCM11*hlgA*	*hlgA* promoter::sGFP	(157)
pCM11*P1sae*	*P1sae* promoter::sGFP	(157)
pRMC2	anhydrotetracycline inducible plasmid	(112)
pRMC2-*nuc*	anhydrotetracycline inducible plasmid containing *nuc*	(119)
**pJB38-Δ*saeP*	AH1263 Δ*saeP* allelic exchange plasmid	Horswill lab
**pJB38-Δ*saeQ*	AH1263 Δ*saeQ* allelic exchange plasmid	Horswill lab

***Strain constructed by Jennifer L. Endres from Bayles laboratory, but has not yet been published.**

****Strains and plasmids constructed in Dr. Alexander Horswill laboratory by Dr. Caralyn Flack, but have not yet been published.**

Table 2. Oligonucleotides

Primer Name	Sequence
cidA-pro-F	5’-CCCGCATGCAGCAAATTATCAATGATGAAGTAGATA-3’
cidA-pro-R	5’-CCCGGATCCCGCCATCCCTTTCTAAATAC-3’
lrgA-pro-F	5’-CCCGCATGCCGATAAAATTCACATGTTAAAGC-3’
lrgA-pro-R	5’-CCCGGATCCCGTTTGATTTAACTAAAGTATAGATGG-3’
ldh1-pro-F	5’-CCCGCATGCATGGCTTTTAATAAATTTTC-3’
ldh1-pro-R	5’-CCCGGATCCTACAAAAACTCCCTTATGAT-3’
cidA-rt-F	5’-GGGTAGAAGACGGTGCAAAC-3’
cidA-rt-R	5’-TTTAGCGTAATTTCGGAAGCA-3’
lrgA-rt-F	5’-GCATCAAAACCAGCACACTTT-3’
lrgA-rt-R	5’-TGATGCAGGCATAGGAATTG-3’
sigA-rt-F	5’-AACTGAATCCAAGTCATCTTAGTC-3’
sigA-rt-R	5’-TCATCACCTTGTTCAATACGTTTG-3’
DsRed-F	5’CAGAGTCGACTGATTAACTTTATAAGGAGGAAATACATATGGACAACACCGAGG-3’
DsRed-R	5’-ACATGCATGCTACAGGAACAGGTGGTGGCGG-3’
sGFP-F	5’CACGAATTCTGATTAACTTTATAAGGAGGAAAAACATATGCCCGGGAGCAAAGGAG-3’
sGFP-R	5’-CCTGGCGCGCCTTCTTATTTGTAGAGCTCATCCATGCC-3
lrgA-R	5’-GCTGGATCCACGTTTGATTTAACTAAAGTATAGATGGCTCAC-3’
cidA-R	5’GCCGGAATTCTAAATACGTCTAAATTGTTACAATAACTATTATAAAGATGGCG-3’
cidABC-lrgAB-F	5’GTTTCCAGTCCATTCAAGCGTTCCGCACATGACCAATACGCAGTACAG-3’
lrgAB-cidABC-F	5’CTGTACTGCGTATTGGTCATGTGCGGAACGCTTGAATGGACTGGAAAC-3’
sDsRed-F	5’-AGCGGATCCAGATAATCTATAAAAGGAGG-3’
sDsRed-R	5’-TCTTGCATGCTTATAAAAACAAATGATGACGAC-3’
MJT240	5’-GTTGTTGAATTCACCTGTATACATTACAGACC-3'
CEF169	5'CAGAAATTGAGTACTAGATCTGTATTCATGCTAACTCCTCATTTC - 3'
CEF170	5’GAATACAGATCTAGTACTCAATTTCTGAGTTAAACTTTTATTTACAAC- 3'
CEF171	5’- GTTGTTGGTACCAAGAAACTAGCAGCATATGC - 3'
CEF172	5' - GTTGTTGAATTCCCTAACAGGTACATTCAGTTC -3'

CEF173	5'GCGAGTACTAGATCTCATTCTTTCTATTTATTGTGTGTAATTTATAT - 3'
CEF174	5' - AGAATGAGATCTAGTACTCGCAAATATAGTTGCACATAC - 3'
CEF175	5’- GTTGTTGGTACCGATGGTATATGTTGTAAAGCTCTC - 3'
icaA-F	5’-CATTGAACAAGAAGCCTGAC-3’
icaA-R	5’-CTGCTGTATTATCTGAACTTCC-3’
Type III-F	5’-CATCGAATGCGTTAAAGGTTAATTATGAGC-3’
Type III-R	5’-CACTATCGTCTCCTGTTAAAGCAACAC-3’
cna-F	5’-AGTGACATGGTCTAATCTTCCGG-3’
cna-R	5’-TCCACTTTTGATGGCTTATCTGG-3’
Dual-coa-F	5’-GCCGCTGCAGGTTTCGCTTTAGTCATTTGAT-3’
Dual-coa-R	5’-GCCGGGATCCATGTAATTGCCCAATCTACAT-3’
Dual-nuc-F	5’-GCCCGCTGCAGGTAAATTATAAGTTATACATCTCG-3’
Dual-nucR	5’GCCGGAATTCCTTTTTAGTTAATTTTAATATTAAACG-3’

Bacterial strains and growth conditions

Staphylococcus aureus and *Escherichia coli* strains used in these studies are described in Table 1. All strains of *E. coli* were grown in Luria-Bertani broth (LB) or LB containing 1.5% agar. All *S. aureus* strains were grown in tryptic soy broth (TSB) (EMD Biosciences, Gibbstown, NJ) or on TSB containing 1.5% agar. All experiments were started from fresh overnight TSB cultures grown at 37°C with shaking at 250 rpm. To determine expression of fluorescent reporters fusions in Chapter III by planktonic aerobic growth, cultures were generated by inoculation of overnight cultures into TSB medium with or without glucose to an OD_{600} of 0.1 and incubation with shaking at 250 rpm at 37˚C using a 10:1 flask to volume ratio. Hypoxic growth was achieved by growing the cells statically at 37˚C in a covered flask at a 5:3 flask to volume ratio. Dissolved oxygen levels were measured using a portable dissolved oxygen meter (Accumet) per the manufacturer's instructions. As needed, chloramphenicol (5 µg ml^{-1}), erythromycin (5 µg ml^{-1}), tetracycline (5 µg ml^{-1}), ampicillin (100 µg ml^{-1}), and spectinomycin (1000 µg ml^{-1}) were added to the growth medium.

Planktonic growth analysis of S. aureus sae mutations

To determine any growth defects of *sae* mutations during planktonic aerobic growth described in Chapter III, cultures were generated by adjusting overnight cultures to an OD_{600} 0.06 in TSB containing 0.25% glucose and then grown for 24 hours with shaking at 250 rpm at 37°C using a 10:1 flask to volume ratio. Subsequently, supernatants were taken at 0, 3, 6, 9, 12 and 24 hours and the OD_{600} were measured and plotted over time.

Determination of exogenous DNA growth and nuc expression on planktonically grown AH1263 and sae mutant cells

At a flask ratio of 10:1, *S. aureus* overnights were adjusted to OD_{600} 0.06 in 25 ml of TSB containing 0.25% glucose buffered in 50 mM 3-(*N*-morpholino)propanesulfonic acid (MOPS) at a pH 7.4 with or without different percentages of exogenous salmon sperm DNA. Cultures were agitated at 250 rpm and grown for up to 24 hrs. To determine the effect on growth and relative fluorescence, OD_{600} supernatants were read first. Next, another supernatant of cells were washed once in 1x PBS and 200 µl were pipetted into a 96-well flat-bottom, black polystyrene plate (COSTAR 3916). Fluorescence was quantified using a Tecan Infinite 200 spectrofluorometer with an excitation wavelength of 490 nm and emission wavelength of 525 nm. Relative fluorescence was determined by normalizing the quantified fluorescence per OD_{600} and plotted using GraphPad Prism. To determine the effect of exogenous DNA on solely growth, the OD_{600} were plotted over time using GraphPad Prism.

Generation of transcriptional reporter fusions

The *S. aureus cidABC*, *lrgAB*, and *ldh1* promoter regions were PCR-amplified using oligonucleotide primers flanking these sequences and Thermolace high fidelity DNA polymerase (Invitrogen, Carlsbad, CA). Specifically, a 689 nt DNA fragment spanning the promoter region of *cidABC* (P_{cidABC}), and a 500 nt DNA fragment spanning the promoter regions of *lrgAB* (P_{lrgAB}) and *ldh1* (P_{ldh1}), were amplified using the cidA-pro, lrgA-pro, and ldh1-pro primer sets, respectively, listed in Table 2. Each promoter fragment was ligated into pCR2.1 using the Invitrogen TA cloning kit (Carlsbad, CA) and the recombinant plasmids were transformed into *E. coli* DH5α cells (Table 1). After confirming the absence of mutations by nucleotide sequencing, the promoter fragments

were excised by digestion with the restriction endonucleases, SphI and BamHI, and used to replace the cadmium-inducible promoter in front of the gene encoding the short half-life GFPaav in the plasmid, pEM64. Due to the weak fluorescence of GFPaav, the GFPaav gene was replaced with the gene encoding superfolder GFP (sGFP) from pCM11 (Table 1).

A dual reporter plasmid (designated pDM4) containing divergently transcribed *cidABC* and *lrgAB* promoter regions fused to genes encoding green and red fluorescent proteins, respectively, was constructed as follows. Primers DsRed-f and DsRed-r (Table 2) were used to amplify the gene encoding DsRed.T3(DNT) fluorescent protein (162). The 717 bp DsRed.T3(DNT) PCR product was ligated into the SalI-SphI sites of the shuttle vector, pBK123 (Table 1), producing pDM1. Using primers lrgA-r, cidA-r, cidABC-lrgAB-f, and lrgAB-cidABC-f (Table 2), the promoter regions spanning 833 bp and 602 bp upstream of *cidABC* and *lrgAB,* respectively, were amplified from the *S. aureus* UAMS-1 chromosome and combined using a SOEing (splicing by overlap extension) technique (163) resulting in a 1,441 bp DNA fragment containing the *cid* and *lrg* promoters in a divergent orientation. After confirmation of this fragment by nucleotide sequencing, it was ligated into the EcoRI and BamHI sites of pDM1 to generate pDM2. Next, a 768 bp DNA fragment encoding sGFP from pEM80 was amplified using the primers, sGFP-r and sGFP-f (Table 2), and then ligated into the EcoRI and AscI sites of pDM2, generating pDM3. Finally, due to the weak expression of the gene encoding DsRed.T3(DNT), the coding region was optimized for codon usage in *S. aureus*, and synthesized by Invitrogen-GeneArt (Carlsbad, CA). This gene was then used to replace the un-optimized DsRed.T3 (DNT) gene in pDM3, resulting in the plasmid, pDM4.

The generation of pDM19 was performed as follows. First, pDM17 was generated by amplifying the promoter region 319 bp upstream of *nuc* transcription start

site from the AH1263 chromosome using the Dual-nuc-F/Dual-nuc-R primer pair (Table 2). After amplification of the *nuc* promoter region, it was digested with EcoRI and PstI and ligated into pSC14, resulting in the dual reporter P*sarA*::sDsRed and P*nuc*::sgfp plasmid pDM17 (Table 1). Upon confirmation, 455 of the *coa* promoter region was ampilified from the AH1263 chromosome using the Dual-coa-F/Dual-coa-R primer pair (Table 2). This 445 promoter region was then digested with PstI and BamHI and ligated into pDM17. The resulting plasmid, P*coa*::sDsRed and P*nuc*::sgfp dual reporter plasmid, was named pDM19 (Table 1).

***Generation of icaA::ΦNΣ mutation in UAMS-1 S. aureus*[2]**

The UAMS-1 *icaA::φNΣ* mutant was generated via transduction using φ11 propogated in the Nebraska Transposon Mutant Library (NTML) mutant, NE37 (155). Due to issues moving the *icaA::φNΣ* transposon into wild-type UAMS-1, initially, the mutation was transduced into a UAMS-1 restriction deficient isolate (153) as described below. Resulting colonies were screened for transposon insertion utilizing primer pair, icaA-F and icaA-R. The transduction process procedure was repeated to move the mutation from the UAMS-1 restriction deficient strain into the wild-type UAMS-1 background. These transductants were confirmed to be UAMS-1 background by PCR amplification of the UAMS-1-specific *cna* gene with the primer pair cna-f and cna-R and primers specific for the type III restriction system, Type III-F and Type III-R. The resulting strain was named KB8037.

The construction of this strain was performed by Jennifer Endres in the Bayles laboratory, but has not yet been published.

***Construction of ∆saeP and ∆saeQ mutations in AH1263 S. aureus*[3]**

To construct the ∆*saeP* mutant in AH1263, two-step overlap PCR was used to create pJB38-∆*saeP*. 600 bp regions directly upstream and downstream of *saeP* were amplified from AH1263 genomic DNA with primer pairs MJT240/CEF169 or CEF170/CEF171 respectively, where CEF169 and CEF 170 contained complementary overlap regions (Table 2). The upstream and downstream PCR products were purified by agarose gel electrophoresis. 2ml of each purified product were mixed and used as the template for the second round of PCR with primer pair MJT240/CEF171. The resulting 1.2kb PCR product was purified, digested with EcoRI and KpnI and ligated into similarly digested pJB38 (158). The resulting plasmid was used to construct a markerless ∆*saeP* strain in the AH1263 background as previously described (158) and was named CEF93 (Table 1).

Similarly, to construct the ∆*saeQ* mutant in AH1263, two-step overlap PCR was used to create pJB38-∆*saeQ* 600 bp region directly upstream and 900 bp region downstream of *saeQ* were amplified from AH1263 genomic DNA with primer pairs CEF172/CEF173 or CEF174/CEF175 respectively, where CEF172 and CEF175 contained complementary overlap regions (Table 2). The upstream and downstream PCR products were purified by agarose gel electrophoresis. 2ml of each purified product were mixed and used as the template for the second round of PCR with primer pair CEF172/CEF175. The resulting 1.2kb PCR product was purified, digested with EcoRI and KpnI and ligated into similarly digested pJB38 (158). The resulting plasmid was used to construct a markerless ∆*saeQ* strain in the AH1263 background as previously described and was named AH3499 (Table 1).

The construction of these strains was performed by Dr. Caralyn Flack in the laboratory of Dr. Alexander Horswill (University of Iowa), but has not yet been published.

Movement of plasmids into S. aureus strains

All plasmids were purified from the *S. aureus* strains or *E. coli* strains using the Wizard Plus SV Minipreps DNA purification system (Promega Corporation) according to manufacturer's instructions, and then electroporated into the highly transformable, restriction-deficient *S. aureus* strain RN4220 (Table 1). Transduction of the plasmids (Table1) into UAMS-1, JE2, or AH1263 (or mutant derivatives) strains was performed using φ11 phage propagated on the plasmid-containing RN4220 strain as previously described (164).

Confocal microscopy imaging of planktonic expressing reporter S. aureus strains

Planktonic *S. aureus* cells expressing fluorescent reporter genes were imaged by CLSM as follows. Overnight cultures were diluted to an OD_{600} of 0.1 into fresh medium and incubated under aerobic and hypoxic conditions as described above. Samples of the cultures were harvested and pelleted by centrifugation at 14,000 × rpm for 3 min. The pellets were resuspended in 0.85% NaCl to an approximate OD_{600} of 5.0, and 2.5 µl of each preparation was placed on a microscope slide and covered with a coverslip. An inverted Zeiss 510 Meta CLSM fitted with a Plan-Apochromat 63×/1.40 Oil DIC M27 objective set to a 3.0× digital zoom was used to image the cells. An argon 488 nm laser was used to excite any GFP present in the cells and the emissions were collected using a 505-550 band pass filter. Images collected were processed using the Imaris 7.0.0 software suite (Bitplane, Saint Paul, MN).

RNA quantification

Total *S. aureus* RNA was isolated as previously described (146) with minor modifications as follows. Briefly, *S. aureus* cells were harvested by centrifugation at 4,100 r.p.m. in a Sorvall Legend table-top centrifuge (Newtown, CT) and the resulting pellets were resuspended in 500 µl of TSB. Then 1.0 ml of RNAprotect Bacteria Reagent (Qiagen, Valencia, CA) was added, samples were vortexed vigorously for 30 sec and incubated at room temp for 15 min. Cells were then pelleted by centrifugation at 5,000 x g for 10 min in a Microfuge 18 centrifuge (Beckman-Coulter, Brea, CA); supernatants were removed and pellets were stored at -80˚C. Once all samples had been collected, the cells were thawed for 10 min, resuspended in 900 µl of RLT buffer, and RNA was isolated using an RNeasy Mini RNA Purification Kit (Qiagen, Valencia, CA) as described previously (146).

Quantitative real-time PCR was performed using *cidA*-, *lrgA*-, and *sigA*-specific primers listed in Table 2. Briefly, 500 ng of total RNA was converted to cDNA using the Quantitect Reverse Transcription Kit from Qiagen (Valencia, CA). The samples were then diluted 1:50 and the *cidA, lrgA*, and *sigA* cDNA products were amplified using 5.0 µM cidA-rt, lrgA-rt, and sigA-rt primers (Table 2), respectively, with the LightCycler DNA Master SYBR Green I kit (Roche Applied Science, Indianapolis, IN), following the manufacturer's instructions. Fold changes in *cidA* and *lrgA* transcript levels were calculated using the comparative C_T method (165), normalizing to the amount of *sigA* transcripts present in the RNA samples. Results were recorded in triplicate, representative of three independent experiments.

Fluorescence-activated cell sorting flow cytometry of cells grown planktonically

To count the number of cells expressing *nuc* in planktonic cells cultures, *S. aureus* strains grown overnight were adjusted to an OD_{600} of 0.06 in 12.5 ml of TSB containing 0.25% glucose and grown for 4 hours with shaking at 250 rpm at 37°C using a 10:1 flask to volume ratio. After 4 hours of growth, 1000 µl of cells were washed with 1x phosphate buffer saline (PBS) and then 200 µl of washed cells were pipetted into a clear 96-well plate and analyzed on a BD LSRII flow cytometer (Beckton and Dickinson, San Jose, California). A total of 10,000 events from each cell culture sample were analyzed at a flow rate of 1000 cell per second. Bacteria were distinguished from background using forward and side scatter light using wild-type cells without a fluorescent reporter plasmid as a negative control. To enumerate sGFP positive cells, samples were excited at 488 nm using an argon laser and detected using a 530$\pm$30 nm (with a 505 nm long-pass filter). The raw data were then analyzed and plotted using FlowJo data analysis software (FlowJo, LLC, Ashland, OR).

Biofilm assays

BioFlux1000 biofilm assays to evaluate gene expression and biofilm morphologies

To monitor gene expression and biofilm morphologies, *S. aureus* biofilm development was assessed using a BioFlux1000 microfluidic system (Fluxion Biosciences Inc., San Francisco, CA) as described previously (148). Using BioFlux1000 48-well plates, the biofilm growth channels were primed by adding 200 µl of TSB to the output wells and initiating a reverse flow for 5 min at 5.0 dyn/cm^2. To seed the channels with bacteria, excess TSB in the output wells was replaced with 200 µl of fresh overnight *S. aureus* cells diluted to an OD_{600} of 0.8 and pumped into the channels at 2.0 dyn/cm^2 for 5 sec. Cells were then allowed to attach to the surface of the plate for 1 hour at 37°C. Remaining inocula was aspirated from the output well and 1.3 ml of 50% TSB was

added to the input wells and pumped at 0.6 dyn/cm^2 for 18 hours (Figure 2-2 depicts macroscopic view of serpentine channels, output and input wells, and the center viewing area). Brightfield and epifluorescence images were acquired in 5-min intervals for a total of 217 time points. All epifluorescence images observing GFP and/or sDsRED expression were acquired using a fluorescein isothiocyanate (FITC) and Tetramethylrhodamine (TRITC) filters, respectively, and kept at constant acquisition settings (FITC; Gain: 20, Exposure: 500 ms and TRITC; Gain: 10, Exposure: 600ms). For a more detailed protocol of utilizing the BioFlux1000 to evaluate staphylococcal biofilm development, refer to reference (166).

To ensure nuclease was actively being made using the inducible aTet plasmid system (pRMC2 and pRMC2-*nuc*) under non-inducing conditions, wild-type and Δ*nuc* mutant strains containing pRMC2 or pRMC2-*nuc* supernatants from effluents of 3-h biofilms grown in the BioFlux without aTet were incubated with *S. aureus* genomic DNA overnight and separated in a 1% agarose gel.

Determination of adding proteinase K, DNaseI, or PAS to biofilms grown in BioFlux1000

To determine the effects of proteinase K (Invitrogen Inc.), DNase I (Fermentas Inc.), or lysis-inhibitor polyanethole sulfonate (PAS) on biofilm development in the BioFlux1000, channel priming and cell seeding were performed as described above and 1 ml of 50% TSB or 1 ml of 50% TSB supplemented with either 100 µg ml^{-1} of proteinase K, 0.5 units ml^{-1} of DNase I, or 50 µg/ml of PAS was pumped at 0.6 dyn/cm^2 for eight hours. Where indicated, flow was stopped intermittently and 1 ml of 50% TSB was replaced with 1 ml of 50% TSB supplemented with proteinase K or DNase I. After restarting the flow, brightfield images were acquired in two-hour intervals.

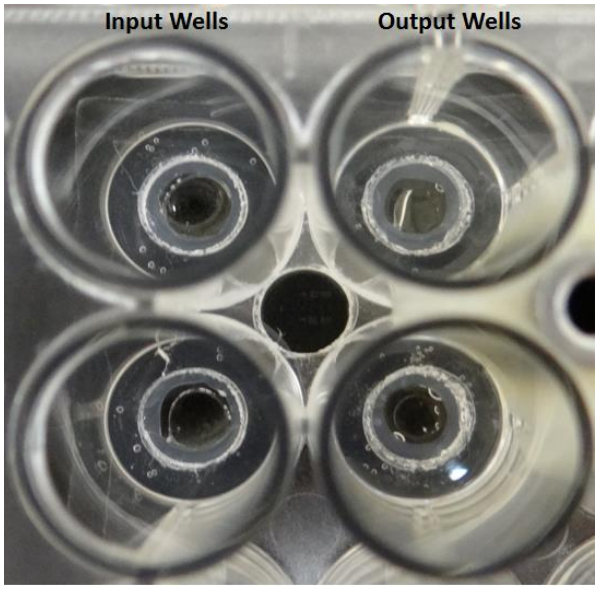

Figure 2-1 Macroscopic view of a 48-well BioFlux plate

Macroscopic view of input and output wells of a 48-well BioFlux plate with media in the center of wells. Circle in the center of wells is the viewing window of the microfluidic channels. To prime channels, 200 µl of TSB is pumped for 5 min from output to input wells. After excess TSB is aspirated from output, 200 µl of adjusted inoculums are seeded into the channels by pumping for 5 s from output to input wells. After 1 h incubation, biofilms are grown in 50 % TSB pumped from input to output wells for 18 h at 0.6 dyn/cm 2 (64 µl/h).

Figure modified from Derek E. Moormeier and Kenneth Bayles. 2013. *Methods Mol Biol*

Determination of adding exogenous DNA to biofilms grown in BioFlux1000

To determine the effects of adding exogenous DNA to *S. aureus* biofilms grown in BioFlux1000, an overnight culture of *S. aureus* wild-type UAMS-1 strain was adjusted to an OD_{600} of 0.8 in TSB containing 0.25% glucose and then seeded and into microchannels of BioFlux1000 plate as described above and allowed to adhere for 1 hour at 37°C. Subsequently, an arbitrary amount of lyophilized salmon sperm DNA (1 µg ml^{-1}) resuspended in 50% TSB buffered in MOPS at a pH 7.4 or 50% TSB buffered in MOPS at a 7.4 were perfused over attached cells for 18 hours at a shear stress of 0.6 dyn/cm^2 and images were acquired in 5 minute intervals. The 6 hour time point of biofilm coverage was quantified as described below and plotted using GraphPad Prism.

Quantification of acquired BioFlux biofilm images

Using BioFlux Montage software (Fluxion Biosciences Inc.), representative brightfield and epifluorescence images were selected and adjusted to similar brightness and calibrated to 0.323445 µm/pixel. For brightfield images, a threshold was set using the Threshold Tool and Slider tool to include all dark objects (biofilm cells) within each image. The total percent area of coverage of the dark objects was designated as percent biofilm coverage and plotted over time. For epifluorescence images, a threshold was set similar to that described above to cover all light objects (fluorescent cells) in each image. The total percent area of coverage was designated percent fluorescence coverage and plotted over time. All time points were plotted in either one hour or 15-min intervals using GraphPad Prism version 5.0 for Windows (GraphPad Software, La Jolla, CA).

Isolation of eDNA from BioFlux biofilms

S. aureus wild-type (UAMS-1) and Δ*nuc* mutant (UAMS-1471) biofilms were grown with or without active DNase I (heat-inactivated 10 min at 95°C) for 4 hours in the BioFlux system in four identical channels as described above. In the output wells, 200 µl of 50 mM TES buffer (TRIS-HCl; pH 8.0, 10 mM EDTA, and 500 mM NaCl) containing 10 µg ml^{-1} chloramphenicol and 50 µg ml^{-1} proteinase K were added to inhibit cell growth in the effluent. After 4 hours of biofilm growth, excess media and effluent were removed from the input and output wells, and the output wells were wiped clean with sterile cotton tipped applicators. To extract biofilms from channels, 400 µl of 50 mM TES buffer containing 100 µg ml^{-1} proteinase K was added to the output wells and then pumped into the input wells for 10 minutes at 5.0 dyn/cm^2 and 10 minutes at 20.0 dyn/cm^2. After ensuring the biofilms had been completely removed from the channels, 350 µl of the flow through from the four replicate channels were pooled into pre-chilled tubes, centrifuged for 5 min at 14,000 rpm, and 1 ml of the supernatant was transferred to new tubes. Excess biofilm supernatants were discarded and pellets were resuspended in 1 ml of water and kept on ice until OD_{600} was determined. The eDNA from supernatants was extracted once with 1 ml of phenol:chloroform:isoamyl alcohol (25:24:1) and once with 900 µl of chloroform:isoamyl alcohol (24:1). To precipitate the eDNA, 500 µl of the aqueous phase was mixed with 50 µl of 3M potassium acetate (pH 5.0) and 1.5 ml of ice-cold 100% ethanol and then stored at -20°C overnight. The following day the precipitated DNA was collected by centrifugation (15,000 × g) for 20 min at 4°C, washed with ice-cold 75% (v/v) ethanol, air-dried at room temperature, and dissolved in 200 µl of TE buffer. To quantify the amount of eDNA present, qRT-PCR was performed on each sample in a LightCycler DNA Master SYBR Green I (Roche) using gyrase primer sets as

previously described (99), and the eDNA concentrations (ng μl^{-1}) were normalized to total OD_{600} in 1 ml of water.

Static biofilm assays

To analyze expression in a static biofilm, overnight cultures of each strain were grown and diluted to an OD_{600} of 0.05 in TSB+0.5% glucose with 1.0 µM Toto-3. Subsequently, 400 µl of each inoculum was placed in one well of an 8-chamber Lab-Tek Chambered #1.0 Borosilicate Coverglass system (Nunc, Rochester, NY). Biofilms were grown for 6 hr at which point they were imaged using an inverted Zeiss 510 Meta Confocal Laser Scanning Microscope (CLSM) with an EC Plan-Neofluar 40x/1.30 na Oil DIC M27 objective. For each sample several z-stack images were acquired using 488 nm excitation of GFP with 505-550 nm bandpass filter detection, as well as the acquisition of DIC images. Moreover, 3D reconstructions of the static biofilm images were completed using the Imaris 7.0.0 software suite (Bitplane, Saint Paul, MN).

Statistical analysis

Differences in eDNA present within the biofilms produced by different strains and under different experimental conditions were analyzed by performing a one-way ANOVA test with a Tukey post-test using GraphPad Prism (GraphPad Software, La Jolla, CA). Data for RNA quantification were analyzed using the Wilcoxon rank-sum test for non-parametric data using GraphPad Prism (GraphPad Software, La Jolla, CA).

CHAPTER III:[4]

The Control of Sae-Dependent Nuclease-Mediated Exodus during Early *Staphylococcus aureus* Biofilm Development

INTRODUCTION

Biofilms are multicellular communities of bacteria aggregated by a self-produced extracellular matrix (ECM) comprised of proteins, carbohydrates, and extracellular DNA (eDNA) (76). In pathogenic bacteria, such as *Staphylococcus aureus*, the formation of biofilms within host tissues and on implanted medical devices leads to chronic infections due to their recalcitrance to antimicrobial therapies and host immune responses (167). Indeed, *S. aureus* is a leading cause of a variety of diseases ranging from skin and soft tissue infections, to more serious illnesses including endocarditis, necrotizing pneumonia, and osteomyelitis (63, 168, 169), and its ability to form biofilms is an important determinant of virulence in many of these infections (67).

S. aureus biofilm development has previously been described to occur in three successive steps: 1) attachment, 2) accumulation/maturation, and 3) detachment/dispersal (76). The initial attachment step has been shown to involve different surface factors including teichoic acids (88), potentially through surface charge interactions, and several different surface-associated proteins that allow the cells to adhere to either polymeric surfaces or host matrix components (170, 171). As the biofilm matures, synthesis of the ECM components allows the cells to mature into three-dimensional structures (100, 148). Production of the self-produced proteases (33),

---

The majority of the work in CHAPTER III has been published in Moormeier DE, Bose JL, Horswill AH, and Bayles KW. 2014. *mBio*.

phenol-soluble modulins (PSMs) (117), and nucleases (100, 119) mediate ECM disruption and the switch from the biofilm lifestyle to planktonic growth. Indeed, adding exogenous enzymes or peptides targeting various ECM components, including DNase I (eDNA), proteinase K (proteins), synthetic PSMs (proteins), and dispersin B (polysaccharide intercellular adhesion [PIA]) have been shown to cause biofilm disassembly (100, 111, 117, 172).

In the studies described in this chapter, we examined the early stages of biofilm development and assessed the matrix composition as the biofilm matured. Unexpectedly, we identified a distinct transition in matrix composition immediately prior to a previously unrecognized exodus of a subpopulation of the biofilm, which was initiated prior to the development of tower structures. In addition, we demonstrated that exodus was dependent on the coordinated, stochastic expression of the gene encoding the secreted staphylococcal nuclease regulated by Sae two-component system. Likewise, we also showed that the coordinated stochastic expression is not only limited to nuclease, but other Sae-regulated factors as well. Together, these findings suggest the existence of a complex regulatory strategy that controls matrix composition during the early stages of biofilm development, and provide novel insight into a nuclease-mediated exodus of biofilm cells and the regulation of Sae-controlled factors.

RESULTS

Defining the early stages of S. aureus biofilm development

Investigation of *S. aureus* UAMS-1 biofilm development using a BioFlux microfluidics system revealed that primary attachment of the *S. aureus* cells is followed by rapid multiplication into a confluent “lawn” (Figure 3-1A). At about the 6-hour time

point, an apparent exodus in a subpopulation of the biofilm was observed, followed by distinct foci of robust biofilm growth, resulting in tower formation.

To further study these early events in biofilm development, we established a method to quantify the amount of biofilm coverage occurring over time (Figure 3-1B). To accomplish this, we set a threshold for dark objects (biofilm cells) within each brightfield image and measured the percent of the area that these objects covered. The data was then plotted as percent biofilm coverage versus time. As seen in Figure 3-1B, after the initial attachment of cells (0 h), there was a gradual increase in the biofilm coverage observed until about six hours, at which time the population began to contract until about 11 hours. It was during this exodus stage (at approximately 8 h) that we observed the initial signs of tower development, which proceeded until the termination of the experiment at 18 hours. To delineate between previously used terminologies of biofilm formation, the terms, “multiplication” and “exodus”, were chosen to describe these previously uncharacterized stages of biofilm development (Figure 3-1).

Protein-dependent attachment and multiplication

To characterize the early stages of biofilm development, the contributions of different ECM components to *S*. *aureus* biofilm attachment and multiplication were examined using the BioFlux system. Unlike other *S*. *aureus* strains that produce biofilms with a PIA-based matrix (92, 95), biofilms produced by both *S*. *aureus* UAMS-1 and USA300 LAC strains have been reported to be PIA-independent (113, 173). In agreement with this, we observed no difference in early biofilm formation with UAMS-1

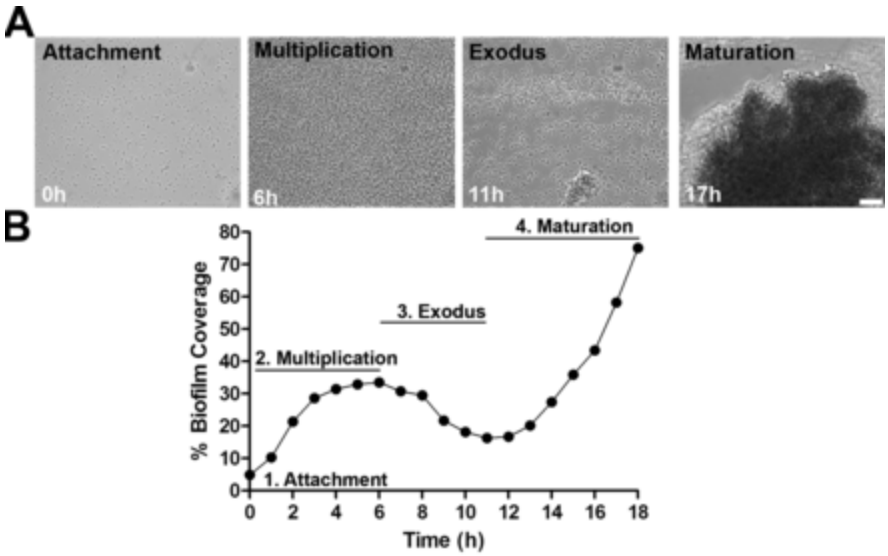

Figure 3-1 Early stages of *S. aureus* biofilm development

S. aureus UAMS-1 (wild-type) biofilms were grown in a BioFlux microfluidics system, and bright-field images were captured throughout an 18-h time course experiment. (A) Representative images at the indicated time points of a typical UAMS-1 *S. aureus* biofilm depicting four stages of development: attachment (stage 1), multiplication (stage 2), exodus (stage 3), and biofilm maturation (stage 4). Attachment of cells to the glass bottom plate is quickly followed by the multiplication of the cell population into a confluent "lawn." An exodus event after multiplication is followed by robust tower formation. Scale bar, 50 µm. (B) Quantification of typical *S. aureus* biofilm development presented as a percentage of biofilm coverage plotted versus time. Labels indicate the duration during which each biofilm stage is occurring.

Figure modified from Moormeier et al. 2014. *mBio.*

or JE2 (a USA300 LAC derivative) (Figure 3-2) mutants in which the genes encoding the PIA biosynthesis machinery have been disrupted.

In previous studies, we reported that eDNA is an important matrix component in *S. aureus* biofilm development and that modulation of the eDNA matrix has a dramatic effect on biofilm maturation (99, 100, 119, 174), including during the initial stages of development in a static assay (22). To gain a better understanding of the contribution of eDNA during early biofilm development under the flow cell conditions used in the current study, we added exogenous DNase I (0.5 Units ml^{-1}) at various time points (2-h intervals) during the biofilm attachment and multiplication phases. Similar to a recent study demonstrating DNase I insensitivity during early biofilm development (175), the addition of DNase I had no effect on the biofilm through eight hours of growth (Figure 3-3A), suggesting that the initial attachment and multiplication stages lack eDNA under these conditions or that the eDNA present in the matrix during this time is insensitive to DNase I treatment.

S. aureus produces a number of surface-associated and secreted proteins important for adherence. Considering the findings that the attachment and multiplication stages are DNase I insensitive (Figure 3-2A), we hypothesized that proteins may play a critical role in these early biofilm formation events. In agreement with this, the staphopain proteases have recently been shown to modulate *S. aureus* biofilm integrity (33). To test the role of proteins, we performed a similar experiment as above except adding proteinase K (100 µg ml^{-1}) at 2-h intervals. As shown in Figure 3-2B, the addition of proteinase K detached the entire biofilm at every time point tested. Taken together with the DNase I data, these results indicate that the attachment and multiplication stages are dependent on protein components produced by the bacteria.

In an attempt to identify specific proteins important in the attachment and multiplication stages, we utilized the BioFlux system to screen the Nebraska Transposon

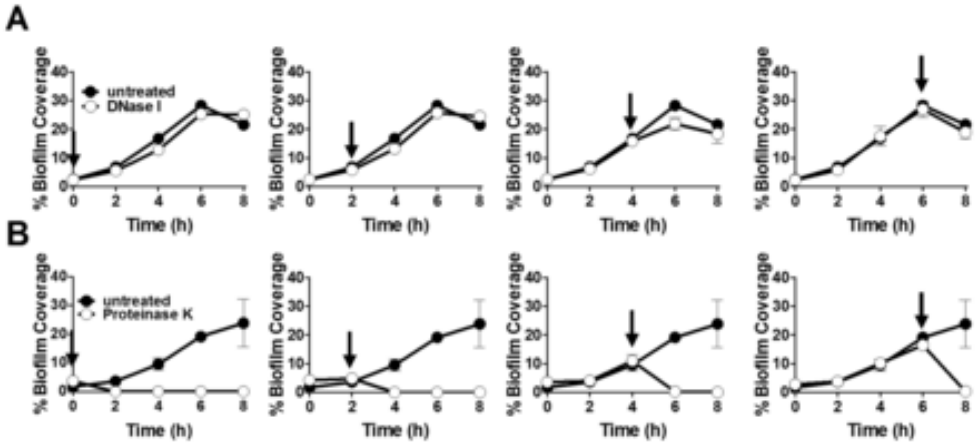

Figure 3-2 Effects of exogenous proteinase K and DNase I on biofilm attachment and multiplication

S. aureus wild-type (UAMS-1) biofilms were grown in the BioFlux system with (open circles) or without (closed circles) exogenously added (A) DNase I (0.5 U ml^{-1}) or (B) proteinase K (100 µg ml^{-1}) at 0, 2, 4, and 6 h after the initiation of the experiment. Arrows in graphs indicate time points at which either proteinase K or DNase I was added to developing biofilm. Each graph shows the mean percentage of biofilm coverage in 2-h intervals. The data represent the means from two independent experiments, each containing at least two technical replicates. Error bars show the standard errors of the means (176) from the two independent experiments.

Figure modified from Moormeier et al. 2014. *mBio.*

Mutant Library (NTML) (155) for mutants that are defective in the production of MSCRAMM proteins, including fibronectin-binding proteins A and B (FnbA and FnbB) (78), Empbp (177), clumping factors A and B (ClfA and ClfB) (81, 82), Protein A (178), elastin-binding protein (EbpS) (179), Sas family proteins (180, 181), and serine-aspartate repeat (Sdr) family proteins (79, 80). In addition, we examined a *srtA* mutant, which is defective in the processing of several LPXTG-motif containing MSCRAMM proteins into the cell wall (182). However, none of these mutants exhibited observable changes in biofilm development when grown in the BioFlux system (Table 3). We also selected mutants defective in the production of secreted proteins such as the as α- and β-hemolysins, which have been previously shown to play a role in biofilm development (108, 183) (Table 3). Again, no noticeable differences in biofilm formation were observed. Finally, we also tested an *atlA* mutant, in which the primary autolysin is disrupted, for early biofilm defects. Consistent with previous findings (104), we saw limited cell attachment and no biofilm multiplication (Figure 3-3) using this strain, suggesting its role in these early stages of biofilm formation. In addition, we added PAS, an autolysis inhibitor, in two hour time points to developing UAMS-1 wild-type biofilms in the BioFlux100 and saw abolishment of the biofilm development (Figure 3-4). Overall, these results support a role for Atl in biofilm attachment and/or multiplication, but fail to identify a role for other cell surface and secreted proteins in these processes, although the requirement for a combination of proteins cannot be ruled out.

Exodus is mediated by staphylococcal nuclease

Quorum sensing is the coordinated expression of genes in response to cell density. In *S. aureus*, it is accomplished through the Agr system, which contributes to biofilm dispersal after tower development through activation of proteases and PSMs (111, 117). Thus, we hypothesized that this exodus stage is also controlled by the Agr

Table 3. NTML mutants screened for involvement in early biofilm development

NTML [a]NE #	*S. aureus* USA300_FPR3757 Locus	[b]Gene Name	[c]Putative Protein	[d]Biofilm Phenotype
NE186	SAUSA300_2441	***fnbA***	**Fibronectin binding protein A**	+
NE728	SAUSA300_2440	***fnbB***	**Fibronectin binding protein B**	+
NE543	SAUSA300_0772	***clfA***	**Clumping factor A**	+
NE391	SAUSA300_2565	***clfB***	**Clumping factor B**	+
NE1558	SAUSA300_0774	***empbp***	**Secretory extracellular matrix and plasma binding protein**	+
NE1561	SAUSA300_1370	***ebps***	**Cell surface elastin binding protein**	+
NE286	SAUSA300_0113	***(spa)***	**Immunoglobulin G binding protein A precursor**	+
NE56	SAUSA300_1702	***(sasC)***	**Cell wall surface anchor family protein**	+
NE825	SAUSA300_2436	***(sasG)***	**Putative cell wall surface anchor family protein**	+
NE33	SAUSA300_2589	-	**LPXTG-motif cell wall surface anchor family protein**	+
NE851	SAUSA300_0883	-	**Putative surface protein**	+
NE1	SAUSA300_1327	-	**Cell surface protein**	+
NE1787	SAUSA300_2467	***srtA***	**Sortase A**	+
NE1363	SAUSA300_1034	***srtB***	**Sortase B**	+
NE460	SAUSA300_0955	***atlA***	**Autolysin**	-
NE37	SAUSA300_2600	***icaA***	**N-glycosyltransferase**	+
NE1167	SAUSA300_2601	***icaB***	**Intercellular adhesion protein B**	+
NE766	SAUSA300_2602	***icaC***	**Intercellular adhesion protein C**	+
NE302	SAUSA300_0152	***cap5A***	**Capsular polysaccharide biosynthesis protein Cap5A**	+
NE1235	SAUSA300_0156	***cap5E***	**Capsular polysaccharide biosynthesis protein Cap5E**	+
NE1286	SAUSA300_2598	***cap1A***	**Capsular polysaccharide biosynthesis protein Cap1A**	+
NE67	SAUSA300_2573	***isaB***	**Immunodominant antigen B**	+
NE1746	SAUSA300_2088	***luxS***	**S-ribosylhomocysteinase**	+
NE1354	SAUSA300_1058	***(hla)***	**Alpha-hemolysin**	+
NE1261	SAUSA300_1973	***(hlb)***	**Truncated-beta hemolysin**	+

Colors indicate functional group: red, LPXTG-motif surface proteins; green, LPXTG-motif protein processing; grey, autolysin; blue, extracellular polysaccharide biosynthesis; orange, other secreted and surface proteins

[a] NE# are obtained from Nebraska Transposon Mutant Library (NTML) website (http://app1.unmc.edu/fgx/)

[b] Gene names are from NTML website. (gene name) indicates gene that is not annotated in the USA300_FPR3757 genome, but replaced with a gene name annotation from other *S. aureus* genomes with similar gene identity. – indicates a putative/hypothetical protein not yet annotated.

[c] Putative proteins as described on NTML website.

[d] + indicates no changes in early *S. aureus* biofilm development (0-8hr) compared to JE2 wild-type. – indicates early *S. aureus* biofilms defective in either biofilm attachment or accumulation (0-8 hr).

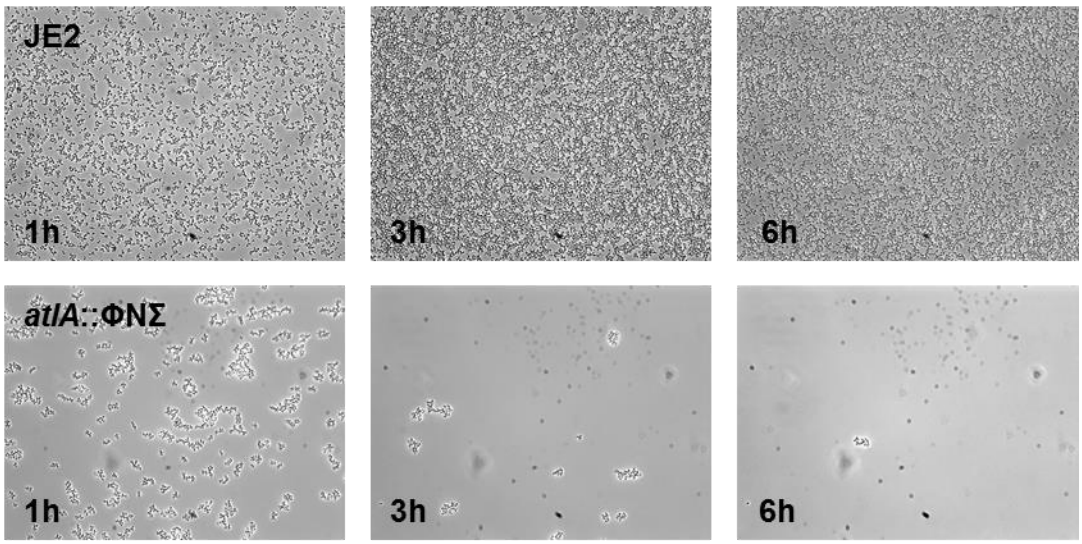

Figure 3-3 Effect of USA300 JE2 *atlA* mutant on early biofilm formation

The *S. aureus* wild-type (USA300 LAC JE2) and *atlA*::ΦNΣ mutant derivative strains were grown in the BioFlux system. Bright-field microscopic images were acquired in 5-min intervals at ×200 magnification. Images at 1 h, 3h, and 6 h are representative of multiple experiments. Note the clumping in the *atlA*::ΦNΣ mutant and the lack of biofilm at 6 h. Scale bar, 50 µm.

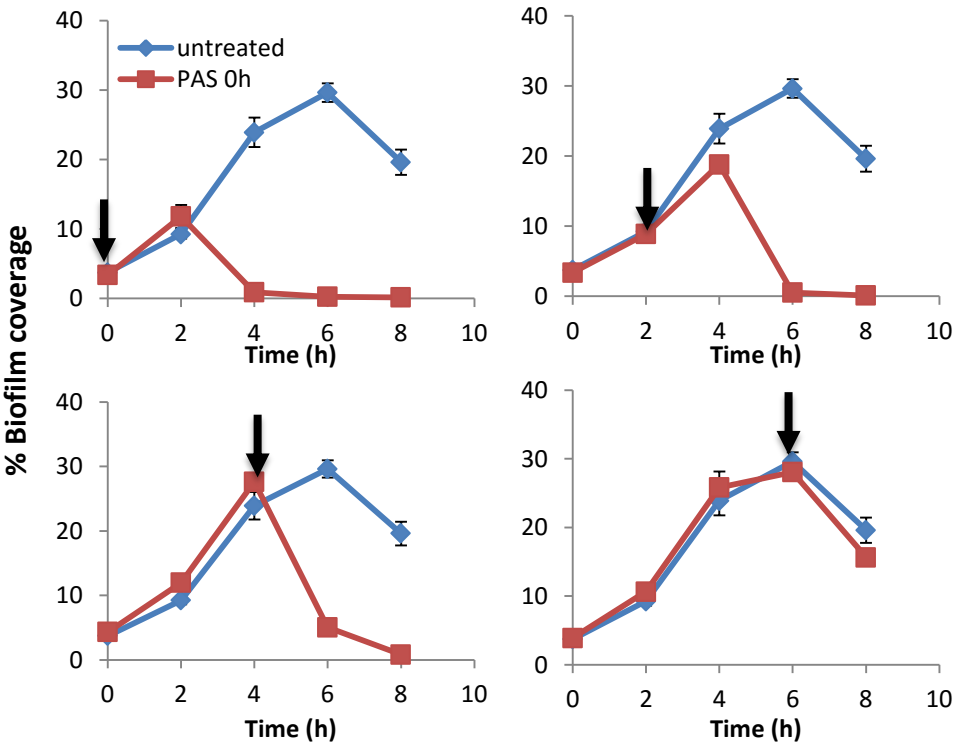

Figure 3-4 Addition of PAS to UAMS-1 wild-type biofilms inhibits proper biofilm development

S. aureus wild-type (UAMS-1) biofilms were grown in the BioFlux system with (184) or without (blue) exogenously added PAS (500 µg ml^{-1}) at 0, 2, 4, and 6 h after the initiation of the experiment. Arrows in graphs indicate time points at which PAS was added to developing biofilm. Each graph shows the mean percentage of biofilm coverage in 2-h intervals. The data represent the means from two independent experiments, each containing at least two technical replicates. Error bars show the standard errors of the means (176) from the two independent experiments.

quorum-sensing system. To test this, we obtained an *agr::tet* mutant (UAMS-155) derivative of UAMS-1 and observed its ability to form a biofilm as described above. Interestingly, although the *agr::tet* mutant exhibited increased initial attachment and biofilm multiplication, exodus of a subpopulation was still clearly evident (Figure 3-5), indicating that this event is largely independent of the Agr system. These results were not specific to this strain as an *agrA::ΦNΣ* transposon mutant of JE2 displayed a similar pattern of exodus during this time period (Figure 3-6). Since previous studies have demonstrated that the Agr P3 promoter is activated in a subpopulation of cells in *S. aureus* biofilms (110, 117), we also tested a GFP reporter that was driven by the Agr-dependent P3 promoter. Consistent with the lack of involvement of *agr* in this exodus event, no P3 promoter activity was detected in the UAMS-1 strain until 13 hours of biofilm growth, where expression was primarily limited to the towers (Figure 3-7) as previously observed (110). Collectively, these findings indicate that the exodus of the biofilm population observed in these assays are independent of the Agr quorum-sensing system, and that this event is distinct from the previously described Agr-dependent dispersal of cells that occurs after tower formation.

S. aureus synthesizes a myriad of extracellular proteins, the stability and processing of which are modulated by ten secreted proteases (34). Our observation that proteinase K disrupted biofilms suggests that *S. aureus* secreted proteases may play a role in the biofilm exodus event. Indeed, recent studies have demonstrated that the staphopain proteases can modulate biofilm integrity (33). However, a USA300 LAC derivative deficient in all ten secreted proteases (AH1919) (156) showed no defects in exodus of the biofilm subpopulation when compared to its parental strain (AH1263) (Figure 3-8), suggesting that this event is independent of these proteases. In this regard, several reports have demonstrated that deletion of the secreted nuclease (Nuc) in *S.*

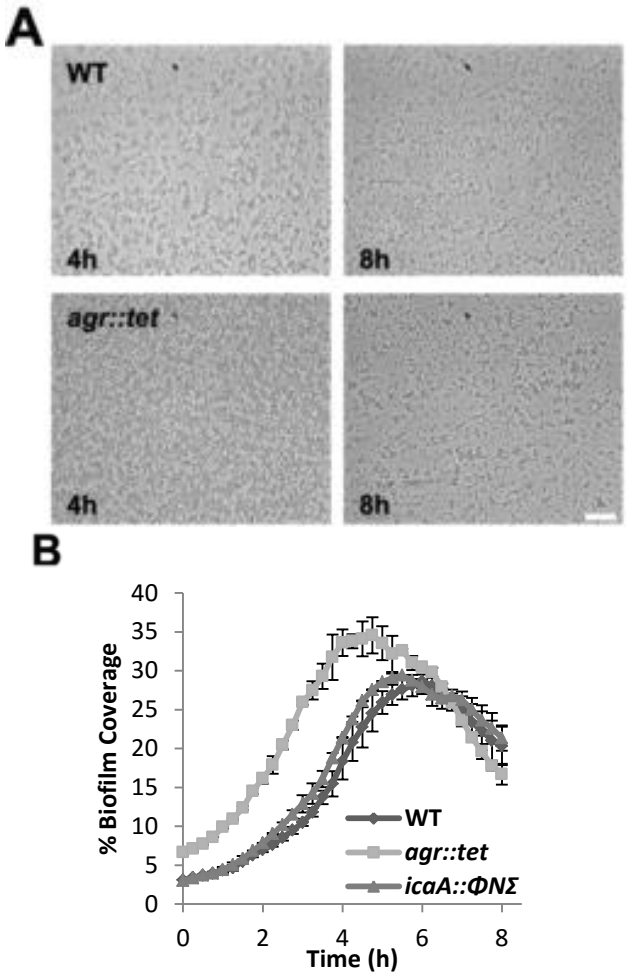

Figure 3-5 Effect of UAMS-1 *agr* and *icaA* mutations on early biofilm development

The *S. aureus agr* and *icaA* mutant strain, UAMS-155 (*agr*::*tet*) and KB8037 (*icaA:: ΦNΣ,* respectively, were inoculated in parallel with UAMS-1 (wild type) in the BioFlux system and allowed to form a biofilm for 18 h (A) Images selected at 4 h and 8 h are representative of wild-type (185) and *agr*::*tet* biofilms from multiple experiments. Scale bar, 50 µm. (B) The graph depicts the percentage of biofilm coverage in 15-min intervals of wild-type (185), *agr*::*tet,* and *icaA*:: *ΦNΣ* mutants biofilms over 8 h of growth. The data represent the means from two independent experiments, each containing three technical replicates. Error bars show the SEM from the two independent experiments.

Figure modified from Moormeier et al. 2014. *mBio.*

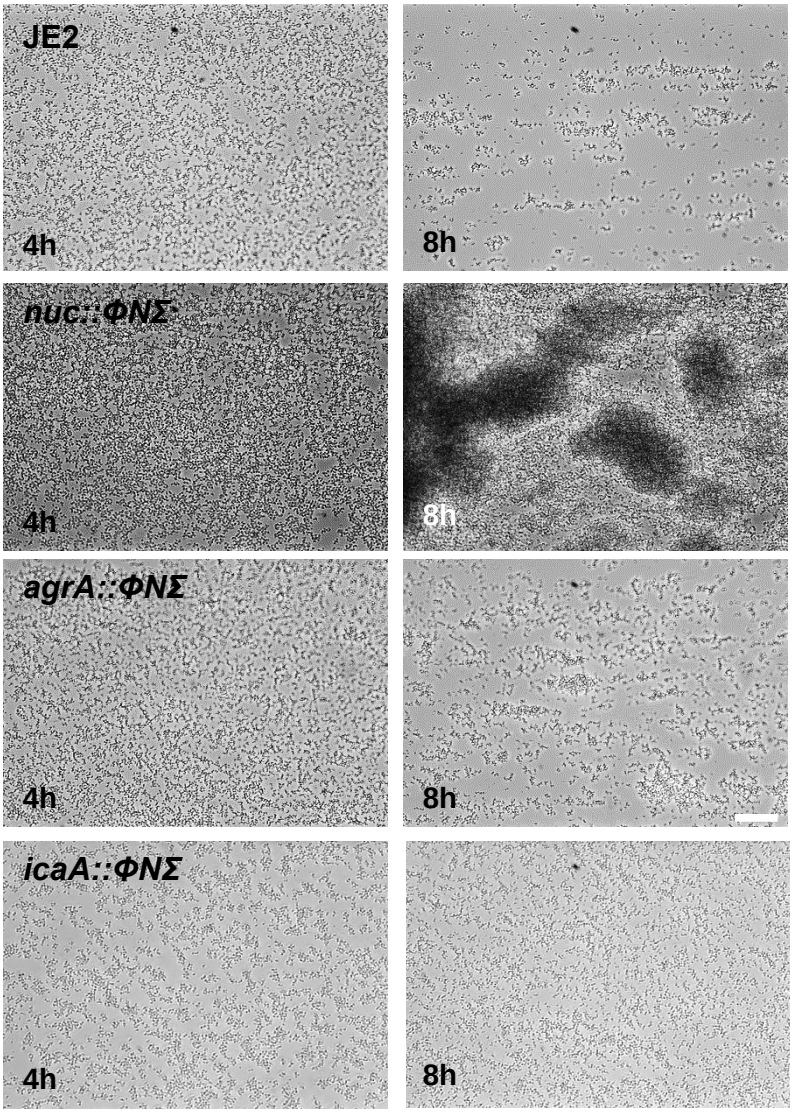

Figure 3-6 Early biofilm development in the *S. aureus* USA300 LAC JE2 strain with *agrA*, *nuc,* and, *icaA* mutant derivatives

The *S. aureus* wild-type (USA300 LAC JE2), *agrA*::ΦNΣ, *nuc*::ΦNΣ, and *icaA*::ΦNΣ mutant derivatives were grown in the BioFlux system. Bright-field microscopic images were acquired in 5-min intervals at ×200 magnification. Images at 4 h and 8 h are representative of multiple experiments. Scale bar, 50 µm.

Figure modified from Moormeier et al. 2014. *mBio.*

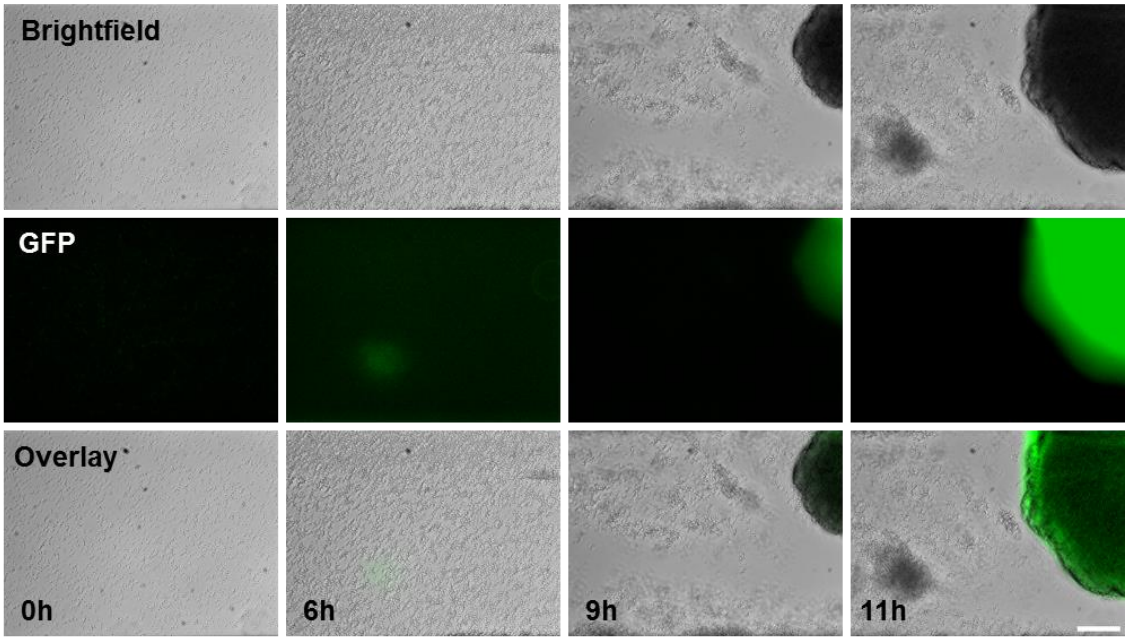

Figure 3-7 Expression of Agr-dependent P3 promoter fusion in biofilm formation

UAMS-1 wild-type *S. aureus* cells containing the Agr P*3*::*gfp* reporter (pKH4) plasmid were inoculated into a BioFlux microfluidic system and allowed to form a biofilm within a flow shear environment at a flow rate of 64 µl/h for a total of 18 h. Bright-field and epifluorescence microscopic images were collected at 5-min intervals at ×200 magnification. The images presented were taken from the complete set of 217 images spanning 0 to 11 h and illustrate typical tower development and GFP expression observed in multiple experiments. Note the lack of P3 expression during early biofilm development (<11 h), and the P3 induction in the large tower. The scale bar represents 50 µm.

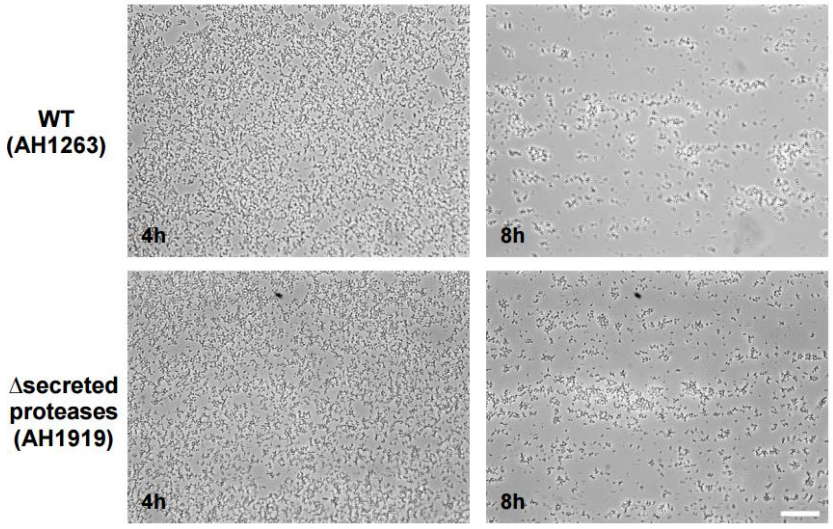

Figure 3-8 Effect of ten major secreted proteases on early biofilms

The *S. aureus* wild-type strain (AH1263) and a mutant derivative lacking all 10 major secreted proteases (AH1919) were grown in the BioFlux system. Bright-field microscopic images were acquired in 5-min intervals at ×200 magnification. Images at 4 h and 8 h are representative of three independent experiments with at least two technical replicates. Scale bar, 50 µm.

Figure modified from Moormeier et al. 2014. *mBio.*

aureus causes an increase in biofilm formation as a result of decreased eDNA degradation in the biofilm ECM (100, 119, 122). Based on this, we hypothesized that exodus of the biofilm population is mediated by the function of staphylococcal nuclease in the degradation of eDNA. To test this, we cultured biofilms produced by the wild-type (UAMS-1) and Δ*nuc* mutant (UAMS-1471) strains harboring a 'leaky' anhydrotetracycline (aTet)-inducible expression vector (pRMC2-*nuc*) driving low-level *nuc* transcription, and then quantified the coverage of the developing biofilm as described above. In support of a role for nuclease in the exodus event, the Δ*nuc* mutant containing the empty vector (pRMC2) failed to initiate exodus, which resulted in considerably thicker biofilms compared to the wild-type harboring either pRMC2 or pRMC2-*nuc* (Figure 3-9A). Quantification of the biofilm over the first eight hours showed considerably more biofilm present past six hours of growth in the Δ*nuc* mutant containing pRMC2 and a reversion to wild-type levels of exodus when grown with pRMC2-*nuc* (Figure 3-9B). To determine if this phenomenon was conserved in another *S. aureus* strain, we also grew wild-type JE2 and its *nuc* mutant derivative (*nuc*::*ΦNΣ*) biofilms in parallel. Like the UAMS-1 strain, the *nuc*::*ΦNΣ* mutant demonstrated biofilm growth that lacked the exodus event, accumulating to a higher cell density over time compared to the wild-type JE2 strain (Figure 3-6). Together, these data demonstrate that the *S. aureus* secreted nuclease plays a major role in the exodus of the biofilm population prior to tower formation and suggests nuclease insensitivity before the exodus event occurs.

To determine if the exodus defect in the Δ*nuc* mutant could be restored by the addition of exogenous nuclease, we grew wild-type, Δ*nuc* mutant, and *nuc* complement biofilms with or without media supplemented with DNase I (0.5 Units ml^{-1}) starting at the 0-h time point. As shown in Figure 3-10, the addition of DNase I had little effect on biofilm multiplication or exodus in the wild-type strain. In contrast, the presence of DNase I caused exodus of the Δ*nuc* mutant biofilm, but not until approximately six hours

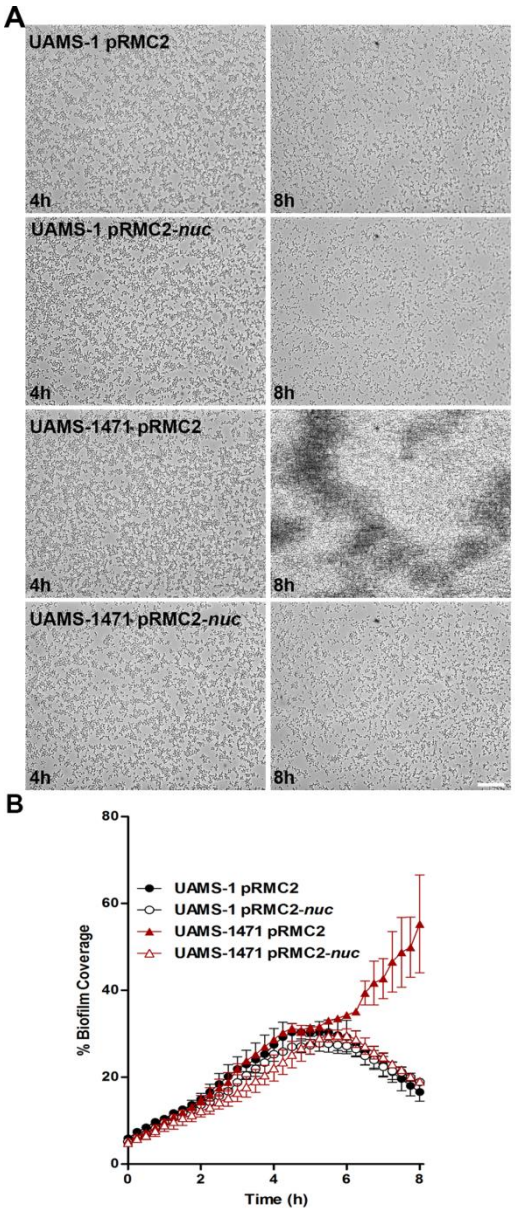

Figure 3-9 Exodus requires staphylococcal nuclease

Biofilms of the *S. aureus* wild-type (UAMS-1) and Δ*nuc* mutant (UAMS-1471) containing pRMC2 or pRMC2-*nuc* were grown in the BioFlux system. (A) Selected bright-field images at 4 h and 8 h are representative of bioflims of the wild-type (UAMS-1) or Δ*nuc* mutant (UAMS-1471) containing pRMC2 or pRMC2-*nuc* from multiple experiments. Scale bar, 50 µm. (B) The graph shows the mean percentage of biofilm coverage in 15-min intervals of biofilms of the wild-type (UAMS-1) and Δ*nuc* mutant (UAMS-1471) containing pRMC2 or pRMC2-*nuc* over 8 h of growth. The data represent the means from two independent experiments, each containing at least three technical replicates. Error bars show the SEM from the two independent experiments.

Figure modified from Moormeier et al. 2014. *mBio.*

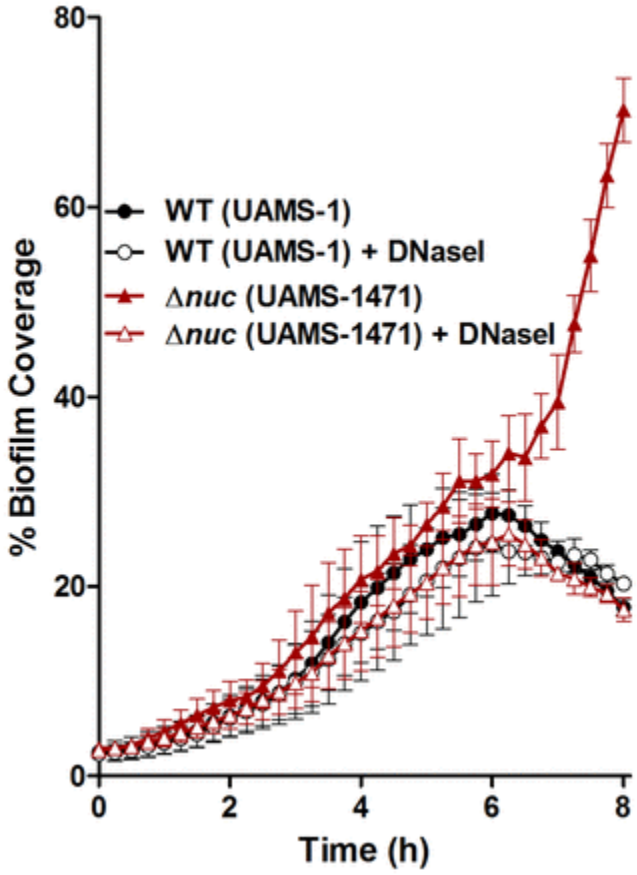

Figure 3-10 Functional complementation of the *nuc* mutant biofilm phenotype by addition of DNase I

S. aureus wild-type (UAMS-1) and Δ*nuc* mutant (UAMS-1471) cells were grown in the BioFlux with or without DNase I (0.5 U ml^{-1}). The graph shows the mean percentage of biofilm coverage in 15-min intervals of wild-type (185) and Δ*nuc* biofilms grown in the presence or absence of DNase I. The data represent the means from two independent experiments, each containing three technical replicates. Error bars show the SEM from the two independent experiments.

Figure modified from Moormeier et al. 2014. *mBio.*

of biofilm development when the exodus event is normally observed (Figure 3-10). To assess whether nuclease insensitivity prior to six hours was a result of the absence of eDNA in the matrix during this time, we isolated eDNA at four hours from wild-type (UAMS-1) and Δ*nuc* mutant (UAMS-1471) biofilms grown in the absence or presence of active DNase I (0.5 Units ml^{-1}). Although eDNA is clearly detectable during the multiplication stage and there is a trend toward differences in the levels of eDNA present between the DNase I treated and untreated biofilms, both wild-type and Δ*nuc* mutant biofilms cultured with and without DNase I showed no significant differences in eDNA levels (Figure 3-11) suggesting that there is some protection from the activity of this nuclease by other components of the biofilm matrix.

Biofilm exodus is preceded by nuclease expression

The data generated so far demonstrates that biofilm exodus is reproducibly initiated in a nuclease-dependent manner at approximately six hours after the initiation of biofilm development. Based on these results, we hypothesized that *nuc* expression would precede biofilm exodus at approximately six hours. To test this, the UAMS-1 and JE2 strains containing a previously constructed *nuc*::*gfp* promoter fusion plasmid (pCM20) were studied to determine the temporal expression of *nuc* during biofilm development. As anticipated, *nuc* expression was induced just prior to the exodus event at six hours, albeit in only a subpopulation (<1%) of the cells (Figure 3-12). To quantify the induction of *nuc* expression, we set a threshold that would enumerate all of the light objects (fluorescent cells) in each image and plotted this as percent fluorescence coverage over time. As seen in Figure 3-13, *nuc* expression was initially observed at three hours and maximally expressed near five hours of biofilm growth, preceding biofilm

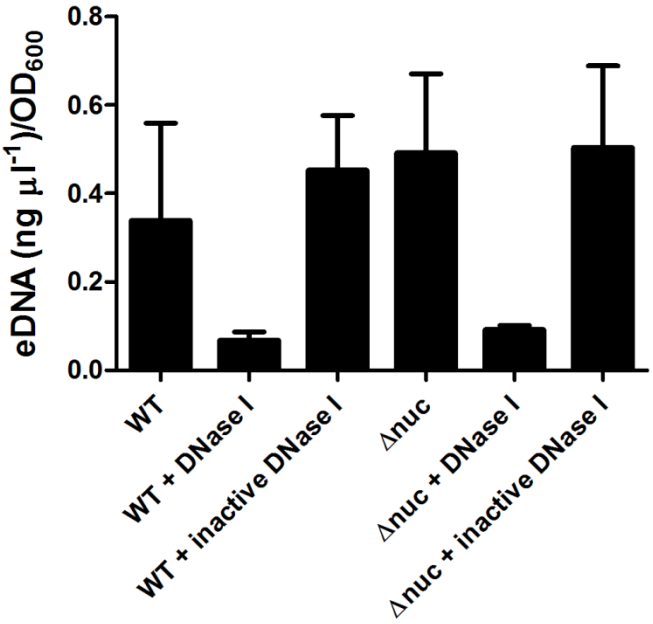

Figure 3-11 Quantification of eDNA isolated from BioFlux biofilms

S. aureus wild-type (UAMS-1) and Δ*nuc* mutant (UAMS-1471) biofilms were grown with or without active DNase I (heat-inactivated 10 min at 95°C) for 4 hours in the BioFlux system in four identical channels. After 4 hours of biofilm growth, eDNA was isolated as described in Materials and Methods. The data represent the means from two independent experiments, each containing three technical replicates. Error bars show the SEM from the two independent experiments.

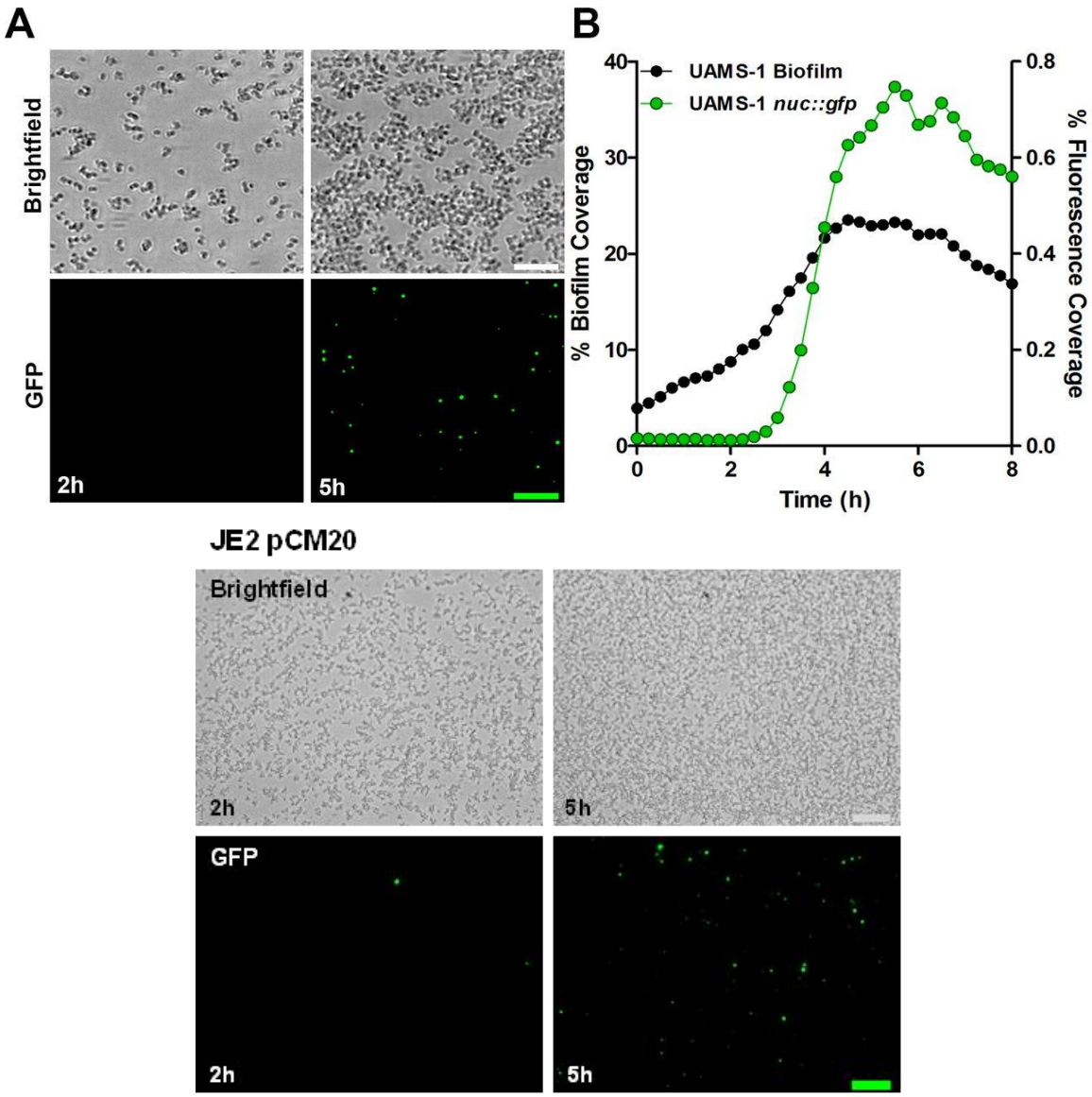

Figure 3-12 Expression of *nuc* precedes exodus of a biofilm subpopulation

S. aureus wild-type UAMS-1 and JE2 cells containing the *nuc*::*gfp* reporter plasmid (pCM20) were grown in the BioFlux system. Bright-field and epifluorescence microscopic images were acquired in 5-min intervals at ×200 magnification. (A) Bright-field and epifluorescence (GFP) images at 2 h and 5 h are representative of multiple experiments of UAMS-1 pCM20. Scale bar, 20 µm. (B) The plot depicts biofilm growth as the mean percentage of UAMS-1 pCM20 biofilm coverage and the *nuc*-expressing cells as the mean fluorescence coverage in 15-min intervals over 8 h of growth. The data represent the means from two independent experiments, each containing at least two technical replicates. Error bars were omitted for clarity.

Figure modified from Moormeier et al. 2014. *mBio.*

exodus. These results indicate that both temporal and stochastic regulatory mechanisms control *nuc* promoter activity during biofilm development.

The Sae two-component regulatory system controls nuc-mediated exodus

Previous results have shown that the Sae two-component system regulates nuclease expression (48). Hence, to gain insight into the regulation of the exodus event, we tested wild-type AH1263 (USA300 LAC derivative) and its *saeQRS::spc* mutant (AH1558) for biofilm development and *nuc* expression. Consistent with its role as a positive regulator of secreted nuclease, the *saeQRS::spc* mutant biofilm developed in a way that was similar to a *nuc* mutant, lacking biofilm exodus and accumulating to a high cell density (Figure 3-13). However, the *saeQRS::spc* mutant also exhibited an apparent decrease in the rate of biofilm multiplication suggesting a role for this regulator in the production of some factor(s) important in this process. Additionally, the *saeQRS::spc* mutant demonstrated much reduced *nuc* expression compared to wild-type AH1263 (Figure 3-13), indicating that the temporal and/or stochastic control of *nuc* expression requires the Sae regulatory system.

To continue to dissect the function that the Sae system has in regulating *nuc* expression and biofilm development, we obtained clean deletion mutations in *saeP*, *saeQ*, *saeS*, and *saePQRS* in the AH1263 strain background and moved the P*nuc::*gfp (pCM20) fluorescent reporter fusion into these genetic backgrounds. To determine if these mutations had any effect on growth, we grew them aerobically for 24 hours in TSB containing 0.25% glucose. Under these growth conditions, we saw no major growth defect demonstrating that these mutations do not have a direct function in regulating expression of genes involved in growth (Figure 3-14). To investigate the effects of the *sae* mutations on biofilm and *nuc* expression, we cultivated these *sae* mutants containing pCM20 in the BioFlux1000 to allow for biofilm formation.

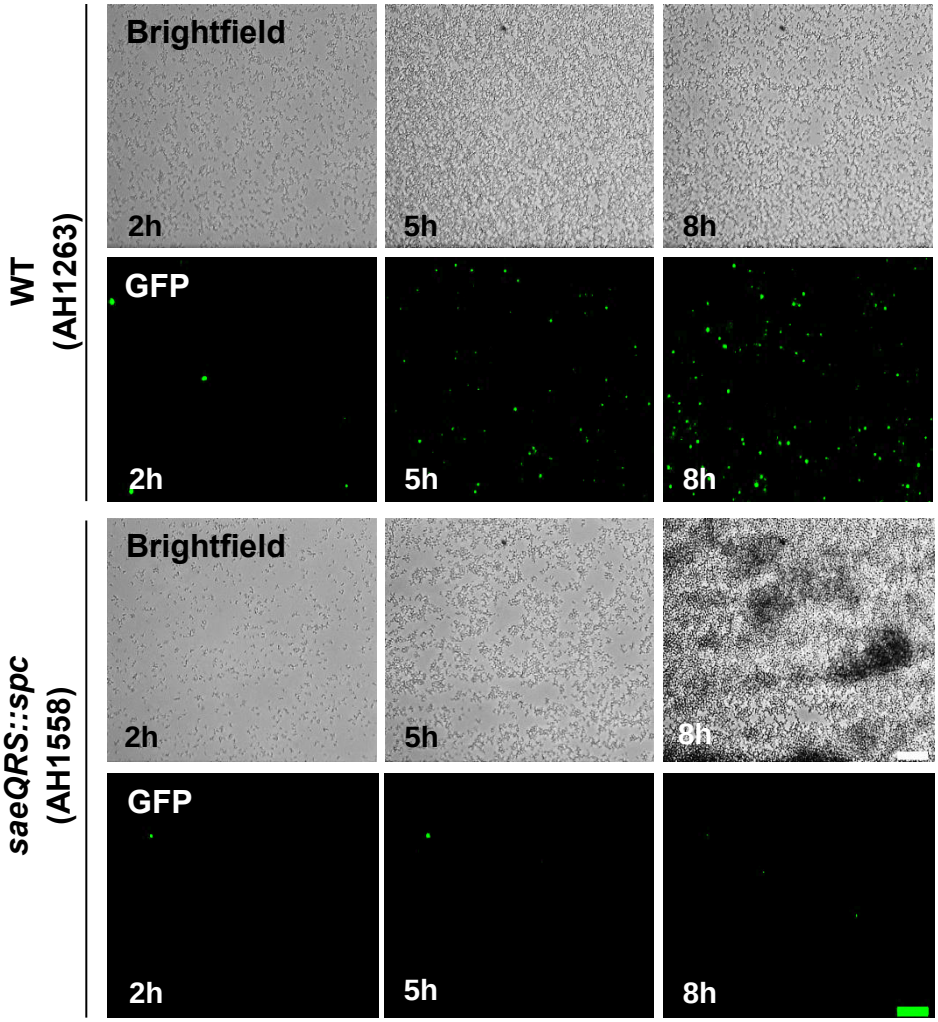
WT (AH1263)
saeQRS::spc (AH1558)
Brightfield
GFP
2h
5h
8h

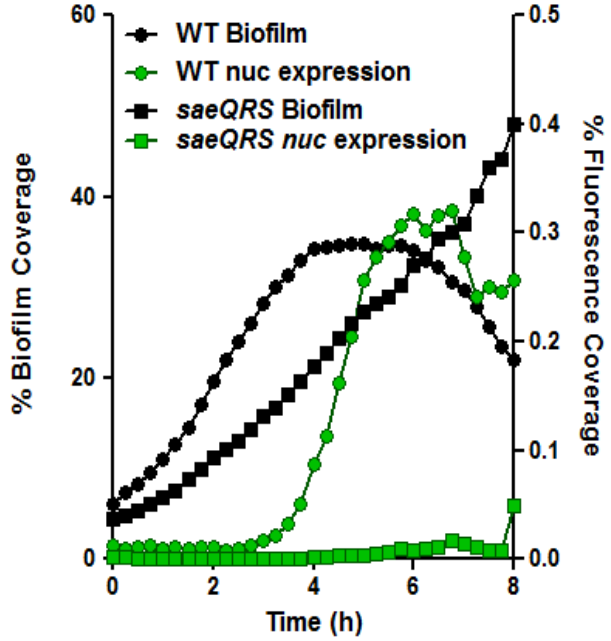
WT Biofilm
WT nuc expression
saeQRS Biofilm
saeQRS nuc expression
% Biofilm Coverage
% Fluorescence Coverage
Time (h)
0
20
40
60
0.0
0.1
0.2
0.3
0.4
0.5
0
2
4
6
8

Figure 3-13 Nuclease-mediated exodus is regulated by Sae

S. aureus wild-type (AH1263) and *saeQRS*::*spc* mutant (AH1558) strains carrying the *nuc*::*gfp* reporter plasmid (pCM20) were grown in the BioFlux system. Bright-field and epifluorescence (GFP) microscopic images were acquired in 5-min intervals at ×200 magnification. Images at 2, 5, and 8 h are representative images from two independent experiments. Scale bar, 50 µm. The plot depicts biofilm growth as the mean percentage of biofilm coverage and the *nuc*-expressing cells as the mean fluorescence coverage in 15-min intervals over 8 h of growth. The data represent the means from two independent experiments, each containing at least two technical replicates. Error bars were omitted for clarity.

Figure modified from Moormeier et al. 2014. *mBio.*

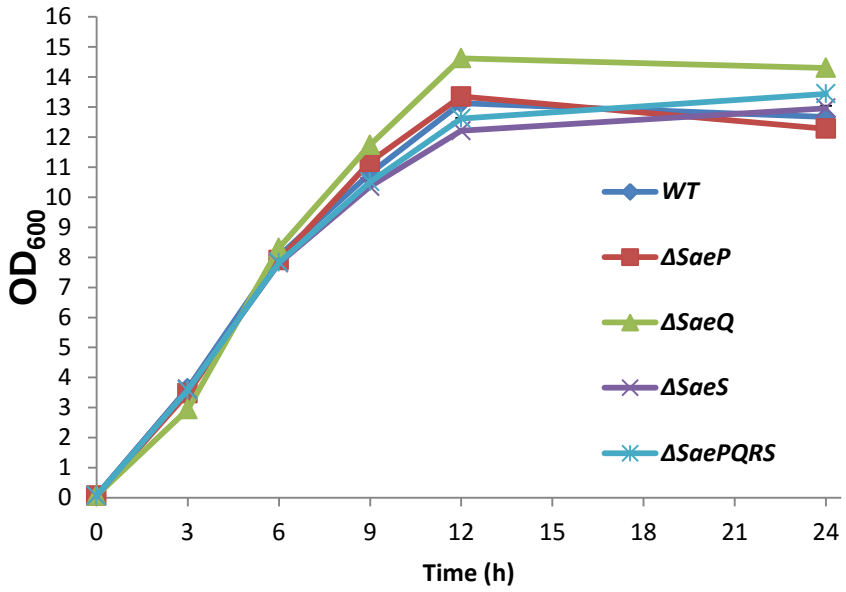

Figure 3-14 Growth analysis of *sae* mutants containing pCM20 grown planktonically

S. aureus AH1263 (185) and *sae* mutants containing P*nuc::*gfp reporter fusion (pCM20) were grown planktonically to determine effect on growth. Cultures were grown for 24 hours with shaking at 250 rpm at 37°C using a 10:1 flask to volume ratio. Subsequently, supernatants were taken at 0, 3, 6, 9, 12 and 24 hours and the OD_{600} were measured and plotted over time**.** Data represents two independent experiments performed in duplicate.

Similar to the *sae::spc* mutant described before (Figure 3-13), we saw little to no *nuc* expression and an abrogated exodus stage in the Δ*saeS* and Δ*saePQRS* mutants (Figure 3-15). In addition, the Δ*saeQ* mutant showed an intermediate phenotype in *nuc* expression when compared to AH1263 and the Δ*saeP* strain (Figure 3-15). Interestingly, however, the Δ*saeP* mutant had an unusual phenotype. While there was little to no *nuc* expression during the first hours of biofilm development in a Δ*saeP* mutant biofilm, at around 3-3.5 hours, instead of only a subpopulation of *nuc* expressing cells like in AH1263 biofilm (Figure 3-13), the entire cell population expressed *nuc* (Figure 3-15). Interestingly, although the entire cell population is expressing *nuc*, there was no effect on the exodus stage itself (Figure 3-15). To determine if stochastic expression is observed in planktonic cells, we grew AH1263 and the *sae* mutant derivatives containing the P*nuc*::gfp fluorescent reporter fusions for 3 hours in shaking flasks and then performed fluorescence-activated cell sorting (FACS). Unlike the subpopulations of cells expressing *nuc* in the parental and Δ*saeQ* strains during biofilm development, this effect is lost during planktonic growth. Indeed, >98% of the cells are expressing *nuc* in all of the strains except for the Δ*saeS* and Δ*saePQRS* mutants, which showed very little *nuc-gfp* positive cells (Figure 3-16). These results suggest that the stochastic expression of *nuc* is a biofilm-specific phenotype not seen in planktonically growing cells. Collectively, these data further demonstrate that the Sae system regulates the exodus stage of biofilm development in a much more complex way than previously thought.

Several different stimuli have been shown to affect the induction of the Sae system including SDS, H_2O_2, low pH, and sub-inhibitory concentrations of antibiotics and α-defensin (HNP-1) (157, 186-189), yet, the exact molecular mechanism in which the Sae system is activated is not known.

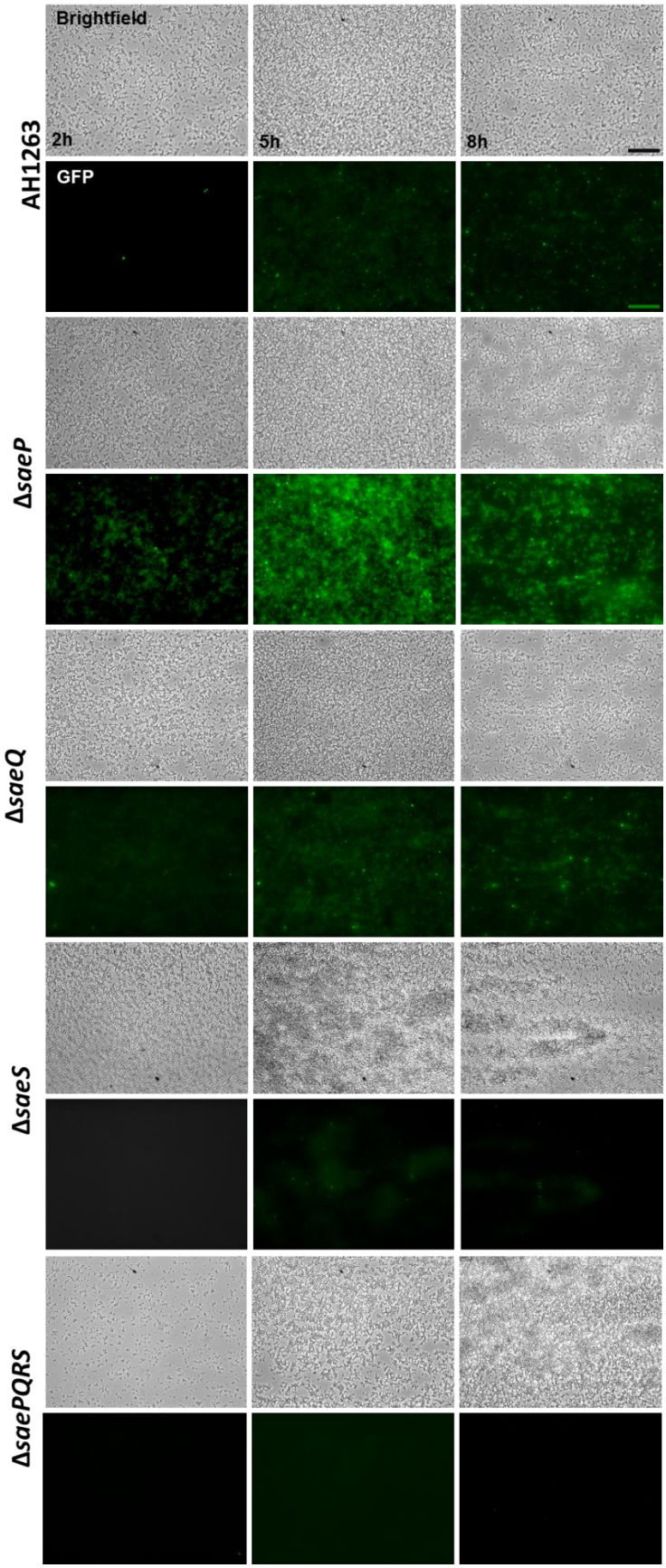
Brightfield
2h
5h
8h
GFP
AH1263
ΔsaeP
ΔsaeQ
ΔsaeS
ΔsaePQRS

Figure 3-15 Effect of Sae mutations on *nuc* expression and early biofilm development

S. aureus wild-type AH1263, Δ***saeP,*** Δ***saeQ,*** Δ***saeS,*** and Δ*saePQRS* mutant derivative strains carrying the *nuc*::*gfp* reporter plasmid (pCM20) were grown in the BioFlux system. Bright-field and epifluorescence (GFP) microscopic images were acquired in 5-min intervals at ×200 magnification. Images at 2, 5, and 8 h are representative images from two independent experiments. Scale bar, 50 µm.

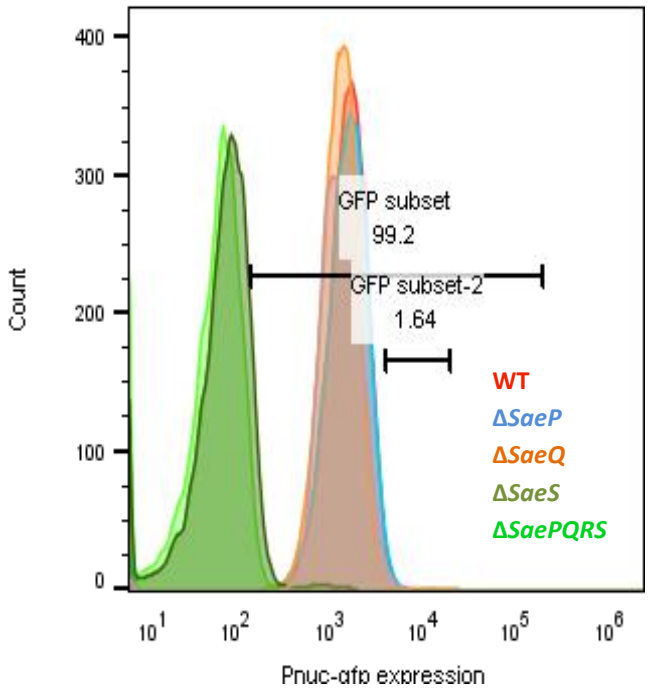

Figure 3-16 FACS analysis of *nuc* expressing cells grown planktonically

S. aureus AH1263 (185) and *sae* mutants containing P*nuc::*gfp reporter fusion (pCM20) were grown planktonically for 4 hours with shaking at 250 rpm at 37°C using a 10:1 flask to volume ratio. Cells were then washed with 1x PBS and 10,000 events of each culture sample were counted using fluorescence-activated cell sorting (FACS) to determine number of GFP-positive cells. Data was plotted using FlowJo software and is representative of three biological replicates.

Additionally, most of these stimuli are not found in our *in vitro* biofilm conditions. Hence, we wanted to continue to evaluate how the Sae system is activated in *S. aureus* biofilms.

Effect of exogenous DNA on planktonic S. aureus cells

Initial data generated from the Horswill laboratory demonstrates that the extracellular lipoprotein SaeP binds eDNA (unpublished data from Horswill lab). Given that the Sae system controls nuclease which degrades eDNA within a biofilm, we hypothesized that eDNA may be the signal that the Sae system is sensing to control expression of nuclease. Therefore, we added exogenous salmon sperm DNA to a wild-type strain containing the P*nuc*-gfp reporter fusion biofilms grown in the BioFlux1000 to see if it would have an effect on *nuc* expression. To our surprise, the exogenously added DNA essentially wiped out the biofilms (Figure 3-17) making it impossible to evaluate its effect on *nuc* expression and suggesting that the additional DNA has an inhibitory effect on *S. aureus* biofilm development. Due to the inhibitory effect of exogenous DNA on *S. aureus* biofilm development, we decided to evaluate the influence that exogenous DNA may have on *nuc* expression in planktonic cells. Thus, we added increasing percentages (w/v) of salmon sperm DNA to planktonically growing wild-type cells containing the P*nuc*::gfp reporter fusion. Surprisingly, we saw an indirect relationship between increasing amounts of DNA and decreasing amounts of nuclease expression at 3 hours of growth (Figure 3-18). However, at six hours of growth, the effect of added DNA on *nuc* expression was not as strong (Figure 3-19). Interestingly, we also saw that the addition of the 2% DNA caused a slight growth defect in wild-type cells (data not shown). Hence, when we sought to determine if a Δ*saeP* mutant would abrogate the effect of adding exogenous DNA seen in wild-type cells, we excluded 2% DNA in further analyses.

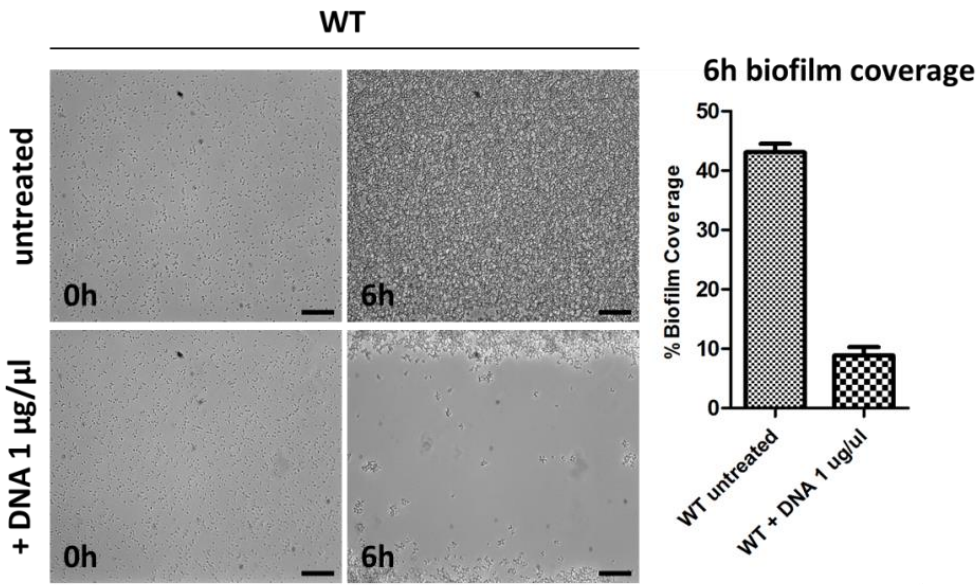

Figure 3-17 Effect of exogenous DNA on biofilm development

S. aureus wild-type (UAMS-1) cells were grown in the BioFlux with or without salmon sperm DNA (1 µg ml^{-1}). The graph shows the mean percentage of biofilm coverage in at six of UAMS-1 wild-type (185) biofilms grown in the presence or absence of DNA. The data represent the means from two independent experiments, each containing at least two technical replicates. Error bars show the SEM from the two independent experiments.

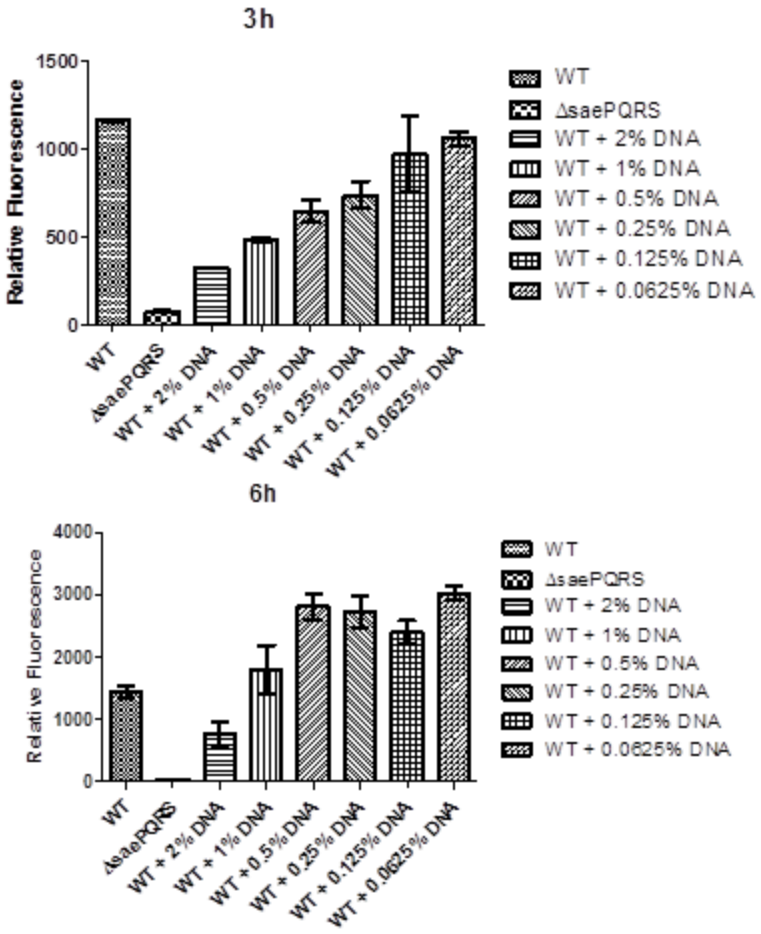

Figure 3-18 Effect of exogenous DNA on *nuc* expression in planktonic AH1263 wild-type cells

AH1263 wild-type and Δ*saePQRS* strains containing P*nuc*::gfp reporter fusion (pCM20) were grown for 3 or 6 hours in TSB containing 0.25% glucose buffered in 50 mM 3-(*N*-morpholino)propanesulfonic acid (MOPS) at pH 7.4 with or without different percentages of exogenous salmon sperm DNA. Fluorescence (*nuc* expression) was quantified using a Tecan Infinite 200 spectrofluorometer with an excitation wavelength of 490 nm and emission wavelength of 525 nm. Relative fluorescence was determined by normalizing the quantified fluorescence per OD_{600} and plotted using GraphPad Prism. Data represents the averages from two independent experiments performed in duplicate. Error bars show the SEM from the two independent experiments.

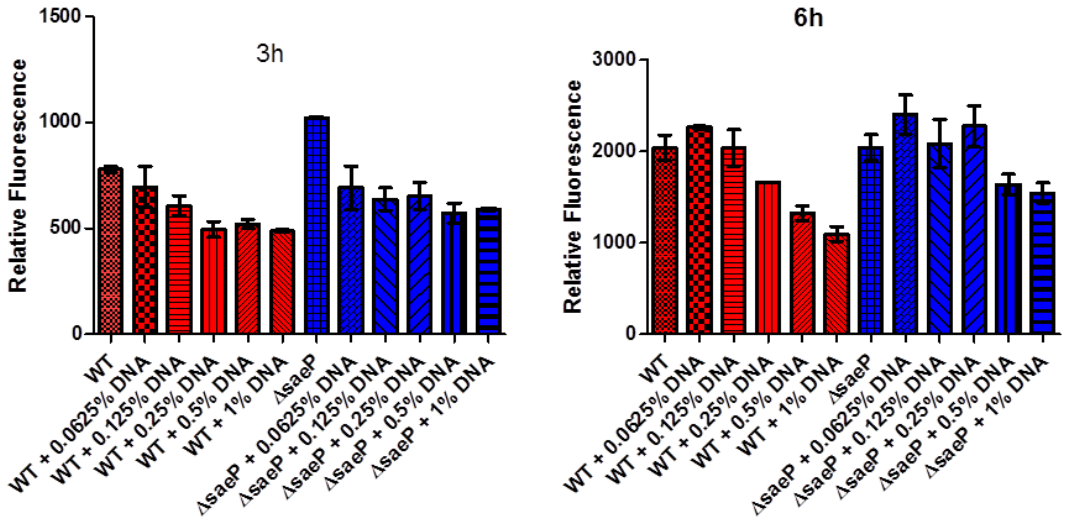

Figure 3-19 Effect of exogenous DNA on *nuc* expression in planktonic Δ*saeP* cells

AH1263 wild-type (184) and Δ*saeP* (blue) strains containing P*nuc*::gfp reporter fusion (pCM20) were grown for 3 or 6 hours in TSB containing 0.25% glucose buffered in 50 mM 3-(*N*-morpholino)propanesulfonic acid (MOPS) at pH 7.4 with or without different percentages of exogenous salmon sperm DNA. Fluorescence (*nuc* expression) was quantified using a Tecan Infinite 200 spectrofluorometer with an excitation wavelength of 490 nm and emission wavelength of 525 nm. Relative fluorescence was determined by normalizing the quantified fluorescence per OD_{600} and plotted using GraphPad Prism. Data represents the averages from two independent experiments performed in duplicate. Error bars show the SEM from the two independent experiments.

Remarkably, there were little differences seen between the wild-type and the Δ*saeP* mutant at both three and six hours (Figure 3-20) suggesting that the SaeP protein may not be the sole contributor to the decrease in nuclease expression in the presence of added DNA, at least under these planktonic conditions.

Given the data that shows a decrease in *nuc* expression in response to increasing amounts of DNA, we also sought to determine if there were any effects on overall *S. aureus* growth in both wild-type, Δ*saeP,* and Δ*saePQRS* strains. Therefore, we grew these strains in the presence of increasing amounts of DNA and plotted the OD_{600} over time. Interestingly in the AH1264 wild-type strain, increased amounts of DNA resulted in larger growth yields at 6-12 hours, yet, there were no differences at 24 hours (Figure 3-20; top color row panels). However, there were no difference between wild-type and the Δ*saeP* and Δ*saePQRS* strains at various percentages of DNA (Figure 3-20; bottom black row panels). This suggests that *S. aureus* may be able to utilize extra DNA as an additional carbon source to cause increases in growth yield or perhaps a reduction in autolysis, though, this ability appears to be independent of the Sae system.

Other Sae-controlled factors demonstrate stochastic expression similar to nuclease

Since the Sae system controls a myriad of other factors, and nuclease is stochastically expressed within a biofilm, we hypothesized that other Sae-controlled factors may be regulated similarly within a biofilm. To test this hypothesis, we obtained *hla* (α-toxin), *hlgA* (γ-toxin), and P1*sae* fluorescent reporter fusions in AH1263 wild-type and *sae* mutant strains and cultivated biofilms in the BioFlux1000.

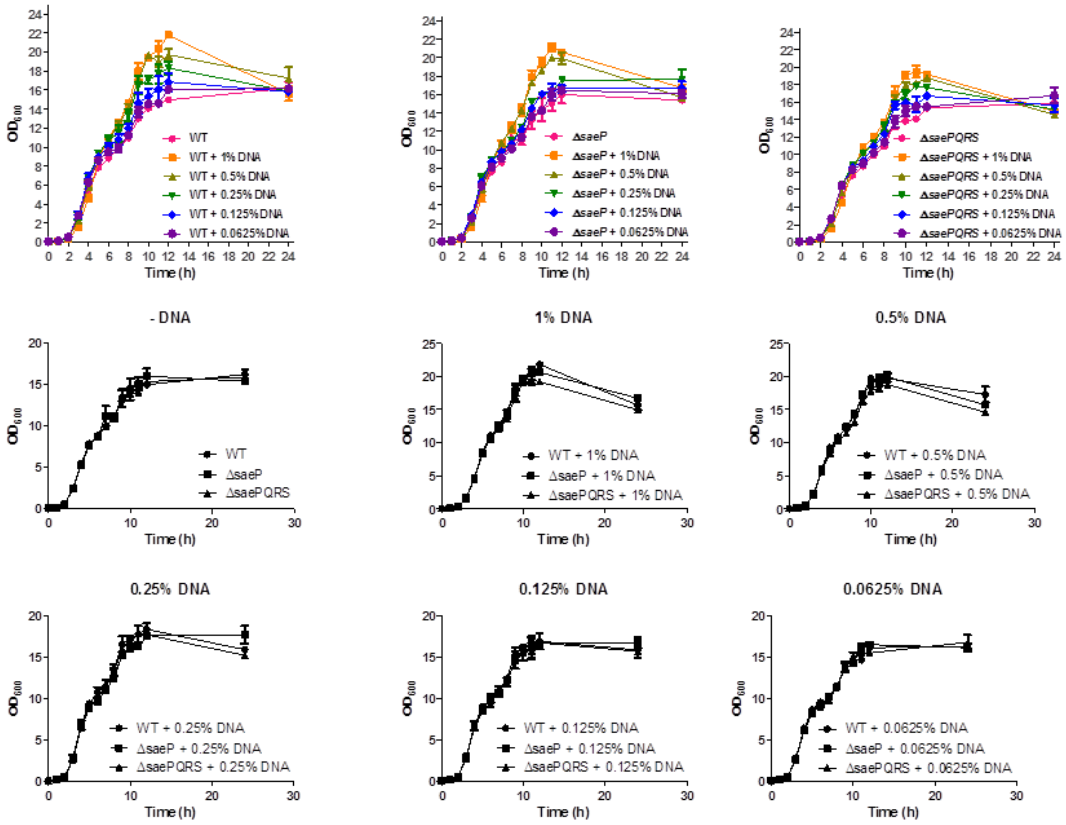

Figure 3-20 Effect of exogenous DNA on planktonic growth

AH1263 wild-type, Δ*saeP,* and Δ*saePQRA* strains containing P*nuc*::gfp reporter fusion (pCM20) were grown for 24 hours in TSB containing 0.25% glucose buffered in 50 mM 3-(*N*-morpholino)propanesulfonic acid (MOPS) at pH 7.4 with or without different percentages of exogenous salmon sperm DNA. OD_{600} were taken at 0, 1, 2, 3, 4, 5, 6 7, 8, 9, 10, 11, 12, and 24 hours and plotted over time using GraphPad prism. Data represents the averages from two independent experiments performed in single flasks. Error bars show the SEM from the two independent experiments. Top row panels (colored) show relation of different percentages of DNA in one strain of *S. aureus*. Bottom two row panels (black) show relation of wild-type and *sae* mutants when grown with a certain percentage of exogenous DNA.

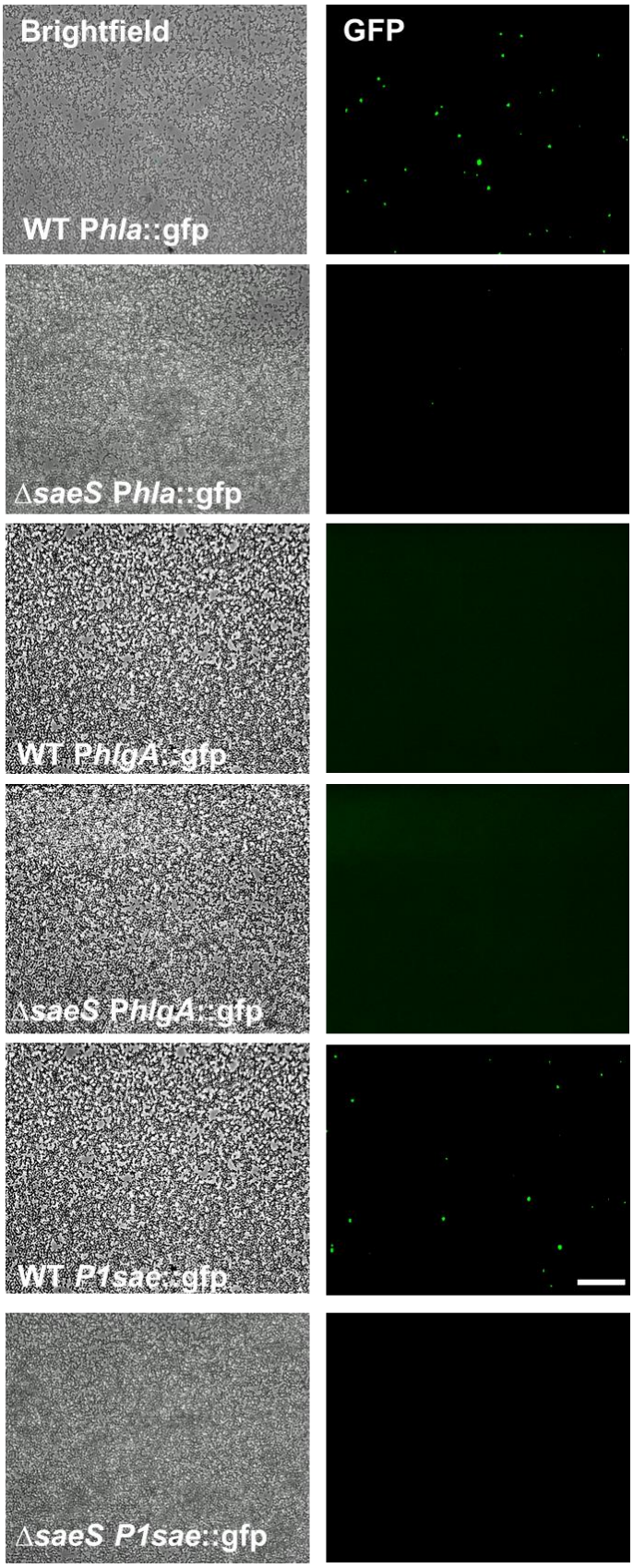
Brightfield
GFP
WT P*hla*::gfp
Δ*saeS* P*hla*::gfp
WT P*hlgA*::gfp
Δ*saeS* P*hlgA*::gfp
WT *P1sae*::gfp
Δ*saeS P1sae*::gfp

Figure 3-21 Expression of Sae-regulated genes *hla, P1sae,* and *hlgA* during biofilm development

S. aureus wild-type AH1263 (185) strain and the Δ*saeS* mutant derivative strain carrying the P*hla*::*gfp* (pCM27), P*hlgA*::*gfp* (pCM11*hlgA*), and P1sae::*gfp* (pcm11P1*sae*) reporter plasmids were grown in the BioFlux system. Brightfield and epifluorescence (GFP) microscopic images were acquired in 5-min intervals at ×200 magnification. Images are at 5 h and are representative images from two independent experiments at least in triplicate. Scale bar, 50 µm.

Strikingly, in support of our hypothesis, the *hla* and P1*sae* reporter fusions demonstrated Sae-dependent stochastic expression (Figure 3-21) similar to *nuc* (Figures 3-12, 3-13, 3-15). In contrast, the *hlgA* reporter showed no expression under our biofilm conditions (Figure 3-21). This is not completely unexpected given the recent results suggesting that *hlgA* is part of the Sae regulon that requires activation by external host signals (157).

Given that the *hla* and P1*sae* reporters demonstrated similar expression to *nuc* in a developing biofilm, we sought to characterize whether or not cells expressing *nuc* were also expressing other Sae-regulated genes. Thus, we generated a dual fluorescent reporter plasmid (pDM19) containing the promoter regions of *nuc* and *coa* (staphylocoagulase) and transduced it into AH1263 and *sae* mutants to simultaneously evaluate expression of two Sae-controlled genes during biofilm development. Remarkably, *coa* and *nuc* demonstrated identical stochastic expression patterns with only a subpopulation of cells expressing the fluorescent reporters in AH1263 wild-type strain (Figure 3-22). Additionally, much like the *nuc* expression studies described above, both the *coa* and *nuc* reporters were expressed in nearly every cell in the Δ*saeP* mutant biofilm. Also, little to no expression of either reporter was observed in the Δ*saePQRS* mutant (Figure 3-22). Altogether, these data suggest that the Sae system coordinates the expression of some Sae-regulated factors in a way that only initiates expression in a subpopulation of cells.

DISCUSSION

Our current understanding of *S. aureus* biofilm development is based on the characterization of three basic steps: 1) attachment, 2) accumulation/maturation, and 3) detachment/dispersal (76). The complexity of these processes was first highlighted in a study by Yarwood et al. (110) who used time-lapse video microscopy to visualize waves of growth and detachment that appeared to coincide with *agr* expression. More recent studies have revealed that detachment is largely dependent on expression of surfactant-

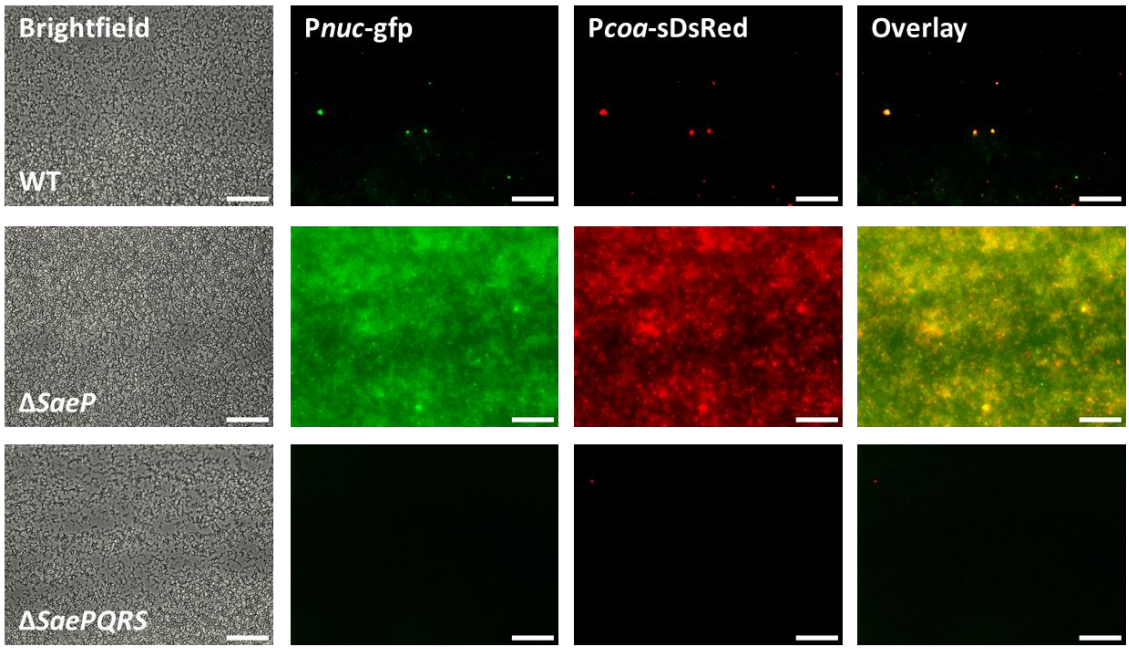

Figure 3-22 *coa* and *nuc* are expressed in the same subpopulation during biofilm development

S. aureus wild-type AH1263 (185), Δ*saeP,* and Δ*saePQRS* mutant derivative strains carrying the P*nuc*::*gfp* P*coa::sdred* dual reporter plasmid (pDM19) were grown in the BioFlux system. Brightfield and epifluorescence (GFP and sDsRed) microscopic images were acquired in 5-min intervals at ×200 magnification. Images are at 5 h and are representative images from two independent experiments at least in duplicate. Scale bar, 50 µm.

like molecules known as phenol-soluble modulins (PSMs) (117). In the current studies, we applied BioFlux microfluidics technology to provide enhanced resolution ofthe events occurring during the early stages of *S. aureus* biofilm development. In doing so, we have identified two additional developmental stages referred to as “multiplication” and “exodus” (Figure 3-1), which are distinct from the *agr*-mediated dispersal events that occur after tower formation. In addition, these studies provide greater insight into tower development associated with biofilm maturation, as well as the complex regulatory strategies that precede this process.

Attachment

The observation that the initial attachment of cells to the substrate could be inhibited by the addition of proteinase K indicates that this process is mediated by protein components associated with the cells (Figure 3-2B). Given that the Agr system is known to regulate expression of secreted and cell wall-associated proteins in *S. aureus* (190), we tested this strain for its ability to attach in our biofilm assay. As shown in Figure 3-5B, we observed an increase in cell attachment in an *agr* mutant derivative of the UAMS-1 strain. This observation is consistent with a previous report showing that *agr*-defective strains exhibit increased adherence to polystyrene in static biofilm assays (85). Within this study, it was demonstrated that increased attachment of the *agr* mutant strains was the result of decreased production of the PSM, δ-toxin, which these authors speculated may act as a strong surfactant preventing hydrophobic interactions between the cell surface and the polystyrene substrate.

In fact, *S. aureus* produces numerous surface proteins including the Sas family of proteins, fibronectin-binding proteins, clumping factors, elastin-binding proteins, protein A, and AtlA that have all been shown to be important for attachment and biofilm

maturation (86, 170). To determine the potential role of these proteins in our system, we identified NTML mutant strains, as well as others, that contain defects in the synthesis of cell surface-associated molecules (i.e. LPXTG-motif proteins, intercellular adhesion, and capsule) and screened them for initial attachment (Table 3). This analysis revealed that only the *atlA::ΦNΣ* mutant exhibited a defect in the initial attachment of cells (Figure 3-3). In addition, we added PAS, an autolysis inhibitor, in two hour time points to developing UAMS-1 wild-type biofilms in the BioFlux1000 and saw abolishment of the biofilm two hour following addition of PAS (Figure 3-4). These data are in agreement with a recent study that demonstrates that the *S. aureus* biofilm matrix relies less on cell surface-associated proteins including protein A and the fibronectin-binding proteins, and more so on cytoplasmic proteins released during stationary phase of growth (191). In addition, while AtlA has been reported to serve as an adhesin (86), results have also indicated that the enzymatic activity of this protein is required for biofilm formation, suggesting the involvement of autolysis and the subsequent release of genomic DNA (104). Arguing against this possibility is the observation that the addition of DNase I to the inoculum (data not shown) or at the 0-h time (Figure 3-2A) had little effect on the attachment of cells. Complicating the interpretation of these results further is the propensity of the *atlA* mutant to form large clusters of cells, which could have detrimental effects on cell attachment. Furthermore, the fact that many of the mutants tested did not show a defect in biofilm development is not completely unexpected since most of the surface proteins are important for binding host matrix components (i.e. MSCRAMMs), which are absent in our biofilm assays. Overall, the finding that attachment was affected by the *agr* and *atlA* mutations, but none of the other cell surface protein mutations, is consistent with the hypothesis that AtlA and δ-toxin are required for this process (85).

Multiplication

Similar to cell attachment, the multiplication stage was also found to be sensitive to protease treatment (Figure 3-2B); however, screening of the NTML for proteins involved in this stage failed to identify a protein important in this process (Table 3). The current studies demonstrated that DNase I had little effect on the biofilm during the multiplication stage (Figure 3-2A and Figure 3-10). This is in agreement with a recent study demonstrating DNase I-insensitivity during early *S. aureus* biofilm development (175). Although these results appear to conflict with our previous findings (99, 100), it is important to note that the biofilm growth conditions used here were distinctly different from the static assay conditions used previously. In addition, the BioFlux assay affords greatly increased resolution of the early events in biofilm maturation through real-time microscopic imaging of the cells, thus, enabling the visualization of developmental events that were previously undetectable in the static assays. In addition, isolation of eDNA from the biofilms at four hours treated with or without active DNase I showed no significant changes in eDNA levels although the eDNA levels were lower when treated (Figure 3-11). Based on these data, we hypothesize that there is a functional shift in the biofilm matrix prior to the exodus event from a protein-based matrix to one that is dependent on both eDNA and protein, most likely the result of eDNA and protein interactions occurring as the biofilm matures. Indeed, precedence for this includes the demonstration that *S. aureus* beta toxin, normally known for its role as a hemolysin, can bind eDNA and covalently cross-link to itself forming an insoluble nucleoprotein matrix within a biofilm (108). However, UAMS-1 does not produce beta toxin due to an insertion of the bacteriophage in the *hlb* gene (108). Like beta toxin, the immunodominant surface antigen B (IsaB) has also been shown to bind DNA, yet an *isaB* mutant previously exhibited no defect in biofilm formation (109). Likewise, an *isaB* mutant showed no

noticeable differences in biofilm development when grown in the BioFlux1000 when compared to it wild-type strain (data not shown).

In contrast to these extracellular DNA-binding proteins, recent reports have demonstrated that cytoplasmic nucleoid-associated proteins (NAPs), normally known for intracellular chromosomal structuring, have emerged as possible biofilm scaffolds in different bacteria. Specifically, biofilm produced by *Burkholderia cenocepacia*, non-typeable *Haemophilus influenza,* and *Escherichia coli* have all shown a requirement for integration host factor (IHF) and/or histone-like protein (HU). In fact, treatment of established biofilms of these species, as well as *S. aureus* and *S. epidermidis,* with antisera specific for these proteins resulted in a considerable decrease in the total amount of biofilm generated (107, 192). The precedence for NAPs in bacterial biofilms and the plethora of NAPs identified in *S. aureus* (193) suggest that these proteins may be important contributors to biofilm development in *S. aureus*. Studies to identify specific eDNA-binding proteins important in biofilm integrity are currently in progress in our laboratory.

Exodus

The observation that Agr P3 promoter activity was not observed until well after tower development (Figure 3-7), in combination with the absence of an effect of an *agr* mutation on the exodus event (Figure 3-5), suggests that the Agr quorum-sensing circuit and the PSMs are not required for exodus. Instead, given the role of eDNA in biofilm development we hypothesized that staphylococcal nuclease may be required. Consistent with this hypothesis was the observation that the biofilm became DNase I-sensitive after six hours of development (Figure 3-10), and the Δ*nuc* mutant failed to initiate exodus at this time point (Figure 3-9). Given the precise timing of the exodus event, we also examined *nuc* expression and, remarkably observed expression limited to

subpopulation of cells preceding the exodus event (Figure 3-12), suggesting that these specialized cells have an impact on the remainder of the biofilm population, much like the specialization that is seen in *Bacillus subtilis* biofilm formation (194). In addition, these data also suggest a model where early Nuc-mediated exodus allows for tower formation and eventual late Agr-mediated dispersal for further dissemination of *S. aureus* cells.

The observation that *nuc* exhibited temporal and stochastic patterns of expression during biofilm development indicates that it is subject to complex regulatory control. While previous reports have suggested that nuclease is regulated by the Agr quorum-sensing circuit (195-197), new evidence demonstrates *nuc* expression is more directly controlled by the Sae regulatory system (198-200). Indeed, recent promoter mapping, Nuc activity measurements, and immunoblot studies have confirmed the Sae-dependent regulation of nuclease expression (48). In support of these findings, an *agr* mutant exhibited both temporal and stochastic regulatory control of *nuc* expression during biofilm development similar to the wild-type strain (data not shown). Additionally, a *saeQRS::spc* mutant failed to initiate exodus of the biofilm population and exhibited much reduced *nuc* expression when compared to its parental strain AH1263 (Figure 3-13). The *saePQRS* operon encodes two auxiliary proteins, SaePQ, and a two-component system, SaeRS, that globally regulate multiple *S. aureus* secreted proteases (201) and virulence factors such as alpha toxin, beta toxin (*hlb*), coagulase (*coa*), fibronectin-binding proteins (*fnbA* and *fnbB*), and extracellular adherence protein (*eap*) (202, 203). To continue to dissect the potential roles that each protein in the *saePQRS* operon has during *nuc* expression and biofilm development, we obtained mutations in three of the four genes (i.e. Δ*saeP*, Δ*saeQ*, and Δ*saeS*) and a complete deletion of the entire operon, Δ*saePQRS*. Most interestingly, the Δ*saeP* demonstrated a unique phenotype where apparently every cell in the developing biofilm expressed nuclease

compared to the subpopulation of cells seen in wild-type (Figure 3-15). This is particularly significant given that work by another group has demonstrated that the SaeP protein can bind eDNA (unpublished data from Alexander Horswill laboratory) and the recent study proposing that the SaeP and SaeQ form a complex to initiate phosphatase activity of the sensor kinase SaeS (203) may explain this unique expression phenotype. Given the former, along with several examples of bacterial cells sensing their ECM to initiate biofilm cell responses (204), we hypothesized that the SaeP protein may be sensing eDNA as a feedback mechanism to control *nuc* expression during biofilm development. Thus, we added exogenous DNA to the developing biofilm, and to our surprise, the additional DNA almost completely prevented biofilm formation (Figure 3-17), making it impossible to evaluate *nuc* expression. Interestingly, this effect was similar to that observed for PAS-treated biofilms, or cells that contain an *atlA* mutation (Figure 3-3), both of which are unable to form biofilms due to a lack of lysis. Considering the recent data demonstrating that the glucosaminidase domain of AtlA binds DNA (205), one possible explanation for this phenomenon is that exogenously added DNA is binding to AtlA and inhibiting its function, and ultimately leading, to inhibition of biofilm development. However, this possibility is still being investigated.

Since we were unable to add additional DNA to a *S. aureus* biofilm, we performed planktonic studies to determine any effects on *nuc* expression. Counterintuitively, when increasing amounts of salmon sperm DNA were added to planktonically growing cells, there was a clear decrease in *nuc* expression (Figure 3-18), yet, it appeared to be SaeP-independent (Figure 3-19). This is in contrast to our expectations considering if more of the substrate for nuclease (i.e. eDNA) is present, one would imagine that an increase in nuclease activity would occur and the Sae-control would be eliminated in a *saeP* mutant. However, this does not appear to be the case. Nonetheless, one possible explanation for the increase in *nuc* expressing cells in the

biofilm in a Δ*saeP* mutant may be due to the fact that SaeQ cannot form a complex with SaeP and activate the phosphatase activity of SaeS resulting in uncontrolled expression of nuclease throughout a biofilm.

In addition to evaluating the effect of exogenous DNA on *nuc* expression, we also evaluated the effect of exogenous DNA on *S. aureus* overall growth. When DNA was added from initial inoculation of planktonically grown cells, there is a clear increase in growth yield from 6-12 hours when compared to strains grown in TSB not containing additional DNA (Figure 3-20). Although this is not a Sae-controlled process (Figure 3-20), it seems that *S. aureus* may be able to use DNA as an additional carbon source. This may be possible considering the primary carbon source, glucose, in TSB is exhausted by six hours (154) and other bacteria such as *Vibrio cholerae* have shown the ability to use DNA as a nutrient source (206). As an alternative hypothesis, the exogenous DNA could be killing the cells but not lysing because the activity of Atl may inhibited.

Lastly, considering that the Sae system regulates so many different genes, we asked whether other Sae-regulated promoters, such as those driving *hla, hlgA, P1sae,* and *coa* expression, demonstrated similar expression patterns in a developing *S. aureus* biofilm. Surprisingly, the *hla, P1sae,* and *coa* promoters all showed similar stochastic expression to *nuc.* In contrast, no *hlgA* expression was observed (Figure 3-21). In addition, a *coa*/*nuc* dual reporter construct revealed overlapping expression patterns (Figure 3-22), demonstrating that subpopulation of cells is responsible for the expression of at least two different secreted proteins. While it is fascinating that these other Sae-regulated factors appear to be stochastically regulated in subpopulation of cells, one interesting observation amongst these data is the fact that *hla* and *coa* have similar expression patterns even though they are in different “classes” of Sae regulation. These classes refer to whether or not the expression of a particular gene is dependent on the

phosphorylation state of SaeR (202). Indeed, class I *sae* target genes (*coa, fnbA, eap, sbi, efb, fib, nuc,* and *sae*) require phosphorylation of SaeR while the class II target genes (*hla, hlb, and cap*) seem to be less reliant on this phosphorylated state (202). Since the *nuc* and *coa* are in the same class, it is not surprising that the two genes are expressed in the same biofilm population. This suggests that a Sae-regulated mechanism is activated to control the overproduction of certain virulence factors and delineate roles to certain subpopulations of cells. In addition, the data demonstrating similar expression patterns between *hla* and *nuc* in a biofilm suggests that there may be much more to the control of *hla,* yet, construction of a *nuc/hla* reporter could provide further insight into whether or not both of these genes are expressed in the same biofilm cell population. This additional control may be under the Agr quorum-sensing system, given that the large 5' untranslated region (5' UTR) of *hla* mRNA can be bound by RNAIII leaving the Shine-Dalgarno sequence to be bound by ribosomes and leaving *hla* under translational control in addition to transcription regulation (207). In addition to *hla* expression patterns, another observation that *hlgA* expression was undetectable even in the wild-type strain. Recent data suggesting that *hlgA* expression is dependent on activation by host cell antimicrobials such as α-defensin (157), may explain why it is not expressed in an *in vitro* biofilm assay. Thus, further studies must be continued to evaluate the regulation of these Sae-factors and others by examining not only Sae control, but also the interplay of other regulators such as Agr or SarA or the newly identified virulence factor regulatory locus, *vfrAB* operon, which appears to be an upstream regulator of the Sae regulon (208)

Tower Maturation Stage

Based on the results of this study, it is apparent that the early exodus event during *S. aureus* biofilm development is essential for the formation of distinct tower structures, which based on our previous studies (148) have variable physiology and

metabolism as seen by the presence or absence of eDNA and dead cells as well as differential gene (*cid* and *lrg*) expression. However, two major questions remain to be answered. First, how do these eDNA-containing towers remain intact if nuclease is active? A recent report testing DNase I efficacy in UAMS-1 *S. aureus* biofilms demonstrated carbohydrates (likely, PIA) and eDNA staining within tower structures and appear to be DNase I insensitive (175). The authors suggest that carbohydrates may be interacting with eDNA and protecting it from DNase I degradation, however, further investigation must be conducted to confirm these findings.

Second, what is the function of towers in *S. aureus* biofilm? Some evidence suggests that tower structures are important for the pathogenesis of *S. aureus* biofilms formed on native heart valves of infective endocarditis where they detach and travel to secondary sites of infection (64, 103, 209). In other organisms, the development of specialized structures is important for survival and/or resistance to environmental stresses. For example, the cystic fibrosis pathogen, *Pseudomonas aeruginosa*, forms robust tower-like structures that have been shown to be important in resisting microbial biocides such as sodium dodecyl sulfate (SDS) detergent and tobramycin (210, 211), as well as mediating biofilm dispersal (138). Additionally, the predator bacterium, *Myxococcus xanthus*, demonstrates complex multicellularity and intercellular signaling through coordinated gene expression to form raised aggregates of cells called fruiting bodies (212-214). Indeed, much like the reduction of the cell population during the exodus phase that precedes tower formation in *S. aureus*, *M. xanthus* demonstrates a reduction of the cell population preceding fruiting body development (215, 216). Based on these similarities, it is likely that tower structures produced by *S. aureus* are also important in survival during environmental stress.

Finally, the results of our studies suggest an alternative to the model proposed by Otto (76) describing how *S. aureus* biofilms develop their characteristic structure. In this

model, it is envisioned that the PSMs act upon a preexisting thick mat of cells, causing cell detachment and leaving behind structures of various forms (e.g. towers and channels). However, the structures present in the biofilms produced in our biofilm system are clearly not generated in this way. Rather, they are formed after the mass exodus of the bulk of the early biofilm, and appear to arise as a result of the rapid growth of only a few remaining cells. In the absence of staphylococcal nuclease, these tower structures are not observed, either because they are overwhelmed by the presence of an unusually robust accumulation of biomass, or because a key developmental switch fails to trigger. Continued studies are required to provide a greater understanding of these fascinating developmental processes, as well as the functions of the structures that are formed.

CHAPTER IV: [5]

Correlation of cell death/extracellular DNA and expression of the *cidABC* and *lrgAB* operons during *Staphylococcus aureus* biofilm development

INTRODUCTION

The primary focus of our laboratory has been the characterization of two *S. aureus* operons, *cidABC* and *lrgAB*, and their roles in programmed cell death (PCD) and biofilm development. Although the exact mechanisms have yet to be elucidated, previous studies of planktonic cultures have shown that the *cid* and *lrg* operons respond to alterations in carbon overflow (overflow metabolism) (217) (218) (219). Although not completely understood, overflow metabolism (i.e. conditions of excess glucose and oxygen) is a phenomenon in which carbon flow into the TCA cycle is limited by carbon catabolite repression (220) (221) (222) (223). Thus, carbon is redirected into various pathways including the Pta/AckA and AlsS/AlsD pathways, accumulating extracellular acetate and acetoin, respectively, and consuming intracellular pyruvate (224). Interestingly, CidR, the LysR-type transcriptional regulator (LTTR) that induces co-expression of *cidABC* and *alsSD* operons, is known to be induced by high concentrations of acetate under conditions of carbon overflow (i.e. 35 mM glucose) (217) (217) (219). Intriguingly, the *cidC* and *alsSD* genes are known to encode three metabolic enzymes, specifically involved in overflow metabolism: pyruvate oxidase (CidC), acetolactate synthase (AlsS), and acetolactate decarboxylase (AlsD), that have also recently been shown to play additional opposing roles in PCD and biofilm development (219). Opposing the *cid* operon in PCD, the *lrgAB* operon is regulated by

---

The majority of the work in CHAPTER IV has been published in Moormeier DE, Endres JL, Mann EE, Sadykov MR, Horswill AR, Rice KC, Fey PD, Bayles KW. *AEM.* 2013.

LytSR, a two-component regulatory system (TCRS) (225) (174). LytSR is known to induce *lrgAB* expression by sensing changes in membrane potential, as demonstrated using membrane-dissipating agents, such as carbonyl cyanide *m*-chlorophenylhydrazone (CCCP) and gramicidin, altering cell death and lysis and leading to biofilm modulations and decreased biofilm adherence (226). Additionally, it has been shown that, under conditions of overflow metabolism, that *lrgAB* is induced in a *LytSR*-dependent manner, coinciding with extracellular acetate accumulation (217). In addition, our results also demonstrate that *lrg* expression can also be induced in a LytS-independent manner as a result of increased levels of acetyl-phosphate, an overflow intermediate metabolite, which acts as a phoshodonor to phosphorylate LytR (227) (228) (229) (230).

Collectively, these data suggest that the *cid and lrg* operons respond to alterations of central metabolism, which are dependent on the conditions of the surrounding environments including oxygen levels, glucose levels, and pH. However, modulations of central metabolism and their roles in biofilm development have yet to be completely illuminated. Thus, the studies described in this chapter were designed to assess the metabolic heterogeneity of developing biofilm microenvironments and the roles they play in the differential expression the *cid* and *lrg* operons.

RESULTS

Induction of cid and lrg expression during hypoxic growth

Previous studies of *cidABC* and *lrgAB* transcription showed that expression of both of these operons was induced during aerobic overflow metabolism (143) where the high rate of glycolysis inhibits aerobic respiration and induces carbon flow through fermentation pathways (231). Since staphylococcal biofilms contain regions of hypoxia (142), we hypothesized that the decrease in oxygen concentrations, leading to activation

of fermentative metabolism, will also affect *cid* and *lrg* expression. To test this, RNA was extracted from aerobically- and hypoxically-grown cells at 4 hr post inoculation and the relative levels of *cid*- and/or *lrg*-transcripts were determined using quantitative reverse transcriptase PCR (qRT-PCR). Measurements of oxygen revealed that hypoxic growth resulted in an oxygen concentration of approximately 1% total saturation, compared to approximately 70% total oxygen saturation under our standard growth conditions (see Chapter II). As anticipated, the levels of the *cid*-specific transcripts were markedly increased (approximately 12 fold) in cells grown under hypoxic conditions compared to cells grown aerobically (Figure 4-1A). Consistent with previous studies (145), *cid* expression was induced under excess glucose conditions in a *cidR*-dependent but *lytSR*-independent manner, respectively (data not shown). Similarly, the induction of *cid* expression under hypoxic conditions was found to be *cidR* dependent and *lytSR* independent (Figure 4-1A). In contrast, *lrgAB* transcription was found to be slightly decreased under hypoxic conditions, but remained *lytSR* dependent (Figure 4-1B) as previously demonstrated (159, 232). Additionally, we found that *lrgAB* expression was not influenced by the *cidR* mutation during growth under hypoxic conditions (Figure 4-1B). Taken together, these data demonstrate that hypoxic conditions induce *cidABC* operon expression in a CidR-dependent manner, similar to its induction observed during overflow metabolism. However, unlike the induction of *lrgAB* expression previously observed during overflow metabolism, hypoxic growth does not affect *lrgAB* transcription.

Expression of cid and lrg in individual cells

To test the hypothesis that the *cid* and *lrg* operons are differentially expressed within a growing biofilm, we generated *cid* and *lrg* transcriptional reporter fusions to facilitate the assessment of expression of these genes in individual cells during different

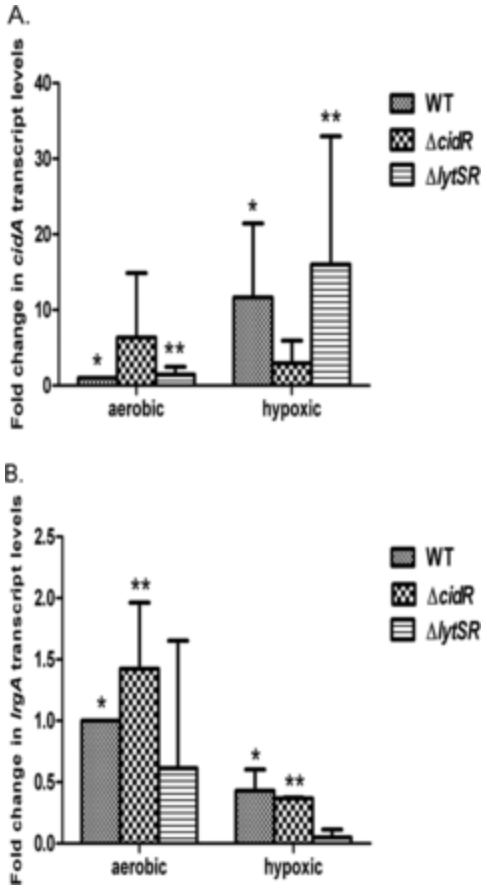

Figure 4-1 Hypoxic induction of *cidABC* and *lrgAB* transcription

Total RNAs were collected from *S. aureus* WT (UAMS-1), *cidR* mutant, and *lytSR* mutant cells at 4 h of growth under aerobic and hypoxic conditions. The *cidABC* (A) and *lrgAB* (B) transcripts present in the RNA were detected by qRT-PCR with *cidA*- and *lrgA*-specific primers, normalized to the levels of *sigA*-specific transcripts detected, and then plotted as *n*-fold changes relative to the *cidABC* and *lrgAB* transcript levels in WT cells grown under aerobic conditions. Error bars represent standard deviations generated from three independent experiments. In panel A, significant differences ($P < 0.05$ for all) between aerobic and hypoxic treatments are denoted as follows: *, WT; **, Δ*lytSR*. In panel B, significant differences ($P < 0.05$ for all) between aerobic and hypoxic treatments are denoted as follows: *, WT; **, Δ*cidR*.

Figure modified from Moormeier et al. 2013. *AEM*

stages of biofilm development. Promoter regions of both the *cid* or *lrg* operons were amplified and inserted upstream of the gene encoding super-folder GFP (sGFP), previously shown to be easily detected in *S. aureus* cultures (160). The resulting constructs were moved into UAMS-1, as well as the *cidR* and *lytSR* derivatives of this clinical isolate. The strains were tested to determine if GFP expression during planktonic growth reflected the transcriptional regulation seen by Northern blot analyses (143, 145, 232) and using qRT-PCR analyses (Figure 4-1). Indeed, when grown in the presence of excess glucose or under hypoxic conditions, the P*cid*::gfp reporter construct produced increased levels of GFP fluorescence (Figure 4-2), as opposed to aerobically grown cells in the absence of glucose, and was *cidR*-dependent (Figure 4-2). In contrast, the P*lrg*::gfp promoter construct did not produce detectable fluorescence under these conditions (Figure 4-2). However, when grown in the presence of CCCP, a membrane potential dissipating agent known to induce *lrgAB* expression, the P*lrg*::gfp promoter construct fluoresced brightly in a *lytSR*-dependent manner (Figure 4-3). As a control, we also generated a *gfp* fusion to the *ldh1* promoter that is specifically expressed during hypoxic growth (233). In wild type cultures containing the P*ldh1*::gfp promoter fusion grown in hypoxic conditions, GFP fluorescence was seen in the majority of cells as compared to the absence of fluorescence in cells grown aerobically in the presence or absence of excess glucose (Figure 4-2).

Expression of cid and lrg operons during biofilm development

To study *cid* and *lrg* expression within a biofilm, we first examined the fluorescent reporter constructs in biofilm grown under static conditions. As shown in Figure 4-4 (panels A and C), GFP fluorescence was observed in biofilm formed by the wild-type strain containing the *cid* fusion, but not in the *cidR* mutant, similar to growth under planktonic conditions (Figure 4-1). Also similar to planktonic growth (Figure 4-2), the

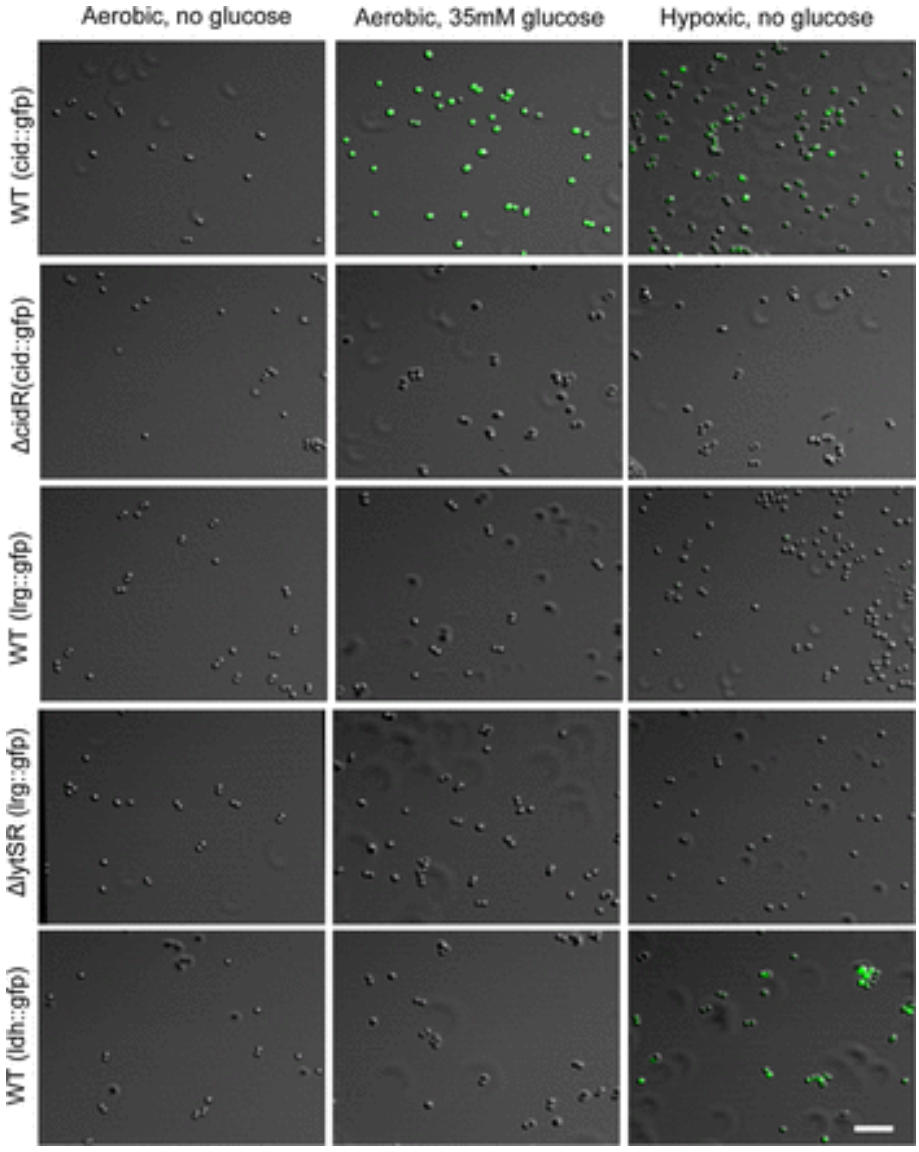

Figure 4-2 Expression of fluorescent reporters during planktonic growth

S. aureus UAMS-1 (185), the *cidR* mutant (Δ*cidR*) strain, and the *lytSR* mutant (Δ*lytSR*) strain containing the P*cid*::*gfp*, P*lrg*::*gfp*, and P*ldh*::*gfp* transcriptional reporter plasmids were grown to exponential phase in the presence or absence of 35 mM glucose and under aerobic and hypoxic conditions as indicated. GFP-positive cells were visualized by CLSM at ×630 magnification as described in Materials and Methods. The scale bar represents 5 μm.

Figure modified from Moormeier et al. 2013. *AEM*

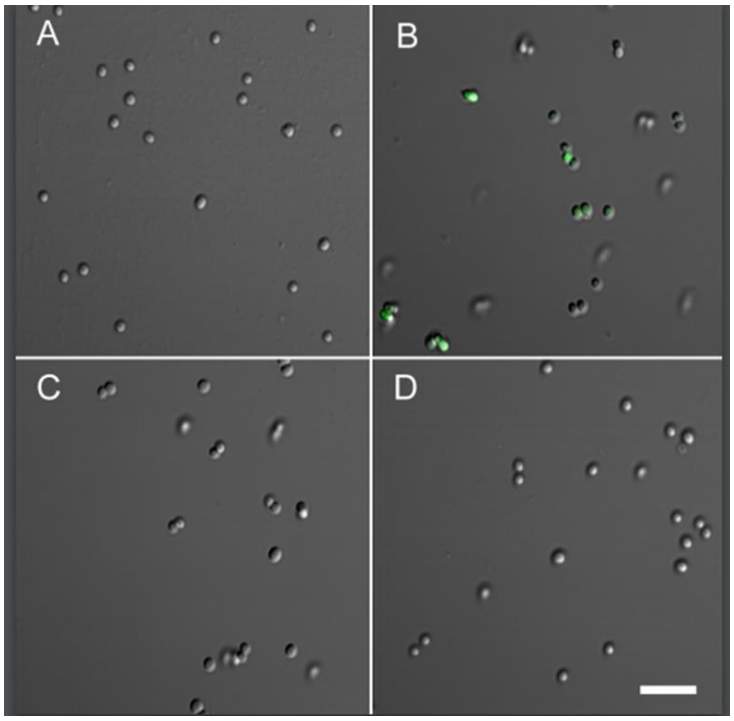

Figure 4-3 CCCP induction of *lrgAB* promoter activity

S. aureus UAMS-1 (panels A and B) and its *lytS* mutant derivative, KB999 (panels C and D), each containing the P*lrg*::gfp promoter fusion plasmid, were grown to mid-exponential phase and treated with CCCP, a depolarizing agent previously shown to induce *lrgAB* transcription. GFP positive cells were visualized by confocal laser scanning microscopy as described in Materials and Methods. Scale bar represents 5 µm.

Figure modified from Moormeier et al. 2013. *AEM*

lrgAB promoter was not expressed in a static biofilm (Figure 4-4D). As anticipated based on previously published results demonstrating the hypoxic nature of static biofilms (142), the *ldh1* promoter fusion construct also expressed GFP fluorescence in our static biofilm assays (Figure 4-4B).

To examine the pattern of *cid* and *lrg* expression during biofilm development under flow cell conditions, we took advantage of BioFlux1000 technology (147) to acquire sequential bright-field and epifluorescence images of a developing biofilm. Analysis of the epifluorescent images revealed distinct patterns of *cid* and *lrg* expression during the development of these biofilms. Using the UAMS-1 P*cid*::gfp fusion strain (Figure 4-5), distinct clusters of cells or "towers" emerged and gradually turned green as they increased in size, similar to the pattern of expression observed with the P*ldh1*::gfp fusion strain (Figure 4-6), consistent with the hypothesis that hypoxic regions of the biofilm (within the interior of the large towers) induce *cid* expression. Unexpectedly, the P*cid*::gfp fusion strain also produced smaller towers with constitutively high levels of fluorescence (Figure 4-7), clearly distinct from the larger towers. These smaller towers appear to emerge from a single highly fluorescent cell that divides (although with a seemingly slower growth rate compared to the other clusters) and remains exclusively associated with its siblings until a large, intensely fluorescent tower was formed. In addition, these towers appeared to be less adherent, as demonstrated by their propensity to release smaller cell clusters (Figure 4-7). Importantly, similar highly fluorescent towers were observed using the P*ldh1*::gfp fusion strain (Figure 4-8), suggesting that overlapping metabolic cues may be responsible for high level *cid* and *ldh1* expression observed in these small towers. Also, no P*cid*::gfp-mediated fluorescence in either tower type was observed in a strain in which the *cidR* gene had been disrupted (data not shown), suggesting that the signals responsible for *cid* expression in both tower types were similar.

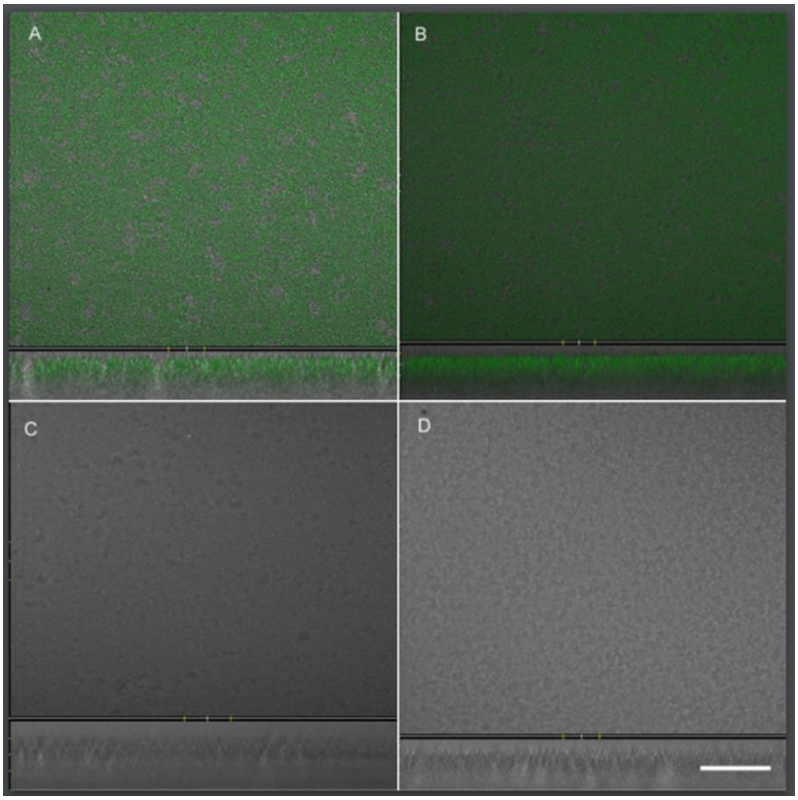

Figure 4-4 Analysis of *cid* and *lrg* expression during static biofilm growth

S. aureus UAMS-1 cells containing: (A) P*cid*::gfp promoter fusion in UAMS-1 [UAMS-1 (pEM81)], (B) P*ldh1*::gfp promoter fusion in UAMS-1 [UAMS-1 (pEM87)], (C) P*cid*::gfp promoter fusion in the *cidR* mutant [KB1090 (pEM81)], and (D) P*lrg*::gfp promoter fusion in UAMS-1 [UAMS-1 (pEM80)]. Three-dimensional images of the biofilms were generated using confocal laser scanning microscopy as described in the Materials and Methods. Images are representative of three independent experiments. Scale bar represents 40 µm.

Figure modified from Moormeier et al. 2013. *AEM*

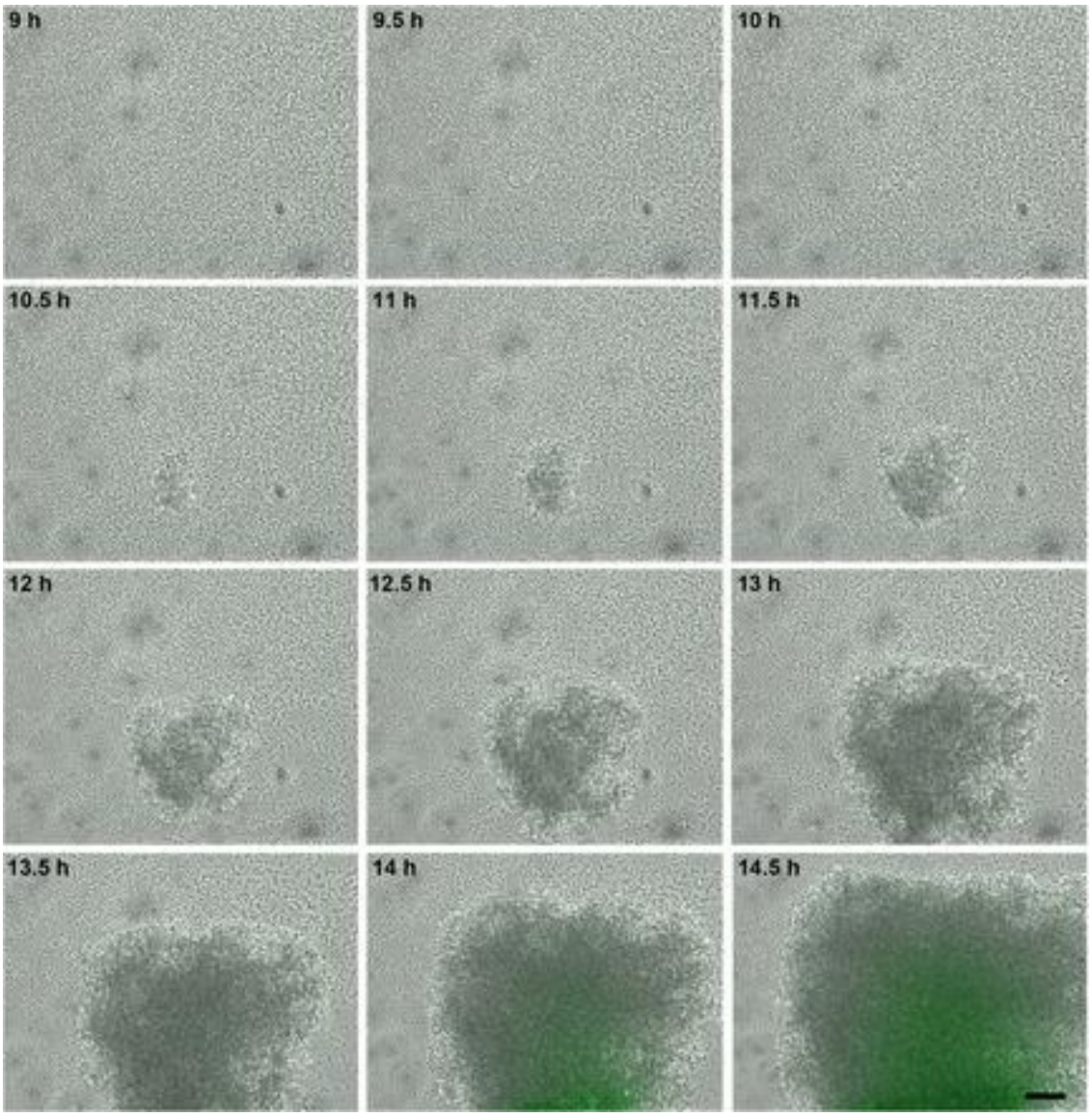

Figure 4-5 Temporal analysis of *cidABC* expression during biofilm development

S. aureus cells containing the P*cid*::*gfp* reporter plasmid were inoculated into a BioFlux microfluidic system and allowed to form a biofilm within a flow shear environment at a flow rate of 64 µl/h for a total of 18 h. Bright-field and epifluorescence microscopic images were collected at 5-min intervals. The images presented were taken from the complete set of 217 images taken at ×200 magnification, spanning 9 to 14.5 h, and illustrate typical tower development and GFP expression observed in multiple experiments. The scale bar represents 50 µm.

Figure modified from Moormeier et al. 2013. *AEM*

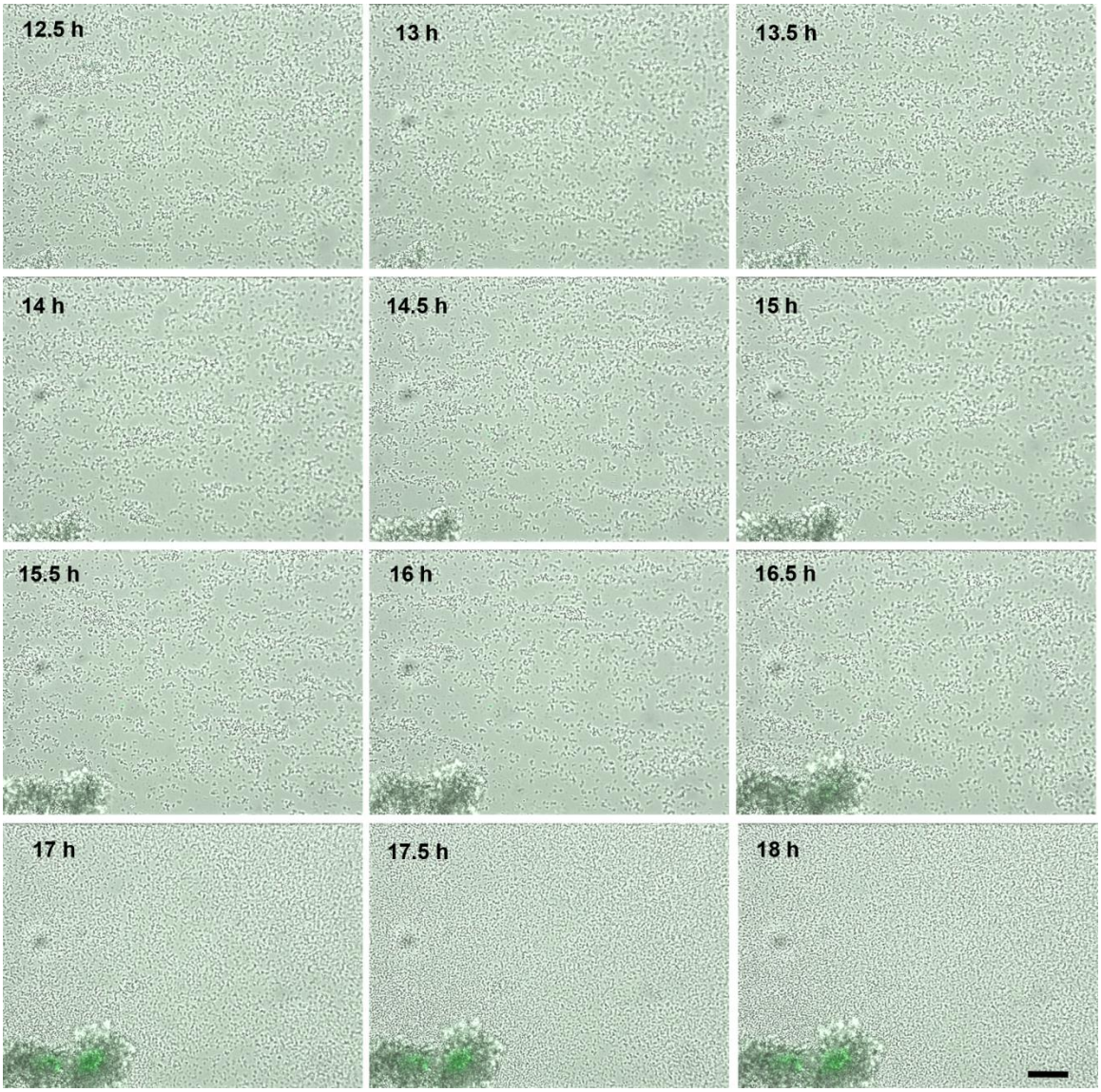

Figure 4-6 Temporal analysis of *ldh1* expression during biofilm development

S. aureus cells containing the P*ldh1*::gfp reporter plasmid were inoculated into a BioFlux microfluidics system and allowed to form a biofilm within a flow-shear environment at a flow rate of 64 µl/h for a total of 18 h. Bright-field and epifluorescence microscopic images were collected at 5-min intervals using 200× magnification. The images presented were taken from the complete set of 217 images spanning 12.5-18 h and illustrate typical tower development and GFP expression observed in multiple experiments. Scale bar represents 50 µm.

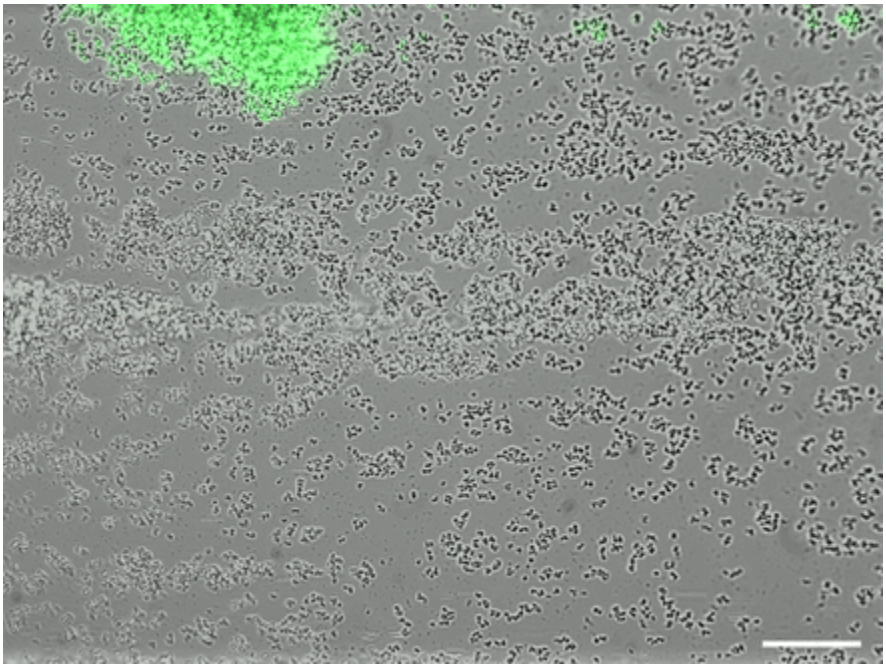

Figure 4-7 High-level *cid* expression in small towers during biofilm formation

S. aureus cells containing the P*cid*::*gfp* reporter plasmid were inoculated into a BioFlux microfluidic system and allowed to form a biofilm as described in the legend to Figure 4-5. The image shown (at ×200 magnification) represents a typical constitutive highly fluorescent “small” tower that is formed by this strain, distinct from the delayed fluorescence produced by the “large” towers depicted in Figure 4-5. Note the presence of detached, highly fluorescent cells “downstream” (to the right) of the tower. The scale bar represents 50 μm.

Figure modified from Moormeier et al. 2013. *AEM*

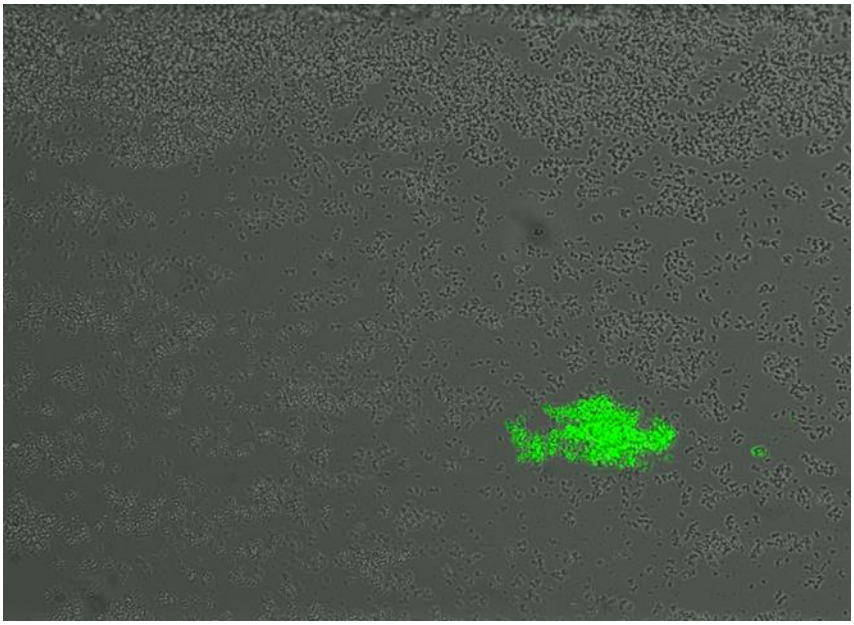

Figure 4-8 High-level *ldh1* expression in small towers during biofilm formation

S. aureus cells containing the P*ldh1*::*gfp* reporter plasmid were inoculated into a BioFlux microfluidic system and allowed to form a biofilm as described in the legend to Figure 4-5. The image shown (at ×200 magnification) represents a typical constitutive highly fluorescent “small” tower that is formed by this strain, distinct from the delayed fluorescence produced by the “large” towers depicted in Figure 4-6. Note the presence of detached, highly fluorescent cells “downstream” (to the right) of the tower.

The UAMS-1 P*lrg*::gfp fusion strain exhibited a different pattern of expression during biofilm development (Figure 4-9). Similar to the *cid* and *ldh1* promoter fusion constructs, the P*lrg*::gfp fusion strain produced fluorescence in what appeared to be the large towers that exhibited inducible *cid* and *ldh1* expression as the towers matured. However, unlike what was observed with the *cid* and *ldh1* promoter fusion constructs, the P*lrg*::gfp fusion strain produced constitutive fluorescence without increasing expression within growing towers, consistent with results indicating that this promoter is not inducible under hypoxic conditions. Importantly, it should be noted that despite the fact that the P*lrg*::gfp fusion strain did not produce detectable fluorescence in planktonic culture or static biofilm assays, this strain produced robust fluorescence within towers formed in this flow-cell system suggesting that this operon is controlled by developmental signals associated with biofilm formation. As expected, the fluorescence produced by the P*lrg*::gfp construct was abolished in a *lytSR* mutant background (101).

To clearly distinguish the coincidence of *cid* and *lrg* expression within the tower structures, a dual *cid*/*lrg* reporter strain was also generated. The *cid* promoter was fused to the gene encoding sGFP, and the *lrg* promoter was fused to the gene encoding DsRed.T3 (DNT). Wild-type UAMS-1 containing this construct was grown using the BioFlux system and observed during biofilm development. As shown in Figure 4-10, *lrg* expression (red fluorescence) was detected early in the development of the towers (12 h) followed by the emergence of *cid* expression (green fluorescence) as the towers increased in size (starting at 16 h). Distinct small towers expressing high levels of *cid* were also observed (arrows), similar to those produced by the P*cid*::gfp fusion strain (Figure 4-6). As shown in Figure 4-11, which illustrates the fluorescence detected using the different filter sets, the small towers clearly express a high level of *cid*-associated sGFP fluorescence and nearly undetectable levels of *lrg*-associated DsRed fluorescence, while the large towers express both promoters, albeit in different temporal

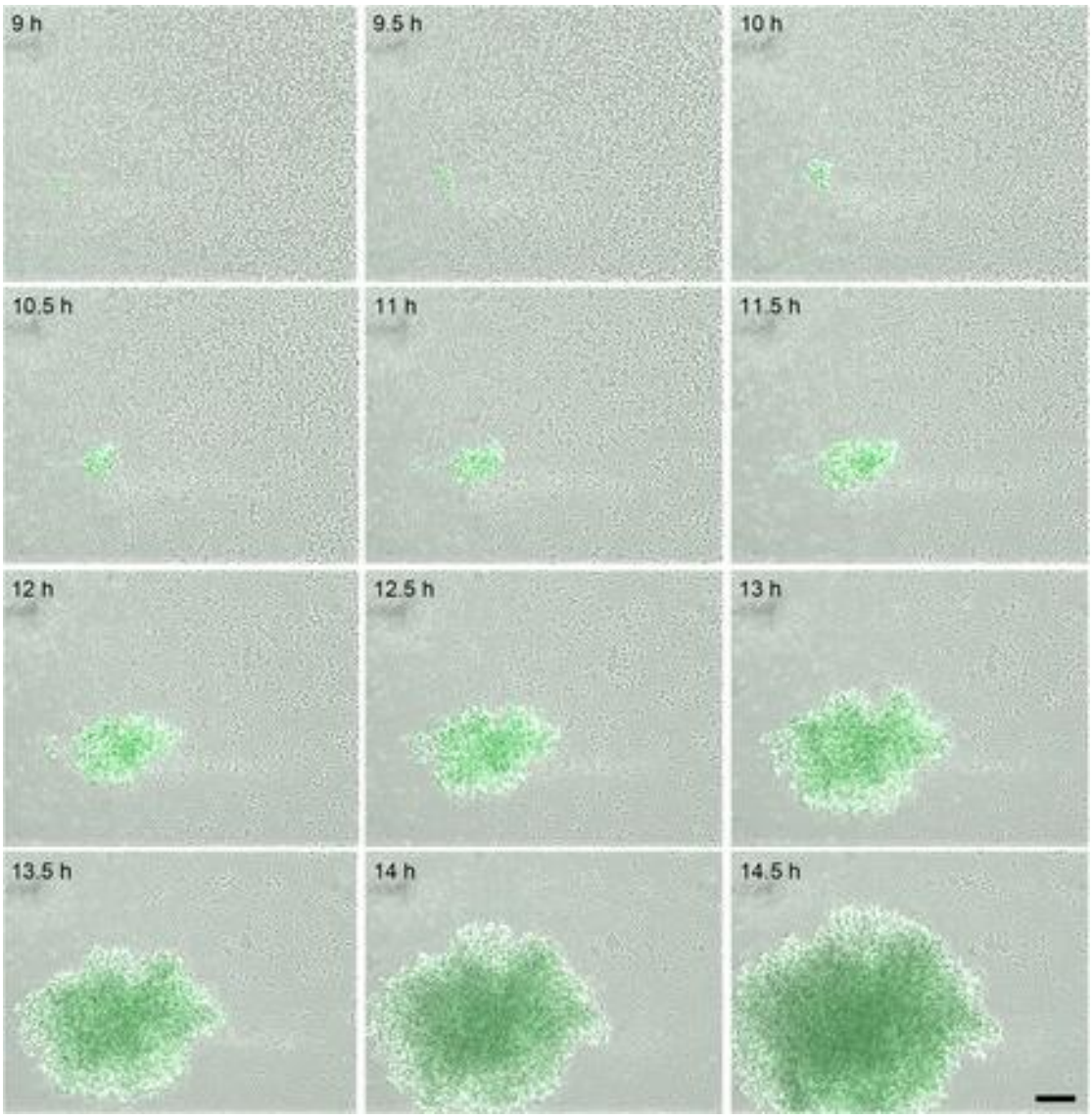

Figure 4-9 Temporal analysis of *lrgAB* expression during biofilm development

S. aureus cells containing the P*lrg*::*gfp* reporter plasmid were inoculated into a BioFlux microfluidic system and allowed to form a biofilm within a flow shear environment at a flow rate of 64 µl/h for a total of 18 h. Bright-field and epifluorescence microscopic images were collected at 5-min intervals at ×200 magnification. The images presented were taken from the complete set of 217 images spanning 9 to 14.5 h and illustrate typical tower development and GFP expression observed in multiple experiments. The scale bar represents 50 µm.

Figure modified from Moormeier et al. 2013. *AEM*

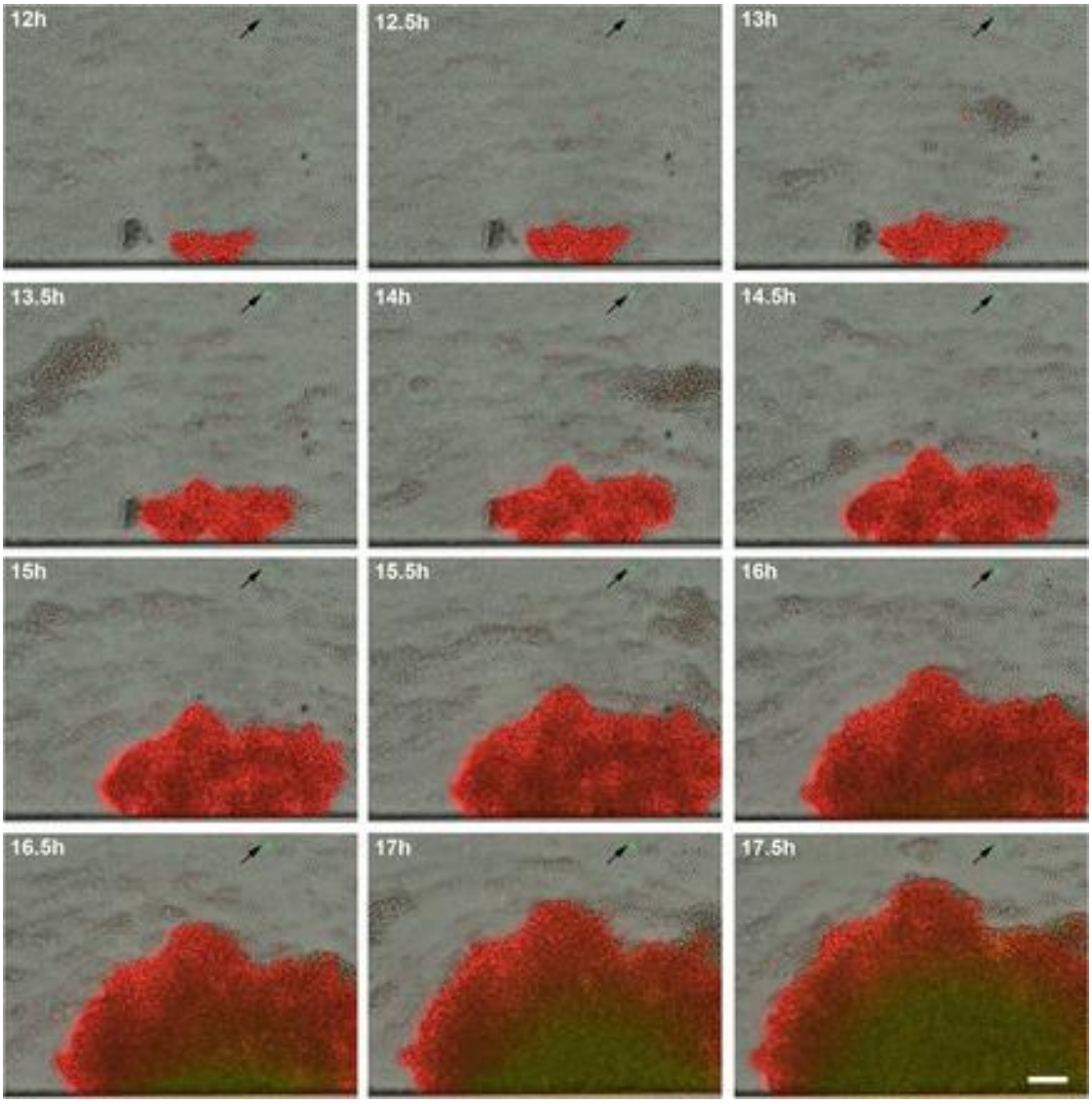

Figure 4-10 Simultaneous temporal analyses of *cidABC* and *lrgAB* expression during biofilm development

S. aureus cells containing the P*cid*::*gfp* and *Plrg*::*sDsRed* dual-reporter plasmid were inoculated into a BioFlux microfluidic system and allowed to form a biofilm within a flow shear environment at a flow rate of 64 µl/h for a total of 18 h. Bright-field and epifluorescence microscopic images were collected at 5-min intervals at ×200 magnification. The images presented were taken from the complete set of 217 images spanning 12 to 17.5 h and illustrate the typical tower development and GFP and DsRed.T3(DNT) expression observed in multiple experiments. The scale bar represents 50 µm. The arrows indicate the small, highly fluorescent *cid*-expressing towers.

Figure modified from Moormeier et al. 2013. *AEM*

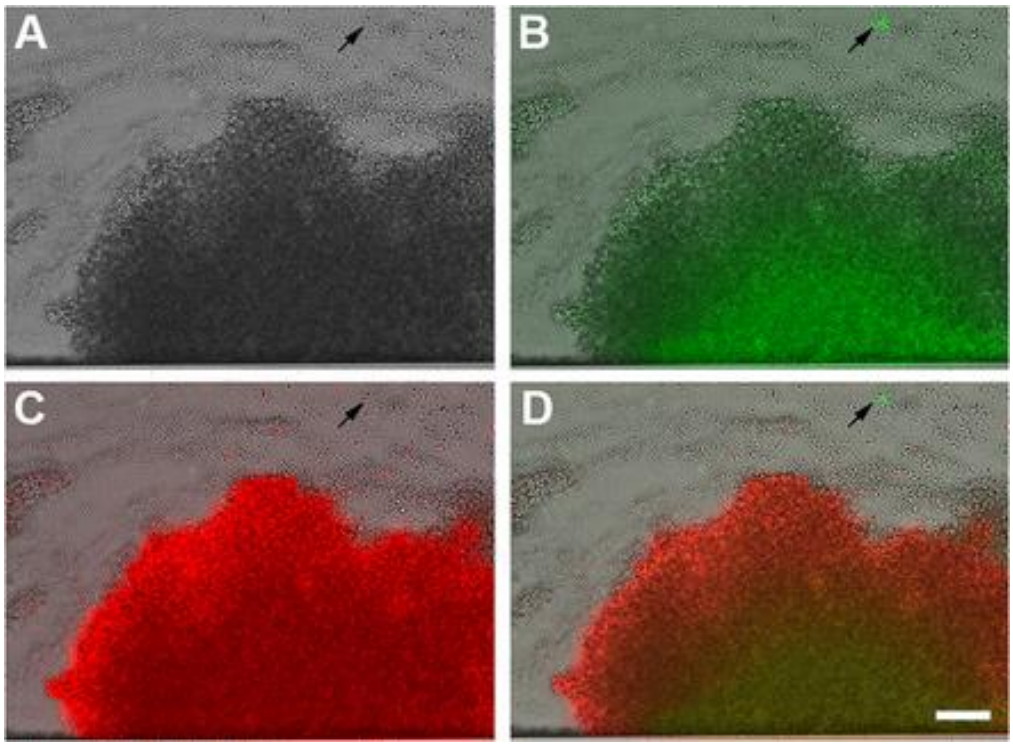

Figure 4-11 Differential expression of *cid* and *lrg* within different towers

The individual images collected at 17 h from Figure 4-10 are presented to better illustrate the green and red fluorescence produced by the *S. aureus* P*cid*::*gfp* and P*lrg*::*sDsRed*dual-reporter strain (at ×200 magnification). The panels include images collected by bright-field microscopy only (A), a bright-field microscopy and FITC overlay (B), a bright-field microscopy and TRITC overlay (C), and a bright-field microscopy, FITC, and TRITC overlay (D). The scale bar represents 50 µm. The arrows indicate the small, highly fluorescent *cid*-expressing towers.

Figure modified from Moormeier et al. 2013. *AEM*

patterns. These data confirm the existence of two distinct towers types, one that is characterized by rapid cell division, constitutive *lrg* expression, and gradual *cid* expression induced presumably as the tower enlarges and becomes hypoxic, and the other that exhibits relatively slow cell division and high, constitutive levels of *cid* expression.

Correlation of lrg expression with cell death and lysis

Previous studies using confocal laser scanning microscopy demonstrated that tower structures contain a high number of dead cells and/or eDNA as indicated using viability staining techniques (100). Subsequent lysis of the dead cells resulted in clear, cell-free voids that likely contain cell debris, including released genomic DNA. This pattern of death and lysis causing a "hollowing out" of tower structures appears to be conserved in other bacterial species (138, 234), including a positive role for *P. aeruginosa cid* and a negative role of *lrg* orthologs in this process (138). To determine if *cid* and/or *lrg* expression correlated with cell death and lysis under these flow-cell conditions, we grew our P*cid*::gfp and P*lrg*::gfp fusion constructs in the BioFlux system and stained the biofilm with propidium iodide (PI) to visualize dead cells and eDNA. As shown in Figure 4-11, the large towers expressing both *cid* and *lrg* were readily stained with PI, exhibiting a relatively uniform fluorescence intensity throughout these structures (see top and bottom panels), similar to the uniform GFP-mediated fluorescence produced by the P*lrg*::gfp fusion construct. Analysis of the temporal pattern of PI staining also corresponded well with *lrg* expression with staining of the tower occurring early in development and continuing as they grew in size. This is in contrast to the P*cid*::gfp reporter construct, which is expressed in the center of the tower structures only after they have reached a certain size, presumably corresponding to the hypoxic regions of the towers (see above). Interestingly, the smaller, intensely fluorescent green towers that

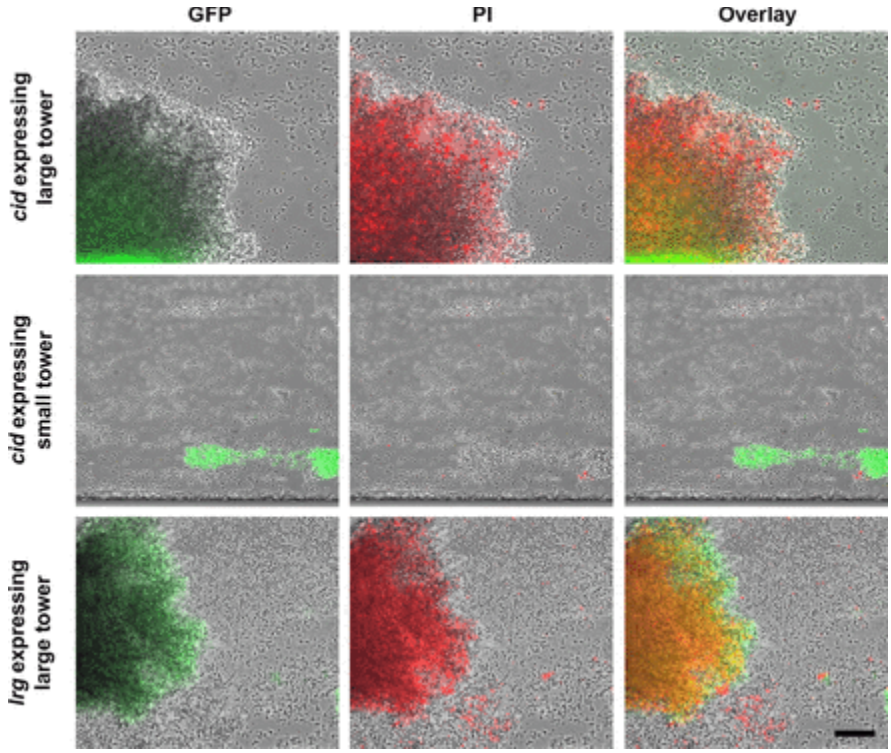

Figure 4-12 Correlation of eDNA/cell death with *cidABC* and *lrgAB* expression within a biofilm

S. aureus WT cells carrying the P*cid*::gfp and P*lrg*::gfp reporter plasmids were inoculated into a BioFlux microfluidic system and grown into biofilms as described in the legend to Figure 4-5. The biofilm was grown in 50% TSB medium containing 0.125 µM PI stain (184) to stain dead cells and eDNA. Individual images captured at 17 h demonstrate an overlap of *lrg* expression (green) and dead cells/eDNA (184) in large towers (top and bottom panels) and the absence of lrg expression and dead cells/eDNA in small towers (middle panels). The scale bar represents 50 µm.

Figure modified from Moormeier et al. 2013. *AEM.*

constitutively express the *cid* promoter (Figure 4-12; middle panels) did not retain the PI stain, also similar to the absence of expression observed in these structures (Figures 4-10 and 4-11). Overall, the results of these studies demonstrate an association with the patterns of *cid* and *lrg* expression within a developing biofilm corresponds with the presence of dead cells and/or eDNA in tower structures.

Mutations in Pta-AckA pathway increase highly-constitutive cid expressing small towers during biofilm development

Given the intimate relationship with overflow metabolic pathways and the changes in expression of the *cidABC* and *lrgAB* operons, we wanted to determine the effects that mutations in different metabolic pathways had on expression of the *cid* and *lrg* operons as wells as biofilm morphology. Recently, inactivation of the phosphotransacetylase-acetate kinase (Pta-AckA) pathway has been demonstrated to increase cell death and increased expression of the CidR regulon, which includes *cidABC* (154). Therefore, we moved our dual *cid* and *lrg* reporter plasmid (pDM4) into Δ*ackA::ermB* and Δ*pta* mutants and evaluated *cid* and *lrg* expression as well as biofilm morphologies. Strikingly, the Δ*ackA::ermB* and Δ*pta* mutants demonstrated increased *cidABC* expression, as well as an increased number of what appear to be the small high *cid*-expressing towers observed in the wild-type strain (Figure 4-13). Additionally, no lrg expression was observed in either mutant strain (Figure 4-13), in contrast to what was previously observed in these mutants grown planktonically (101). Together, these results demonstrate an intimate relationship between metabolic pathways and the expression of the *cid* and *lrg* operons and the changes that can occur during tower development in the later stages of biofilm development.

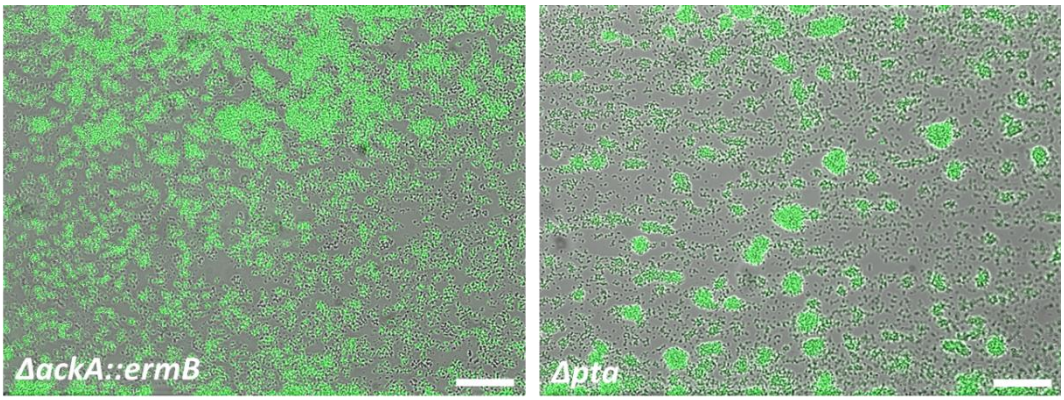

Figure 4-13 High-level *cid* expression and increased small towers in *ackA* and *pta* mutants during small formation

S. aureus mutants Δ*ackA::ermB* and Δ*pta* cells containing the P*cid*::*gfp* reporter plasmid were inoculated into a BioFlux microfluidic system and allowed to form a biofilm as described in the legend to Figure 4-5. The image shown (at ×200 magnification) represents a typical constitutive highly fluorescent “small” tower that is formed by this strain. The scale bar represents 50 μm.

DISCUSSION

Previous studies in our laboratory have suggested a role for *S. aureus cid*- and *lrg*-mediated cell death and lysis during biofilm development (99, 100). Implicit in this model is that there is heterogeneity in the expression of these operons such that only subpopulations of the biofilm cells will die and lyse. Indeed, viability stains clearly revealed marked heterogeneity in the distribution of dead cells within the basal biofilm layers, and more pronounced cell death and lysis associated with tower structures (100). Although these observations suggest that variations in *cid* and *lrg* expression may exist within different regions of a biofilm, our current understanding of *cid* and *lrg* regulation has been limited to studies in which the expression of these operons was assessed during planktonic growth, where the results generated represent an average level of expression throughout the population. For example, glucose metabolism in planktonic cultures was shown to induce *cidABC* expression via the LysR-type transcriptional regulator (LTTR) encoded by the *cidR* gene (143-145). Additionally, the two-component regulatory system, LytSR, was shown to induce *lrgAB* transcription in response to changes in membrane potential (146, 159). Although both of these studies provided an appreciation for the metabolic signals important in the control of *cid* and *lrg* expression, neither afforded any insight into the heterogeneity of gene expression within the population nor how expression of these operons might be affected by growth in the context of a multicellular biofilm. Thus, a key focus of this study is to gain a better understanding of how these and/or related metabolic signals are involved in coordinating *cid* and *lrg* expression during biofilm development.

In the first part of this study, we demonstrate that in addition to being induced by growth in the presence of excess glucose, *cid* expression is also induced during growth in a hypoxic environment (Figure 4-1), conditions known to predominate within a biofilm.

In fact, aerobic growth in the presence of excess glucose is well-known to induce a physiological change in cells that results in a shift from oxidative phosphorylation to substrate-level phosphorylation in which less oxygen is consumed (235). This so-called “Crabtree effect” may, thus, produce metabolic intermediates during aerobic growth that stimulate CidR-dependent expression of the *cid* operon that would normally be produced during hypoxic growth. In agreement with the notion that similar metabolic signals are sensed during these seemingly disparate conditions is the observation that *cid* expression under hypoxic conditions was found to be *cidR* dependent, similar to the induction of this operon during growth in the presence of excess glucose (Figure 4-1). As *cidR* encodes a member of the LysR-type transcription regulator (LTTR) family of proteins, whose members are activated by the binding of specific small effector molecules, the effector interacting with CidR likely reflects the metabolic similarities that form the basis of the Crabtree effect. Although the identity of this molecule remains to be determined, it was recently speculated that pyruvate or an intermediate of pyruvate metabolism could serve this purpose based on the observations that CidR-mediated control occurs under conditions favoring fermentative metabolism, as well as the fact that the CidR regulon includes two operons, both of which encode enzymes involved in pyruvate metabolism (231). Interestingly, recent studies indicate that pyruvate plays a key role in the formation of microcolonies in *Pseudomonas aeruginosa* (236).

It seems clear that the expression and/or function of the *cid* and *lrg* operons must be a population-dependent phenomenon, given the observation that there is a mixture of live and dead cells within biofilms. Because cell death and lysis are particularly predominant within tower structures (100), we hypothesized that the level of *cid* expression relative to *lrg* is increased in tower structures compared to the surrounding basal layer of cells (123). The differences in expression may be a function of localized

microenvironments in which reduced oxygen is present. Indeed, oxygen and nutrient gradients have been shown to exist in biofilm and have been implicated in signaling heterogeneity within the biofilm (142, 237, 238). Furthermore, *P. aeruginosa* (239, 240) and *B. subtilis* (241-243) demonstrate heterogeneous expression of genes within the biofilms they produce. Based on the impact of hypoxic growth on *cid* and *lrg* expression, we reasoned that variations in oxygen levels within a biofilm play an important role in the differential control of *cid* and *lrg* expression, and subsequent cell death and lysis within these metabolically diverse communities. Thus, to examine the differential control of *cid* and *lrg* expression during biofilm development, transcriptional fusions of *cid* and *lrg* promoter regions with a *gfp* reporter gene were generated and introduced into *S. aureus* wild-type, *cidR*, and *lytSR* mutant strains. We took advantage of newly developed BioFlux technology (147) that allowed us to simultaneously monitor biofilm growth and reporter gene expression under flow-cell conditions over an extended time-course experiment, mimicking a more physiologically relevant environment. Strikingly, growth of the *cid* and *lrg* reporter strains revealed clear temporal and spatial control of these genes. For the *cid::gfp* strain, fluorescence increased over time in large tower structures (Figure 4-5 and Figure 4-10), similar to the *ldh::gfp* strain (Figure 4-6) and consistent with the hypothesis that reduced oxygen levels within these structures was responsible for the up-regulation of these genes. In addition, a second highly fluorescent subpopulation of cells was observed in the *cid::gfp* fusion strain that was clearly distinct from those associated with large tower structures (Figures 4-7, 4-10, and 4-11). In contrast to the latter, the highly fluorescent subpopulation appeared to emerge from single cells that multiplied and formed distinct tower structures that appeared less adherent as evidenced by the observation that they tended to release small cell clusters likely as a result of shear forces in this flow-cell environment (Figure 4-7). Thus, the differences in gene expression observed between the two tower types identified in this

study appear to be associated with fundamentally distinct physical characteristics, such as matrix composition, although this remains to be investigated. Importantly, the lack of a genetically stable highly fluorescent population of cells within the effluent (data not shown) suggests these highly fluorescent towers are not a result of a regulatory mutation (e.g. - within the *cidR* gene).

The *lrgAB::gfp* strain also generated a fluorescent signal that was associated with tower structures (Figure 4-9). Although the kinetics of this induction were clearly distinct compared to the delayed, gradual emergence of fluorescence observed in the large towers produced by the P*cid::gfp* and P*ldh1::gfp* fusion strains, it was similar in some respects to the small towers expressing high levels of GFP fluorescence. However, a dual reporter construct allowed us to determine the relationship between *cid* and *lrg* expression within individual towers and clearly demonstrated that towers exhibiting a gradual increase in *cid* expression were also constitutively expressing *lrg*. In contrast, towers expressing constitutively high *cid* levels were expressing low to undetectable levels of *lrg*. The differences in *cid* and *lrg* expression undoubtedly reflect the fact that expression of these operons is controlled by distinct regulatory systems that respond to different metabolic signals. Thus, gaining a better appreciation for the metabolic cues sensed by the CidR and LytSR regulatory systems, as well as the metabolic differences between these tower types, will be essential for understanding the basis for the expression differences observed.

Given the proposed functions of the *cid* and *lrg* operons, we next wanted to examine the correlation between expression of these genes in a biofilm, and the death and lysis that occurs in these structures. As shown in Figure 4-12, analyses of the *cid* reporter construct revealed that the GFP signal produced by the *cid::gfp* strain overlapped with the PI staining, which was previously shown to be particularly evident in

these structures (100). However, it is clear that this overlap is incomplete as evidenced by the observation that the high-level expression observed in the smaller towers was not associated with PI staining (Figure 4-12, middle row panels). In contrast, fluorescence produced by the *lrg::gfp* strain correlated much better with the PI-stained structures (Figure 4-12, bottom row panels) exhibiting homogeneous fluorescence throughout the large towers and no fluorescence in the small towers. Since the *cidA* and *lrgA* gene products are proposed effectors of cell death and lysis, one might predict that the disruption of these genes would affect the death and/or lysis observed by PI staining. However, similar experiments using *cid* and *lrg* mutants harboring the *cid* and *lrg* GFP reporter constructs revealed no obvious effect on the pattern of cell death and lysis (as indicated by PI staining; data not shown), suggesting that the roles of these genes are not readily detectable under these conditions. One scenario is that the Cid and Lrg proteins encoded by these operons simply potentiate cell death and under biofilm conditions makes this process more efficient. In fact, holin proteins function much like this as they are expressed and inserted in the membrane in an inactive form and can be induced by lethal agents that dissipate the membrane potential (244). Similarly, altered expression of members of the Bcl-2 family of proteins, critical in the control of apoptosis, does not directly affect cell viability but instead, potentiates cell death or survival depending on the relative levels of death effectors or inhibitors that are present in the cell (245). Another hypothesis is that this BioFlux1000 system uses two-dimensional image acquisition software and microfluidic flow-cell conditions. These capabilities may not have the sensitivity to evaluate slight changes in biofilm morphology like previously described flow-cell biofilms that have taken advantage of confocal scanning laser microscopy to render three-dimensional images and quantify subtle changes using sophisticated biofilm quantification software called COMSTAT (246).

Given the apparent fundamental differences in gene expression and physical properties of large versus small towers, a better understanding of the relative physiological differences between these tower types should provide valuable information about the control of cell death during biofilm development. Furthermore, insight into the potential functional differences that are associated with spatially and temporally regulated genes within the biofilm, as has been observed in *Bacillus subtilis* (247), could be particularly enlightening. Thus, current studies using Bioflux technology are aimed at using fluorescent metabolic probes that will allow us to correlate the temporal and spatial aspects of *cid* and *lrg* expression with differential physiological states within biofilm microenvironments, providing more mechanistic and functional insights into the heterogeneous control of cell death and lysis observed within a developing biofilm.

CHAPTER V:

CONCLUSIONS AND FUTURE DIRECTIONS

In this dissertation, we have developed a model of *S. aureus* biofilm development using the BioFlux1000 microfluidic device that is described in five sequential stages: 1. attachment, 2. multiplication, 3. exodus, 4. tower maturation, and 5. dispersal (Figure 5-1). More specifically, *S. aureus* biofilms cells first attach to the bottom of the glass bottom plates (Figure 5-1A). Then, as fresh media is perfused across attached cells, the biofilm develops into a confluent 'mat' of cells (multiplication) (Figure 5-1B). Upon reaching confluency, a period of mass exodus of cells occurs in which a subpopulation of cells is released from the biofilm (Figure 5-1C) allowing the formation of distinct three-dimensional structures. These structures, designated as towers, form from distinct foci of cells that rapidly divide to form robust aggregations (Figure 5-1D). It is at this point that portions of the tower begin to disperse to start the process again (Figure 5-1E).

Attachment and Multiplication

During the attachment and multiplication stages, we discovered under these flow-cell conditions that this phase appears to rely primarily on proteins, rather than eDNA or PIA, given that the initial stages of development are susceptible to proteinase K treatment. In addition, we also discovered that proteins such as AtlA and δ-toxin potentially interact with the glass surface of the BioFlux plate presumably through charge interactions. Additionally, by screening the Nebraska Transposon Mutant Library, we found that most LPXTG-motif containing proteins and MSCRAMM proteins appeared to not have a major role during the initial stages. However, it cannot be ruled out

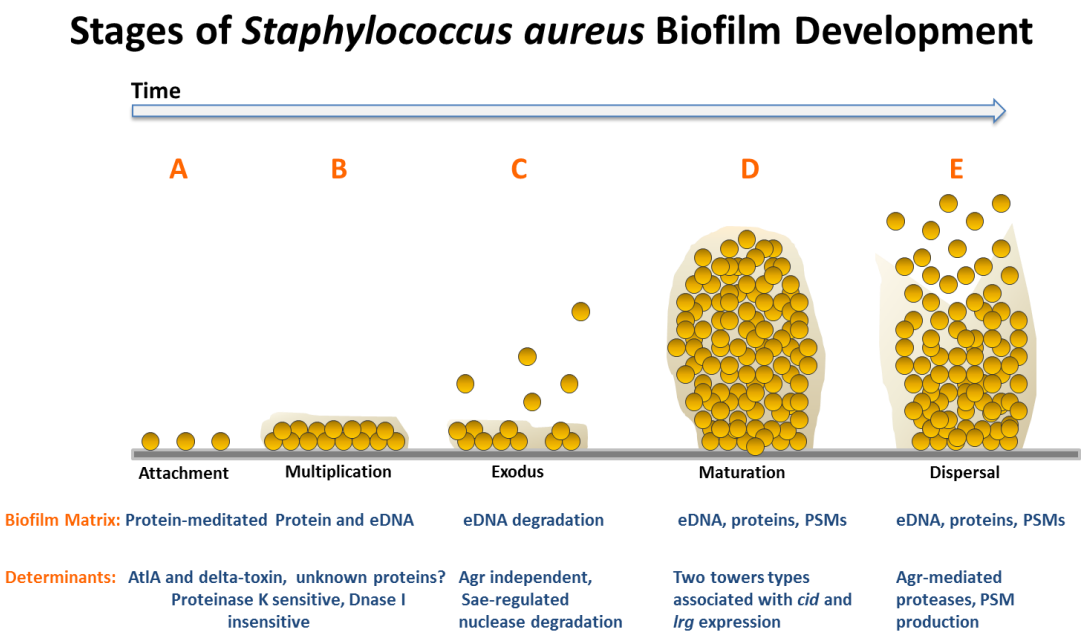

Figure 5-1 Working model of *Staphylococcus aureus* biofilm development in BioFlux1000

S. aureus biofilm development using the BioFlux1000 microfluidic device is described in five stages: 1. attachment, 2. multiplication, 3. exodus, 4. tower maturation, and 5. dispersal. (Figure 5-1A; Attachment) *S. aureus* biofilms cells first attach to the bottom of the glass bottom plates. (Figure 5-1B; Multiplication) As fresh media is perfused across attached cells, the biofilm develops into a confluent 'mat' of cells. (Figure 5-1C; Exodus) Upon reaching confluency, a period of mass exodus of cells occurs in which a subpopulation of cells is released from the biofilm allowing the formation of distinct three-dimensional structures. (Figure 5-1D; Tower Maturation) These structures, designated as towers, form from distinct foci of cells that rapidly divide to form robust aggregations. (Figure 5-1E; Dispersal) It is at this point that portions of the tower begin to disperse to start the process again.

that there may be involvement of more than one of these proteins, and that disruption of a single gene encoding one of these proteins may not cause a large enough defect to see any changes in biofilm development.

To continue to determine the functions that the AtlA protein has during biofilm development, a more detailed approach must be taken. Given that AtlA is the major autolysin of *S. aureus,* we cannot rule out that the fact that a defect in this protein will generate cells with a defective cell wall that could lead to drastic effects on the placement of extracellular proteins of the cell surface or in a developing biofilm. Therefore, further genetic approaches using point mutations aimed at dissecting the enzymatic activity in conjunction with extracellular protein profiling of these may provide results that can determine whether or not a defective AtlA is disrupting proper extracellular protein placement. In addition to processing the cell wall of *S. aureus*, the glucosaminidase domain of AtlA has also been shown to bind DNA suggesting that there may be a potential eDNA-protein interaction that is occurring within the biofilm matrix. Hence, using DNA-specific stains and/or antibodies in combination with genetic mutations of the DNA-binding domain may aid in determining the effects that AtlA has a possible eDNA-binding protein. Lastly, AtlA also serves as a mediator of lysis and eDNA release during biofilm development. In order to better understand this process, genetic mutations disrupting functional enzymatic activity may provide immense information on how this process is occurring.

The PSMs including δ-toxin are well-characterized in their functions in *S. aureus* biofilm development. Nonetheless, to determine if there is a direct function of δ-toxin under our biofilm conditions, either a δ-toxin mutant must be obtained or constructed and then evaluated for biofilm development in the BioFlux1000. One complicating issue with studying the δ-toxin is that the *hld* gene resides within the RNAIII-transcript (116).

Therefore, a mutant with a generated translational termination site that does not interfere with the RNAIII transcript would need to be generated. Based, on previous reports evaluating the role of δ-toxin and the other PSMS in biofilm development (117), we hypothesize that we would see robust biofilm growth after the exodus stage in a δ-toxin mutant when compared to wild-type.

In addition to the large contribution of extracellular proteins to the biofilm ECM during the attachment and multiplication stages, there also appears to be a contribution of eDNA, given that a defective nuclease causes abrogation of the exodus event. As discussed before, there may be eDNA-protein interactions that act as scaffold for the biofilm matrix. One particularly interesting group of eDNA-binding proteins are the nucleoid- associated proteins (NAPs) which have been shown to have a function in the ECM of staphylococcal biofilms (107). To determine if NAPs indeed have function in biofilm scaffolding, the first thought would be to construct a mutation in the gene encoding the NAP protein. However, this is impossible because the protein is essential to *S. aureus* survival (193). An additional factor that may complicate studying this protein is that disruption of a gene that is important for chromosomal condensation may have drastic effects on global regulation within the cell and not solely on eDNA-protein interactions in the biofilm ECM. Thus, non-mutational microscopy approaches utilizing eDNA specific stains and/or antibodies in conjunction with NAP-specific antibodies are currently being conducted to determine if there are NAP-eDNA interactions contributing to the ECM within the multiplication stage.

One major complicating issue that often causes disagreement between investigators on which molecular determinants are important for biofilm development is that researchers use varying degrees of biofilm conditions including different types of media, shear stresses, and plasma coating. Therefore, to continue to determine the

potential functions that some of these previously described proteins have in biofilm development, we must test our mutants in several experimental conditions. One simple experimental condition to change would be to coat the microfluidic channels of the BioFlux with host substrates that are found in human plasma rather than allowing the cells to adhere directly to the glass bottom of the BioFlux plate. This has already been performed in a recent study where the *S. aureus* cells were allowed to adhere to human plasma. Under these conditions, the authors discovered that *saeRS* mutants actually generated less overall biofilm development when compared to their respective UAMS-1 and JE2 wild-types even under similar shear stress conditions (42). This is directly opposing to what was discovered in our studies in this dissertation. Thus, the mutants used throughout in this dissertation must also be examined under various experimental biofilm conditions to determine if their functions are dependent on other biological conditions.

Exodus

The exodus stage is an early biofilm dispersal stages that precedes the maturation of tower structures. It was first described in these studies and was named this to delineate between the Agr-mediated dispersal events that have been described vigorously in the literature. While exodus was first described in these studies, in the past, there have been several reports describing that *S. aureus* produces nucleases that modulate biofilm development by degrading eDNA within the ECM. However, none of these previous studies provided as much detail into the timing and regulation. As described in these studies, exodus is clearly mediated by the degradation of eDNA by the secreted nuclease, and is tightly regulated by the multi-component Sae system.

Indeed, the Sae system regulates the exodus process so tightly that only a subpopulation of cells expresses nuclease. In further support of this, the subpopulation of cells becomes highly dysregulated when genes within the sae operon begin to be mutated.

One question is why does disruption of the gene encoding the SaeP protein cause every cell within the biofilm to express nuclease and other Sae-regulated factors? As previously discussed, this may be because deletion of SaeP cannot form a complex with SaeQ to activate the phosphatase activity of SaeS causing the cells to lack a mediator of self-control in SaeS phosphorylation, and uncontrolled transcription levels of Sae-regulated factors. Another thought is that the SaeP protein located on the surface of the subpopulation of cells is binding eDNA within the ECM, and thus, unable to interact with SaeQ to repress transcription of Sae-regulated genes. This makes sense considering when *saeP* is deleted all of the cells in the biofilm transcribe the gene encoding nuclease and staphylocoagulase. From these data, it's obvious that the next steps are to determine the eDNA-binding sites in SaeP, and then genetically mutate these sites and determine the effect on nuclease expression in both biofilm and planktonic studies. Considering that there are recent examples of different bacterial species including *B. subtilis, P. aeruginosa*, and *Caulobacter crescentus* (204) that sense the constituents of the biofilm matrix and regulate specific genetic programs within the biofilm cells, *S. aureus* may also undergo a similar process to utilize the Sae system to sense eDNA concentrations with ECM to trigger a dispersal mechanism.

Another obvious question that can easily be addressed is how many different Sae-regulated genes demonstrate similar expression patterns within a biofilm when compared to nuclease? This can addressed by constructing additional dual fluorescent promoter fusion constructs of Sae-controlled genes such as *hla, hlb, fnbA, efb, P1sae,*

sbi, fib and *cap*, and then moving these constructs into the *sae* mutant backgrounds and evaluating the effects that they have on expression within a developing biofilm. Indeed, these constructs are currently being generated in the laboratory. In combination with this method, our laboratory is also attempting to remove the biofilms from the microfluidic channels by using enzymatic destruction of the biofilm matrix, and then conducting fluorescence-activated cell sorting flow cytometry to not only count the number of fluorescently positive cells, but to also sort the cells for further transcriptomic and proteomic analyses. Considering that there are two target classes of Sae regulation that rely on the phosphorylation of SaeS, we hypothesize that not all of the Sae-controlled genes will be demonstrate stochastic expression in a subpopulation of cells like nuclease. However, we predict that genes in the same Sae target class will demonstrate similar expression patterns.

Tower Maturation

The studies presented here provide further confirmation that biofilms are multicellular communities that contain both physiologic and metabolic heterogeneity. Perhaps, one of the most obvious examples of heterogeneity in *S. aureus* biofilm development is the tower maturation stage. It is in this stage where two distinct tower types are formed. First, following the exodus stage, there are the large tower types that rapidly divide from a distinct to foci to form large robust structures. Within these developing towers, we observed differential regulation of the cell death operons, *cidABC* and *lrgAB.* More specifically, the large towers demonstrated constitutive expression of the *lrgAB* operon throughout the entire time of development. Conversely, *cidABC* expression was not observed until the tower reached a particular robust size, at which

point, expression was seen within the most internal regions of the tower. We hypothesized that this internal *cid* expression was due to hypoxic conditions with the tower structure. Thus, we tested an *ldh1* reporter fusion, known to be expressed under hypoxic conditions, to determine similar expression patterns. This suggested an intimate connection with the metabolic status of the cell within the towers. In addition to the large tower types, there were was also the emergence of small tower types that developed from distinct foci of cells also. However, the small towers appeared to be less cohesive and grew more slowly when compared to their larger counterparts. In addition, these smaller tower types constitutively expressed *cid,* but interestingly, did not express *lrg,* suggesting another form of differential regulation. Strikingly, cell death and eDNA were only observed in the large tower types.

Given the intimate relationship that these operons have shown with the metabolic status of the cell, in particular overflow metabolism, we hypothesize that these expression differences are in response to metabolic status in the cells. In support of this when we evaluated mutations Pta-AckA pathway, we saw increased *cid* expression as well as the increased prevalence of small towers. Expanding upon these data, a recent study from our laboratory also demonstrated a direct relationship with acid stress and *S. aureus* biofilm formation. Under the BioFlux biofilm conditions, there were no distinguishable differences in biofilm morphology between mutations in either the *cid* or *lrg* operons. However, under other flow cell conditions there was a clear connection in tower formation and regulation of cell death genes, *cidC* and *alsSD,* both of which are regulated by the CidR regulon, (103). In addition to this, another study from the laboratory showed that genetic mutations effecting the signal transduction of the LytSR two-component, the primary regulator of *lrgAB,* developed unique biofilm characteristics (101).

Considering the close relationship with *cid* and *lrg* operons and the effects seen on *S. aureus* biofilm development, one would think that an obvious way to evaluate the effects of metabolism on these cell death operons would be to delete genes encoding important enzymes in key metabolic pathways. However, this produces a couple of caveats when looking at biofilm formation. One, deletion of metabolic enzymes often has significant grown defects, making it extremely difficult to compare biofilm morphologies of mutants to wild-type. Two, *S. aureus* is very adaptable organism and has several ways to obtain and utilize carbon to ensure survival; therefore, mutating one metabolic enzyme may cause a shift in carbon to another pathway making it difficult to determine differences in biofilm formation. Last, some metabolic enzymes are essential to the growth of the organism and cannot be disrupted. To circumvent these caveats, we are currently designing fluorescent promoter reporter fusions to key enzymes involved in carbon metabolism. Although these may not provide a direct indication of activity of these enzymes, they can provide insight in to where these enzymes are being expressed and whether or not they correlate with the expression of *cid* and *lrg* during biofilm formation. Additionally, if cells expressing these reporter fusions linked to metabolic enzymes can be sorted using flow cytometry, transcriptomic and proteomic analyses may be performed to provide further insight to protein production and activity. In conjunction with fluorescent reporters, the use of stains or dyes that indicate the metabolic state of the cell are also currently being considered to aid in determining the metabolism within a developing biofilm.

Another interesting question is why does *S. aureus* want to form towers? Typically, we think of thicker biofilms as being more resistant to antibiotics and other antimicrobials. While this is usually the case, there is some data in other bacterial species like *Pseudomonas* species suggesting that formation of tower-like structures in

aid in resistance to antimicrobials (211). Hence, we are also currently designing experiments to test the resistance of cells within the towers to antibiotics or other antimicrobials.

In conclusion, the standardization of the BioFlux1000 microfluidic flow-cell system to cultivate *S. aureus* biofilms has provided unprecedented views of the stages of biofilm development in real-time manner. The results of these studies also further demonstrate the unique multicellular and heterogeneity characteristics of *S. aureus* biofilms. Clearly, there is much more to be learned about the regulation of the Sae-controlled nuclease-mediated exodus event and the signal that triggers nuclease expression as well as the metabolic heterogeneity that determines the expression of the *cidABC* and *lrgAB* operons. Still, these studies have laid the fundamental groundwork for further studies to expand upon these fascinating processes in hope of a better understanding *S. aureus* biofilm development to create novel anti-biofilm therapeutic strategies.

REFERENCES

1. **Kuehnert MJ, Kruszon-Moran D, Hill HA, McQuillan G, McAllister SK, Fosheim G, McDougal LK, Chaitram J, Jensen B, Fridkin SK, Killgore G, Tenover FC.** 2006. Prevalence of Staphylococcus aureus nasal colonization in the United States, 2001-2002. J Infect Dis **193:**172-179.
2. **DeLeo FR, Otto M, Kreiswirth BN, Chambers HF.** 2010. Community-associated meticillin-resistant Staphylococcus aureus. Lancet **375:**1557-1568.
3. **Frank DN, Feazel LM, Bessesen MT, Price CS, Janoff EN, Pace NR.** 2010. The human nasal microbiota and Staphylococcus aureus carriage. PloS one **5:**e10598.
4. **Wertheim HF, Melles DC, Vos MC, van Leeuwen W, van Belkum A, Verbrugh HA, Nouwen JL.** 2005. The role of nasal carriage in Staphylococcus aureus infections. Lancet Infect Dis **5:**751-762.
5. **Tong SY, Davis JS, Eichenberger E, Holland TL, Fowler VG, Jr.** 2015. Staphylococcus aureus infections: epidemiology, pathophysiology, clinical manifestations, and management. Clin Microbiol Rev **28:**603-661.
6. **Fowler VG, Jr., Miro JM, Hoen B, Cabell CH, Abrutyn E, Rubinstein E, Corey GR, Spelman D, Bradley SF, Barsic B, Pappas PA, Anstrom KJ, Wray D, Fortes CQ, Anguera I, Athan E, Jones P, van der Meer JT, Elliott TS, Levine DP, Bayer AS, Investigators ICE.** 2005. Staphylococcus aureus endocarditis: a consequence of medical progress. JAMA **293:**3012-3021.
7. **Wenzel RP, Edmond MB.** 2001. The impact of hospital-acquired bloodstream infections. Emerg Infect Dis **7:**174-177.
8. **Parvizi J, Pawasarat IM, Azzam KA, Joshi A, Hansen EN, Bozic KJ.** 2010. Periprosthetic joint infection: the economic impact of methicillin-resistant infections. J Arthroplasty **25:**103-107.

9. **Song X, Perencevich E, Campos J, Short BL, Singh N.** 2010. Clinical and economic impact of methicillin-resistant Staphylococcus aureus colonization or infection on neonates in intensive care units. Infect Control Hosp Epidemiol **31:**177-182.

10. **Kirby WM.** 1944. Extraction of a Highly Potent Penicillin Inactivator from Penicillin Resistant Staphylococci. Science **99:**452-453.

11. **Barber M, Rozwadowska-Dowzenko M.** 1948. Infection by penicillin-resistant staphylococci. Lancet **2:**641-644.

12. **Rountree PM, Freeman BM.** 1955. Infections caused by a particular phage type of Staphylococcus aureus. Med J Aust **42:**157-161.

13. **Barber M.** 1961. Methicillin-resistant staphylococci. J Clin Pathol **14:**385-393.

14. **Herold BC, Immergluck LC, Maranan MC, Lauderdale DS, Gaskin RE, Boyle-Vavra S, Leitch CD, Daum RS.** 1998. Community-acquired methicillin-resistant Staphylococcus aureus in children with no identified predisposing risk. JAMA **279:**593-598.

15. **Moran GJ, Krishnadasan A, Gorwitz RJ, Fosheim GE, McDougal LK, Carey RB, Talan DA, Group EMINS.** 2006. Methicillin-resistant S. aureus infections among patients in the emergency department. N Engl J Med **355:**666-674.

16. **Fridkin SK, Hageman JC, Morrison M, Sanza LT, Como-Sabetti K, Jernigan JA, Harriman K, Harrison LH, Lynfield R, Farley MM, Active Bacterial Core Surveillance Program of the Emerging Infections Program N.** 2005. Methicillin-resistant Staphylococcus aureus disease in three communities. N Engl J Med **352:**1436-1444.

17. **Hiramatsu K, Aritaka N, Hanaki H, Kawasaki S, Hosoda Y, Hori S, Fukuchi Y, Kobayashi I.** 1997. Dissemination in Japanese hospitals of strains of

Staphylococcus aureus heterogeneously resistant to vancomycin. Lancet **350:**1670-1673.

18. **Weigel LM, Clewell DB, Gill SR, Clark NC, McDougal LK, Flannagan SE, Kolonay JF, Shetty J, Killgore GE, Tenover FC.** 2003. Genetic analysis of a high-level vancomycin-resistant isolate of Staphylococcus aureus. Science **302:**1569-1571.
19. **Otto M.** 2014. Staphylococcus aureus toxins. Curr Opin Microbiol **17:**32-37.
20. **Berube BJ, Bubeck Wardenburg J.** 2013. Staphylococcus aureus alpha-toxin: nearly a century of intrigue. Toxins (Basel) **5:**1140-1166.
21. **Valeva A, Walev I, Pinkernell M, Walker B, Bayley H, Palmer M, Bhakdi S.** 1997. Transmembrane beta-barrel of staphylococcal alpha-toxin forms in sensitive but not in resistant cells. Proceedings of the National Academy of Sciences of the United States of America **94:**11607-11611.
22. **Wilke GA, Bubeck Wardenburg J.** 2010. Role of a disintegrin and metalloprotease 10 in Staphylococcus aureus alpha-hemolysin-mediated cellular injury. Proceedings of the National Academy of Sciences of the United States of America **107:**13473-13478.
23. **Spaan AN, Henry T, van Rooijen WJ, Perret M, Badiou C, Aerts PC, Kemmink J, de Haas CJ, van Kessel KP, Vandenesch F, Lina G, van Strijp JA.** 2013. The staphylococcal toxin Panton-Valentine Leukocidin targets human C5a receptors. Cell host & microbe **13:**584-594.
24. **DuMont AL, Yoong P, Day CJ, Alonzo F, 3rd, McDonald WH, Jennings MP, Torres VJ.** 2013. Staphylococcus aureus LukAB cytotoxin kills human neutrophils by targeting the CD11b subunit of the integrin Mac-1. Proceedings of the National Academy of Sciences of the United States of America **110:**10794-10799.

25. **Alonzo F, 3rd, Kozhaya L, Rawlings SA, Reyes-Robles T, DuMont AL, Myszka DG, Landau NR, Unutmaz D, Torres VJ.** 2013. CCR5 is a receptor for Staphylococcus aureus leukotoxin ED. Nature **493:**51-55.

26. **Spaan AN, Vrieling M, Wallet P, Badiou C, Reyes-Robles T, Ohneck EA, Benito Y, de Haas CJ, Day CJ, Jennings MP, Lina G, Vandenesch F, van Kessel KP, Torres VJ, van Strijp JA, Henry T.** 2014. The staphylococcal toxins gamma-haemolysin AB and CB differentially target phagocytes by employing specific chemokine receptors. Nature communications **5:**5438.

27. **Peschel A, Otto M.** 2013. Phenol-soluble modulins and staphylococcal infection. Nature reviews. Microbiology **11:**667-673.

28. **de Haas CJ, Veldkamp KE, Peschel A, Weerkamp F, Van Wamel WJ, Heezius EC, Poppelier MJ, Van Kessel KP, van Strijp JA.** 2004. Chemotaxis inhibitory protein of Staphylococcus aureus, a bacterial antiinflammatory agent. J Exp Med **199:**687-695.

29. **Hennekinne JA, De Buyser ML, Dragacci S.** 2012. Staphylococcus aureus and its food poisoning toxins: characterization and outbreak investigation. FEMS Microbiol Rev **36:**815-836.

30. **Bergdoll MS, Crass BA, Reiser RF, Robbins RN, Davis JP.** 1981. A new staphylococcal enterotoxin, enterotoxin F, associated with toxic-shock-syndrome Staphylococcus aureus isolates. Lancet **1:**1017-1021.

31. **Schlievert PM, Shands KN, Dan BB, Schmid GP, Nishimura RD.** 1981. Identification and characterization of an exotoxin from Staphylococcus aureus associated with toxic-shock syndrome. J Infect Dis **143:**509-516.

32. **Li H, Llera A, Malchiodi EL, Mariuzza RA.** 1999. The structural basis of T cell activation by superantigens. Annu Rev Immunol **17:**435-466.

33. **Mootz JM, Malone CL, Shaw LN, Horswill AR.** 2013. Staphopains modulate *Staphylococcus aureus* biofilm integrity. Infection and immunity **81:**3227-3238.

34. **Kolar SL, Ibarra JA, Rivera FE, Mootz JM, Davenport JE, Stevens SM, Horswill AR, Shaw LN.** 2013. Extracellular proteases are key mediators of *Staphylococcus aureus* virulence via the global modulation of virulence-determinant stability. Microbiologyopen **2:**18-34.

35. **Nickerson NN, Joag V, McGavin MJ.** 2008. Rapid autocatalytic activation of the M4 metalloprotease aureolysin is controlled by a conserved N-terminal fungalysin-thermolysin-propeptide domain. Molecular microbiology **69:**1530-1543.

36. **Nickerson N, Ip J, Passos DT, McGavin MJ.** 2010. Comparison of Staphopain A (ScpA) and B (SspB) precursor activation mechanisms reveals unique secretion kinetics of proSspB (Staphopain B), and a different interaction with its cognate Staphostatin, SspC. Molecular microbiology **75:**161-177.

37. **Drapeau GR.** 1978. Role of metalloprotease in activation of the precursor of staphylococcal protease. Journal of bacteriology **136:**607-613.

38. **Massimi I, Park E, Rice K, Muller-Esterl W, Sauder D, McGavin MJ.** 2002. Identification of a novel maturation mechanism and restricted substrate specificity for the SspB cysteine protease of Staphylococcus aureus. The Journal of biological chemistry **277:**41770-41777.

39. **Cheng AG, McAdow M, Kim HK, Bae T, Missiakas DM, Schneewind O.** 2010. Contribution of coagulases towards Staphylococcus aureus disease and protective immunity. PLoS Pathog **6:**e1001036.

40. **Vanassche T, Peetermans M, Van Aelst LN, Peetermans WE, Verhaegen J, Missiakas DM, Schneewind O, Hoylaerts MF, Verhamme P.** 2013. The role of

staphylothrombin-mediated fibrin deposition in catheter-related Staphylococcus aureus infections. J Infect Dis **208:**92-100.

41. **Thomer L, Schneewind O, Missiakas D.** 2013. Multiple ligands of von Willebrand factor-binding protein (vWbp) promote Staphylococcus aureus clot formation in human plasma. The Journal of biological chemistry **288:**28283-28292.

42. **Zapotoczna M, McCarthy H, Rudkin JK, O'Gara JP, O'Neill E.** 2015. An Essential Role for Coagulase in Staphylococcus aureus Biofilm Development Reveals New Therapeutic Possibilities for Device-Related Infections. J Infect Dis **212:**1883-1893.

43. **Christner RB, Boyle MD.** 1996. Role of staphylokinase in the acquisition of plasmin(ogen)-dependent enzymatic activity by staphylococci. J Infect Dis **173:**104-112.

44. **Molkanen T, Tyynela J, Helin J, Kalkkinen N, Kuusela P.** 2002. Enhanced activation of bound plasminogen on Staphylococcus aureus by staphylokinase. FEBS Lett **517:**72-78.

45. **Rooijakkers SH, van Wamel WJ, Ruyken M, van Kessel KP, van Strijp JA.** 2005. Anti-opsonic properties of staphylokinase. Microbes Infect **7:**476-484.

46. **Berends ET, Horswill AR, Haste NM, Monestier M, Nizet V, von Kockritz-Blickwede M.** 2010. Nuclease expression by Staphylococcus aureus facilitates escape from neutrophil extracellular traps. J Innate Immun **2:**576-586.

47. **Thammavongsa V, Missiakas DM, Schneewind O.** 2013. Staphylococcus aureus degrades neutrophil extracellular traps to promote immune cell death. Science **342:**863-866.

48. **Olson ME, Nygaard TK, Ackermann L, Watkins RL, Zurek OW, Pallister KB, Griffith S, Kiedrowski MR, Flack CE, Kavanaugh JS, Kreiswirth BN, Horswill**

AR, Voyich JM. 2013. *Staphylococcus aureus* nuclease is an SaeRS-dependent virulence factor. Infection and immunity **81:**1316-1324.

49. **Costerton JW, Cheng KJ, Geesey GG, Ladd TI, Nickel JC, Dasgupta M, Marrie TJ.** 1987. Bacterial biofilms in nature and disease. Annual review of microbiology **41:**435-464.
50. **Hall-Stoodley L, Costerton JW, Stoodley P.** 2004. Bacterial biofilms: from the natural environment to infectious diseases. Nature reviews. Microbiology **2:**95-108.
51. **Flemming HC, Wingender J.** 2010. The biofilm matrix. Nature reviews. Microbiology **8:**623-633.
52. **Davey ME, O'Toole G A.** 2000. Microbial biofilms: from ecology to molecular genetics. Microbiology and molecular biology reviews : MMBR **64:**847-867.
53. **Kostakioti M, Hadjifrangiskou M, Hultgren SJ.** 2013. Bacterial biofilms: development, dispersal, and therapeutic strategies in the dawn of the postantibiotic era. Cold Spring Harb Perspect Med **3:**a010306.
54. **Claessen D, Rozen DE, Kuipers OP, Sogaard-Andersen L, van Wezel GP.** 2014. Bacterial solutions to multicellularity: a tale of biofilms, filaments and fruiting bodies. Nature reviews. Microbiology **12:**115-124.
55. **Vlamakis H, Chai Y, Beauregard P, Losick R, Kolter R.** 2013. Sticking together: building a biofilm the Bacillus subtilis way. Nature reviews. Microbiology **11:**157-168.
56. **Lopez D, Kolter R.** 2010. Extracellular signals that define distinct and coexisting cell fates in Bacillus subtilis. FEMS Microbiol Rev **34:**134-149.
57. **Zusman DR, Scott AE, Yang Z, Kirby JR.** 2007. Chemosensory pathways, motility and development in Myxococcus xanthus. Nature reviews. Microbiology **5:**862-872.

58. **Stewart PS, Franklin MJ.** 2008. Physiological heterogeneity in biofilms. Nature reviews. Microbiology **6:**199-210.

59. **Capra EJ, Laub MT.** 2012. Evolution of two-component signal transduction systems. Annual review of microbiology **66:**325-347.

60. **Parsek MR, Greenberg EP.** 2005. Sociomicrobiology: the connections between quorum sensing and biofilms. Trends Microbiol **13:**27-33.

61. **Monds RD, O'Toole GA.** 2009. The developmental model of microbial biofilms: ten years of a paradigm up for review. Trends Microbiol **17:**73-87.

62. **Otto M.** 2006. Bacterial evasion of antimicrobial peptides by biofilm formation. Curr Top Microbiol Immunol **306:**251-258.

63. **Costerton JW, Stewart PS, Greenberg EP.** 1999. Bacterial biofilms: a common cause of persistent infections. Science **284:**1318-1322.

64. **Donlan RM, Costerton JW.** 2002. Biofilms: survival mechanisms of clinically relevant microorganisms. Clin Microbiol Rev **15:**167-193.

65. **McConoughey SJ, Howlin R, Granger JF, Manring MM, Calhoun JH, Shirtliff M, Kathju S, Stoodley P.** 2014. Biofilms in periprosthetic orthopedic infections. Future Microbiol **9:**987-1007.

66. **Ribeiro M, Monteiro FJ, Ferraz MP.** 2012. Infection of orthopedic implants with emphasis on bacterial adhesion process and techniques used in studying bacterial-material interactions. Biomatter **2:**176-194.

67. **Darouiche RO.** 2004. Treatment of infections associated with surgical implants. N Engl J Med **350:**1422-1429.

68. **Bhattacharya M, Wozniak DJ, Stoodley P, Hall-Stoodley L.** 2015. Prevention and treatment of Staphylococcus aureus biofilms. Expert Rev Anti Infect Ther **13:**1499-1516.

69. **Thurlow LR, Hanke ML, Fritz T, Angle A, Aldrich A, Williams SH, Engebretsen IL, Bayles KW, Horswill AR, Kielian T.** 2011. Staphylococcus aureus biofilms prevent macrophage phagocytosis and attenuate inflammation in vivo. J Immunol **186:**6585-6596.

70. **Hanke ML, Heim CE, Angle A, Sanderson SD, Kielian T.** 2013. Targeting macrophage activation for the prevention and treatment of Staphylococcus aureus biofilm infections. J Immunol **190:**2159-2168.

71. **Hanke ML, Angle A, Kielian T.** 2012. MyD88-dependent signaling influences fibrosis and alternative macrophage activation during Staphylococcus aureus biofilm infection. PloS one **7:**e42476.

72. **Secor PR, James GA, Fleckman P, Olerud JE, McInnerney K, Stewart PS.** 2011. Staphylococcus aureus Biofilm and Planktonic cultures differentially impact gene expression, mapk phosphorylation, and cytokine production in human keratinocytes. BMC microbiology **11:**143.

73. **Scherr TD, Hanke ML, Huang O, James DB, Horswill AR, Bayles KW, Fey PD, Torres VJ, Kielian T.** 2015. Staphylococcus aureus Biofilms Induce Macrophage Dysfunction Through Leukocidin AB and Alpha-Toxin. MBio **6**.

74. **Keren I, Kaldalu N, Spoering A, Wang Y, Lewis K.** 2004. Persister cells and tolerance to antimicrobials. FEMS Microbiol Lett **230:**13-18.

75. **Lewis K.** 2001. Riddle of biofilm resistance. Antimicrob Agents Chemother **45:**999-1007.

76. **Otto M.** 2013. Staphylococcal infections: mechanisms of biofilm maturation and detachment as critical determinants of pathogenicity. Annu Rev Med **64:**175-188.

77. **Foster TJ, Geoghegan JA, Ganesh VK, Hook M.** 2014. Adhesion, invasion and evasion: the many functions of the surface proteins of Staphylococcus aureus. Nature reviews. Microbiology **12:**49-62.

78. **O'Neill E, Pozzi C, Houston P, Humphreys H, Robinson DA, Loughman A, Foster TJ, O'Gara JP.** 2008. A novel *Staphylococcus aureus* biofilm phenotype mediated by the fibronectin-binding proteins, FnBPA and FnBPB. Journal of bacteriology **190:**3835-3850.

79. **Corrigan RM, Miajlovic H, Foster TJ.** 2009. Surface proteins that promote adherence of *Staphylococcus aureus* to human desquamated nasal epithelial cells. BMC microbiology **9:**22.

80. **Josefsson E, McCrea KW, Ni Eidhin D, O'Connell D, Cox J, Hook M, Foster TJ.** 1998. Three new members of the serine-aspartate repeat protein multigene family of *Staphylococcus aureus*. Microbiology **144 (Pt 12):**3387-3395.

81. **McDevitt D, Francois P, Vaudaux P, Foster TJ.** 1994. Molecular characterization of the clumping factor (fibrinogen receptor) of *Staphylococcus aureus*. Molecular microbiology **11:**237-248.

82. **Ni Eidhin D, Perkins S, Francois P, Vaudaux P, Hook M, Foster TJ.** 1998. Clumping factor B (ClfB), a new surface-located fibrinogen-binding adhesin of *Staphylococcus aureus*. Molecular microbiology **30:**245-257.

83. **Zong Y, Xu Y, Liang X, Keene DR, Hook A, Gurusiddappa S, Hook M, Narayana SV.** 2005. A 'Collagen Hug' model for Staphylococcus aureus CNA binding to collagen. EMBO J **24:**4224-4236.

84. **Vazquez V, Liang X, Horndahl JK, Ganesh VK, Smeds E, Foster TJ, Hook M.** 2011. Fibrinogen is a ligand for the Staphylococcus aureus microbial surface components recognizing adhesive matrix molecules (MSCRAMM) bone sialoprotein-binding protein (Bbp). The Journal of biological chemistry **286:**29797-29805.

85. **Vuong C, Saenz HL, Gotz F, Otto M.** 2000. Impact of the *agr* quorum-sensing system on adherence to polystyrene in Staphylococcus aureus. J Infect Dis **182:**1688-1693.

86. **Biswas R, Voggu L, Simon UK, Hentschel P, Thumm G, Gotz F.** 2006. Activity of the major staphylococcal autolysin Atl. FEMS Microbiol Lett **259:**260-268.

87. **Houston P, Rowe SE, Pozzi C, Waters EM, O'Gara JP.** 2011. Essential role for the major autolysin in the fibronectin-binding protein-mediated Staphylococcus aureus biofilm phenotype. Infection and immunity **79:**1153-1165.

88. **Gross M, Cramton SE, Gotz F, Peschel A.** 2001. Key role of teichoic acid net charge in *Staphylococcus aureus* colonization of artificial surfaces. Infection and immunity **69:**3423-3426.

89. **Cramton SE, Gerke C, Schnell NF, Nichols WW, Gotz F.** 1999. The intercellular adhesion (ica) locus is present in Staphylococcus aureus and is required for biofilm formation. Infection and immunity **67:**5427-5433.

90. **Cramton SE, Ulrich M, Gotz F, Doring G.** 2001. Anaerobic conditions induce expression of polysaccharide intercellular adhesin in Staphylococcus aureus and Staphylococcus epidermidis. Infection and immunity **69:**4079-4085.

91. **O'Gara JP.** 2007. ica and beyond: biofilm mechanisms and regulation in Staphylococcus epidermidis and Staphylococcus aureus. FEMS Microbiol Lett **270:**179-188.

92. **Fitzpatrick F, Humphreys H, O'Gara JP.** 2005. Evidence for icaADBC-independent biofilm development mechanism in methicillin-resistant Staphylococcus aureus clinical isolates. J Clin Microbiol **43:**1973-1976.

93. **Toledo-Arana A, Merino N, Vergara-Irigaray M, Debarbouille M, Penades JR, Lasa I.** 2005. Staphylococcus aureus develops an alternative, ica-independent

biofilm in the absence of the arlRS two-component system. Journal of bacteriology **187:**5318-5329.

94. **Brooks JL, Jefferson KK.** 2014. Phase variation of poly-N-acetylglucosamine expression in Staphylococcus aureus. PLoS Pathog **10:**e1004292.

95. **O'Neill E, Pozzi C, Houston P, Smyth D, Humphreys H, Robinson DA, O'Gara JP.** 2007. Association between methicillin susceptibility and biofilm regulation in Staphylococcus aureus isolates from device-related infections. J Clin Microbiol **45:**1379-1388.

96. **Rohde H, Burandt EC, Siemssen N, Frommelt L, Burdelski C, Wurster S, Scherpe S, Davies AP, Harris LG, Horstkotte MA, Knobloch JK, Ragunath C, Kaplan JB, Mack D.** 2007. Polysaccharide intercellular adhesin or protein factors in biofilm accumulation of Staphylococcus epidermidis and Staphylococcus aureus isolated from prosthetic hip and knee joint infections. Biomaterials **28:**1711-1720.

97. **Boles BR, Thoendel M, Roth AJ, Horswill AR.** 2010. Identification of genes involved in polysaccharide-independent *Staphylococcus aureus* biofilm formation. PloS one **5:**e10146.

98. **Foulston L, Elsholz AK, DeFrancesco AS, Losick R.** 2014. The extracellular matrix of Staphylococcus aureus biofilms comprises cytoplasmic proteins that associate with the cell surface in response to decreasing pH. MBio **5:**e01667-01614.

99. **Rice KC, Mann EE, Endres JL, Weiss EC, Cassat JE, Smeltzer MS, Bayles KW.** 2007. The *cidA* murein hydrolase regulator contributes to DNA release and biofilm development in *Staphylococcus aureus*. Proceedings of the National Academy of Sciences of the United States of America **104:**8113-8118.

100. **Mann EE, Rice KC, Boles BR, Endres JL, Ranjit D, Chandramohan L, Tsang LH, Smeltzer MS, Horswill AR, Bayles KW.** 2009. Modulation of eDNA release and degradation affects *Staphylococcus aureus* biofilm maturation. PLoS One **4:**e5822.

101. **Lehman MK, Bose JL, Sharma-Kuinkel BK, Moormeier DE, Endres JL, Sadykov MR, Biswas I, Bayles KW.** 2015. Identification of the amino acids essential for LytSR-mediated signal transduction in Staphylococcus aureus and their roles in biofilm-specific gene expression. Molecular microbiology **95:**723-737.

102. **Sadykov MR, Bayles KW.** 2012. The control of death and lysis in staphylococcal biofilms: a coordination of physiological signals. Curr Opin Microbiol **15:**211-215.

103. **Thomas VC, Sadykov MR, Chaudhari SS, Jones J, Endres JL, Widhelm TJ, Ahn JS, Jawa RS, Zimmerman MC, Bayles KW.** 2014. A central role for carbon-overflow pathways in the modulation of bacterial cell death. PLoS Pathog **10:**e1004205.

104. **Bose JL, Lehman MK, Fey PD, Bayles KW.** 2012. Contribution of the *Staphylococcus aureus* Atl AM and GL murein hydrolase activities in cell division, autolysis, and biofilm formation. PloS one **7:**e42244.

105. **Dengler V, Foulston L, DeFrancesco AS, Losick R.** 2015. An Electrostatic Net Model for the Role of Extracellular DNA in Biofilm Formation by Staphylococcus aureus. Journal of bacteriology **197:**3779-3787.

106. **Schwartz K, Ganesan M, Payne DE, Solomon MJ, Boles BR.** 2015. Extracellular DNA facilitates the formation of functional amyloids in Staphylococcus aureus biofilms. Molecular microbiology.

107. **Goodman SD, Obergfell KP, Jurcisek JA, Novotny LA, Downey JS, Ayala EA, Tjokro N, Li B, Justice SS, Bakaletz LO.** 2011. Biofilms can be dispersed

by focusing the immune system on a common family of bacterial nucleoid-associated proteins. Mucosal Immunol **4:**625-637.

108. **Huseby MJ, Kruse AC, Digre J, Kohler PL, Vocke JA, Mann EE, Bayles KW, Bohach GA, Schlievert PM, Ohlendorf DH, Earhart CA.** 2010. Beta toxin catalyzes formation of nucleoprotein matrix in staphylococcal biofilms. Proceedings of the National Academy of Sciences of the United States of America **107:**14407-14412.

109. **Mackey-Lawrence NM, Potter DE, Cerca N, Jefferson KK.** 2009. *Staphylococcus aureus* immunodominant surface antigen B is a cell-surface associated nucleic acid binding protein. BMC microbiology **9:**61.

110. **Yarwood JM, Bartels DJ, Volper EM, Greenberg EP.** 2004. Quorum sensing in *Staphylococcus aureus* biofilms. Journal of bacteriology **186:**1838-1850.

111. **Boles BR, Horswill AR.** 2008. *agr*-mediated dispersal of *Staphylococcus aureus* biofilms. PLoS Pathog **4:**e1000052.

112. **Tsang LH, Cassat JE, Shaw LN, Beenken KE, Smeltzer MS.** 2008. Factors contributing to the biofilm-deficient phenotype of *Staphylococcus aureus sarA* mutants. PloS one **3:**e3361.

113. **Lauderdale KJ, Boles BR, Cheung AL, Horswill AR.** 2009. Interconnections between Sigma B, *agr*, and proteolytic activity in *Staphylococcus aureus* biofilm maturation. Infection and immunity **77:**1623-1635.

114. **Mrak LN, Zielinska AK, Beenken KE, Mrak IN, Atwood DN, Griffin LM, Lee CY, Smeltzer MS.** 2012. saeRS and sarA act synergistically to repress protease production and promote biofilm formation in Staphylococcus aureus. PloS one **7:**e38453.

115. **Mootz JM, Benson MA, Heim CE, Crosby HA, Kavanaugh JS, Dunman PM, Kielian T, Torres VJ, Horswill AR.** 2015. Rot is a key regulator of Staphylococcus aureus biofilm formation. Molecular microbiology **96:**388-404.

116. **Wang R, Braughton KR, Kretschmer D, Bach TH, Queck SY, Li M, Kennedy AD, Dorward DW, Klebanoff SJ, Peschel A, DeLeo FR, Otto M.** 2007. Identification of novel cytolytic peptides as key virulence determinants for community-associated MRSA. Nat Med **13:**1510-1514.

117. **Periasamy S, Joo HS, Duong AC, Bach TH, Tan VY, Chatterjee SS, Cheung GY, Otto M.** 2012. How Staphylococcus aureus biofilms develop their characteristic structure. Proceedings of the National Academy of Sciences of the United States of America **109:**1281-1286.

118. **Schwartz K, Syed AK, Stephenson RE, Rickard AH, Boles BR.** 2012. Functional amyloids composed of phenol soluble modulins stabilize Staphylococcus aureus biofilms. PLoS Pathog **8:**e1002744.

119. **Kiedrowski MR, Kavanaugh JS, Malone CL, Mootz JM, Voyich JM, Smeltzer MS, Bayles KW, Horswill AR.** 2011. Nuclease modulates biofilm formation in community-associated methicillin-resistant *Staphylococcus aureus*. PloS one **6:**e26714.

120. **Moormeier DE, Bose JL, Horswill AR, Bayles KW.** 2014. Temporal and stochastic control of *Staphylococcus aureus* biofilm development. MBio **5:**e01341-01314.

121. **Kiedrowski MR, Crosby HA, Hernandez FJ, Malone CL, McNamara JO, 2nd, Horswill AR.** 2014. Staphylococcus aureus Nuc2 is a functional, surface-attached extracellular nuclease. PloS one **9:**e95574.

122. **Beenken KE, Spencer H, Griffin LM, Smeltzer MS.** 2012. Impact of extracellular nuclease production on the biofilm phenotype of *Staphylococcus*

aureus under in vitro and in vivo conditions. Infection and immunity **80:**1634-1638.

123. **Bayles KW.** 2007. The biological role of death and lysis in biofilm development. Nat. Rev. Microbiol. **5:**721-726.

124. **Rice KC, Bayles KW.** 2008. Molecular control of bacterial death and lysis. Microbiol. Mol. Biol. Rev. **72:**85-109.

125. **Whitchurch CB, Tolker-Nielsen T, Ragas PC, Mattick JS.** 2002. Extracellular DNA required for bacterial biofilm formation. Science **295:**1487.

126. **Allesen-Holm M, Barken KB, Yang L, Klausen M, Webb JS, Kjelleberg S, Molin S, Givskov M, Tolker-Nielsen T.** 2006. A characterization of DNA release in *Pseudomonas aeruginosa* cultures and biofilms. Mol. Microbiol. **59:**1114-1128.

127. **Guiton PS, Hung CS, Kline KA, Roth R, Kau AL, Hayes E, Heuser J, Dodson KW, Caparon MG, Hultgren SJ.** 2009. Contribution of autolysin and Sortase a during Enterococcus faecalis DNA-dependent biofilm development. Infection and immunity **77:**3626-3638.

128. **Thomas VC, Thurlow LR, Boyle D, Hancock LE.** 2008. Regulation of autolysis-dependent extracellular DNA release by Enterococcus faecalis extracellular proteases influences biofilm development. Journal of bacteriology **190:**5690-5698.

129. **Webb JS, Thompson LS, James S, Charlton T, Tolker-Nielsen T, Koch B, Givskov M, Kjelleberg S.** 2003. Cell death in *Pseudomonas aeruginosa* biofilm development. J. Bacteriol. **185:**4585-4592.

130. **Godeke J, Paul K, Lassak J, Thormann KM.** 2011. Phage-induced lysis enhances biofilm formation in Shewanella oneidensis MR-1. Isme J **5:**613-626.

131. **Rice SA, Tan CH, Mikkelsen PJ, Kung V, Woo J, Tay M, Hauser A, McDougald D, Webb JS, Kjelleberg S.** 2009. The biofilm life cycle and

virulence of Pseudomonas aeruginosa are dependent on a filamentous prophage. Isme J **3:**271-282.

132. **Webb JS, Lau M, Kjelleberg S.** 2004. Bacteriophage and phenotypic variation in *Pseudomonas aeruginosa* biofilm development. J. Bacteriol. **186:**8066-8073.

133. **Klausen M, Aaes-Jorgensen A, Molin S, Tolker-Nielsen T.** 2003. Involvement of bacterial migration in the development of complex multicellular structures in Pseudomonas aeruginosa biofilms. Mol Microbiol **50:**61-68.

134. **Groicher KH, Firek BA, Fujimoto DF, Bayles KW.** 2000. The *Staphylococcus aureus lrgAB* operon modulates murein hydrolase activity and penicillin tolerance. J. Bacteriol. **182:**1794-1801.

135. **Patton TG, Rice KC, Foster MK, Bayles KW.** 2005. The *Staphylococcus aureus cidC* gene encodes a pyruvate oxidase that affects acetate metabolism and cell death in stationary phase. Mol. Microbiol. **56:**1664-1674.

136. **Rice KC, Firek BA, Nelson JB, Yang SJ, Patton TG, Bayles KW.** 2003. The *Staphylococcus aureus cidAB* operon: evaluation of its role in the regulation of murein hydrolase activity and penicillin tolerance. J. Bacteriol. **185:**2635-2643.

137. **Rice KC, Bayles KW.** 2003. Death's toolbox: examining the molecular components of bacterial programmed cell death. Mol. Microbiol. **50:**729-738.

138. **Ma L, Conover M, Lu H, Parsek MR, Bayles K, Wozniak DJ.** 2009. Assembly and development of the Pseudomonas aeruginosa biofilm matrix. PLoS Pathog **5:**e1000354.

139. **Yang Y, Jin H, Chen Y, Lin W, Wang C, Chen Z, Han N, Bian H, Zhu M, Wang J.** 2012. A chloroplast envelope membrane protein containing a putative LrgB domain related to the control of bacterial death and lysis is required for chloroplast development in Arabidopsis thaliana. New Phytol **193:**81-95.

140. **Yamaguchi M, Takechi K, Myouga F, Imura S, Sato H, Takio S, Shinozaki K, Takano H.** 2012. Loss of the plastid envelope protein AtLrgB causes spontaneous chlorotic cell death in Arabidopsis thaliana. Plant Cell Physiol **53:**125-134.

141. **Pang X, Moussa SH, Targy NM, Bose JL, George NM, Gries C, Lopez H, Zhang L, Bayles KW, Young R, Luo X.** 2011. Active Bax and Bak are functional holins. Genes Dev **25:**2278-2290.

142. **Rani SA, Pitts B, Beyenal H, Veluchamy RA, Lewandowski Z, Davison WM, Buckingham-Meyer K, Stewart PS.** 2007. Spatial patterns of DNA replication, protein synthesis, and oxygen concentration within bacterial biofilms reveal diverse physiological states. Journal of bacteriology **189:**4223-4233.

143. **Rice KC, Nelson JB, Patton TG, Yang SJ, Bayles KW.** 2005. Acetic acid induces expression of the *Staphylococcus aureus cidABC* and *lrgAB* murein hydrolase regulator operons. J. Bacteriol. **187:**813-821.

144. **Yang SJ, Dunman PM, Projan SJ, Bayles KW.** 2006. Characterization of the *Staphylococcus aureus* CidR regulon: elucidation of a novel role for acetoin metabolism in cell death and lysis. Mol. Microbiol. **60:**458-468.

145. **Yang SJ, Rice KC, Brown RJ, Patton TG, Liou LE, Park YH, Bayles KW.** 2005. A LysR-type regulator, CidR, is required for induction of the *Staphylococcus aureus cidABC* operon. J. Bacteriol. **187:**5893-5900.

146. **Patton TG, Yang SJ, Bayles KW.** 2006. The role of proton motive force in expression of the *Staphylococcus aureus cid* and *lrg* operons. Mol. Microbiol. **59:**1395-1404.

147. **Benoit MR, Conant CG, Ionescu-Zanetti C, Schwartz M, Matin A.** 2010. New device for high-throughput viability screening of flow biofilms. Appl Environ Microbiol **76:**4136-4142.

148. **Moormeier DE, Endres JL, Mann EE, Sadykov MR, Horswill AR, Rice KC, Fey PD, Bayles KW.** 2013. Use of Microfluidic Technology To Analyze Gene Expression during Staphylococcus aureus Biofilm Formation Reveals Distinct Physiological Niches. Appl Environ Microbiol **79:**3413-3424.

149. **Hanahan D.** 1983. Studies on transformation of Escherichia coli with plasmids. J Mol Biol **166:**557-580.

150. **Kreiswirth BN, Lofdahl S, Betley MJ, O'Reilly M, Shlievert PM, Bergdoll MS, Novick RP.** 1983. The toxic shock syndrome exotoxin structural gene is not detectably transmitted by a prophage. Nature **305:**709-712.

151. **Gillaspy AF, Hickmon SG, Skinner RA, Thomas JR, Nelson CL, Smeltzer MS.** 1995. Role of the accessory gene regulator (*agr*) in pathogenesis of staphylococcal osteomyelitis. Infect. Immun. **63:**3373-3380.

152. **Blevins JS, Beenken KE, Elasri MO, Hurlburt BK, Smeltzer MS.** 2002. Strain-dependent differences in the regulatory roles of *sarA* and *agr* in *Staphylococcus aureus*. Infection and immunity **70:**470-480.

153. **Corvaglia AR, Francois P, Hernandez D, Perron K, Linder P, Schrenzel J.** 2010. A type III-like restriction endonuclease functions as a major barrier to horizontal gene transfer in clinical Staphylococcus aureus strains. Proceedings of the National Academy of Sciences of the United States of America **107:**11954-11958.

154. **Sadykov MR, Thomas VC, Marshall DD, Wenstrom CJ, Moormeier DE, Widhelm TJ, Nuxoll AS, Powers R, Bayles KW.** 2013. Inactivation of the Pta-AckA pathway causes cell death in Staphylococcus aureus. Journal of bacteriology **195:**3035-3044.

155. **Fey PD, Endres JL, Yajjala VK, Widhelm TJ, Boissy RJ, Bose JL, Bayles KW.** 2013. A Genetic Resource for Rapid and Comprehensive Phenotype Screening of Nonessential Staphylococcus aureus Genes. MBio **4**.

156. **Wormann ME, Reichmann NT, Malone CL, Horswill AR, Grundling A.** 2011. Proteolytic cleavage inactivates the *Staphylococcus aureus* lipoteichoic acid synthase. Journal of bacteriology **193:**5279-5291.

157. **Flack CE, Zurek OW, Meishery DD, Pallister KB, Malone CL, Horswill AR, Voyich JM.** 2014. Differential regulation of staphylococcal virulence by the sensor kinase SaeS in response to neutrophil-derived stimuli. Proceedings of the National Academy of Sciences of the United States of America **111:**E2037-2045.

158. **Bose JL, Fey PD, Bayles KW.** 2013. Genetic tools to enhance the study of gene function and regulation in Staphylococcus aureus. Appl Environ Microbiol **79:**2218-2224.

159. **Sharma Kuinkel BK, Mann EE, Ahn JS, Kuechenmeister LJ, Dunman PM, Bayles KW.** 2009. The Staphylococcus aureus LytSR two-component regulatory system affects biofilm formation. J Bacteriol.

160. **Lauderdale KJ, Malone CL, Boles BR, Morcuende J, Horswill AR.** 2010. Biofilm dispersal of community-associated methicillin-resistant Staphylococcus aureus on orthopedic implant material. J Orthop Res **28:**55-61.

161. **Shompole S, Henon KT, Liou LE, Dziewanowska K, Bohach GA, Bayles KW.** 2003. Biphasic intracellular expression of Staphylococcus aureus virulence factors and evidence for Agr-mediated diffusion sensing. Molecular microbiology **49:**919-927.

162. **Dunn AK, Millikan DS, Adin DM, Bose JL, Stabb EV.** 2006. New *rfp*- and pES213-derived tools for analyzing symbiotic *Vibrio fischeri* reveal patterns of infection and *lux* expression in situ. Appl. Environ. Microbiol. **72:**802-810.

163. **Horton RM.** 1995. PCR-mediated recombination and mutagenesis. SOEing together tailor-made genes. Mol Biotechnol **3:**93-99.

164. **Novick RP.** 1991. Genetic systems in staphylococci. Methods Enzymol **204:**587-636.

165. **Schmittgen TD, Livak KJ.** 2008. Analyzing real-time PCR data by the comparative C(T) method. Nat Protoc **3:**1101-1108.

166. **Moormeier DE, Bayles KW.** 2014. Examination of Staphylococcus epidermidis biofilms using flow-cell technology. Methods in molecular biology **1106:**143-155.

167. **Otto M.** 2008. Staphylococcal biofilms. Curr Top Microbiol Immunol **322:**207-228.

168. **Lowy FD.** 1998. *Staphylococcus aureus* infections. N Engl J Med **339:**520-532.

169. **Boucher H, Miller LG, Razonable RR.** 2010. Serious infections caused by methicillin-resistant *Staphylococcus aureus*. Clin Infect Dis **51 Suppl 2:**S183-197.

170. **Foster TJ, Hook M.** 1998. Surface protein adhesins of *Staphylococcus aureus*. Trends Microbiol **6:**484-488.

171. **Patti JM, Allen BL, McGavin MJ, Hook M.** 1994. MSCRAMM-mediated adherence of microorganisms to host tissues. Annual review of microbiology **48:**585-617.

172. **Izano EA, Amarante MA, Kher WB, Kaplan JB.** 2008. Differential roles of poly-N-acetylglucosamine surface polysaccharide and extracellular DNA in *Staphylococcus aureus* and *Staphylococcus epidermidis* biofilms. Appl Environ Microbiol **74:**470-476.

173. **Beenken KE, Dunman PM, McAleese F, Macapagal D, Murphy E, Projan SJ, Blevins JS, Smeltzer MS.** 2004. Global gene expression in *Staphylococcus aureus* biofilms. Journal of bacteriology **186:**4665-4684.

174. **Sharma-Kuinkel BK, Mann EE, Ahn JS, Kuechenmeister LJ, Dunman PM, Bayles KW.** 2009. The Staphylococcus aureus LytSR two-component regulatory system affects biofilm formation. Journal of bacteriology **191:**4767-4775.

175. **Grande R, Nistico L, Sambanthamoorthy K, Longwell M, Iannitelli A, Cellini L, Di Stefano A, Hall Stoodley L, Stoodley P.** 2014. Temporal expression of *agrB*, *cidA*, and *alsS* in the early development of *Staphylococcus aureus* UAMS-1 biofilm formation and the structural role of extracellular DNA and carbohydrates. Pathog Dis.

176. **Yau YC, Ratjen F, Tullis E, Wilcox P, Freitag A, Chilvers M, Grasemann H, Zlosnik J, Speert D, Corey M, Stanojevic S, Matukas L, Leahy TR, Shih S, Waters V.** 2015. Randomized controlled trial of biofilm antimicrobial susceptibility testing in cystic fibrosis patients. J Cyst Fibros **14:**262-266.

177. **Christner M, Franke GC, Schommer NN, Wendt U, Wegert K, Pehle P, Kroll G, Schulze C, Buck F, Mack D, Aepfelbacher M, Rohde H.** 2010. The giant extracellular matrix-binding protein of *Staphylococcus epidermidis* mediates biofilm accumulation and attachment to fibronectin. Molecular microbiology **75:**187-207.

178. **Merino N, Toledo-Arana A, Vergara-Irigaray M, Valle J, Solano C, Calvo E, Lopez JA, Foster TJ, Penades JR, Lasa I.** 2009. Protein A-mediated multicellular behavior in *Staphylococcus aureus*. Journal of bacteriology **191:**832-843.

179. **Campoccia D, Montanaro L, Ravaioli S, Cangini I, Speziale P, Arciola CR.** 2009. Description of a new group of variants of the *Staphylococcus aureus* elastin-binding protein that lacks an entire DNA segment of 180 bp. Int J Artif Organs **32:**621-629.

180. **Roche FM, Massey R, Peacock SJ, Day NP, Visai L, Speziale P, Lam A, Pallen M, Foster TJ.** 2003. Characterization of novel LPXTG-containing proteins of *Staphylococcus aureus* identified from genome sequences. Microbiology **149:**643-654.

181. **Roche FM, Meehan M, Foster TJ.** 2003. The *Staphylococcus aureus* surface protein SasG and its homologues promote bacterial adherence to human desquamated nasal epithelial cells. Microbiology **149:**2759-2767.

182. **Mazmanian SK, Liu G, Ton-That H, Schneewind O.** 1999. *Staphylococcus aureus* sortase, an enzyme that anchors surface proteins to the cell wall. Science **285:**760-763.

183. **Caiazza NC, O'Toole GA.** 2003. Alpha-toxin is required for biofilm formation by *Staphylococcus aureus*. Journal of bacteriology **185:**3214-3217.

184. **Ferguson DJ, McColm AA, Ryan DM, Acred P.** 1986. A morphological study of experimental staphylococcal endocarditis and aortitis. II. Inter-relationship of bacteria, vegetation and cardiovasculature in established infections. Br J Exp Pathol **67:**679-686.

185. **Stack CM, Caffrey CR, Donnelly SM, Seshaadri A, Lowther J, Tort JF, Collins PR, Robinson MW, Xu W, McKerrow JH, Craik CS, Geiger SR, Marion R, Brinen LS, Dalton JP.** 2008. Structural and functional relationships in the virulence-associated cathepsin L proteases of the parasitic liver fluke, Fasciola hepatica. The Journal of biological chemistry **283:**9896-9908.

186. **Geiger T, Goerke C, Mainiero M, Kraus D, Wolz C.** 2008. The virulence regulator Sae of *Staphylococcus aureus*: promoter activities and response to phagocytosis-related signals. Journal of bacteriology **190:**3419-3428.

187. **Novick RP, Jiang D.** 2003. The staphylococcal saeRS system coordinates environmental signals with agr quorum sensing. Microbiology **149:**2709-2717.

188. **Kuroda H, Kuroda M, Cui L, Hiramatsu K.** 2007. Subinhibitory concentrations of beta-lactam induce haemolytic activity in Staphylococcus aureus through the SaeRS two-component system. FEMS Microbiol Lett **268:**98-105.

189. **Makgotlho PE, Marincola G, Schafer D, Liu Q, Bae T, Geiger T, Wasserman E, Wolz C, Ziebuhr W, Sinha B.** 2013. SDS interferes with SaeS signaling of Staphylococcus aureus independently of SaePQ. PloS one **8:**e71644.

190. **Dunman PM, Murphy E, Haney S, Palacios D, Tucker-Kellogg G, Wu S, Brown EL, Zagursky RJ, Shlaes D, Projan SJ.** 2001. Transcription profiling-based identification of *Staphylococcus aureus* genes regulated by the *agr* and/or *sarA* loci. Journal of bacteriology **183:**7341-7353.

191. **Foulston L EA, DeFrancesco AS, Losick R.** 2014. The extracellular matrix of *Staphylococcus aureus* biofilms comprises cytoplasmic proteins that associate with the cell surface in response to decreasing pH. MBio **5:**01667-01614.

192. **Novotny LA, Amer AO, Brockson ME, Goodman SD, Bakaletz LO.** 2013. Structural stability of *Burkholderia cenocepacia* biofilms is reliant on eDNA structure and presence of a bacterial nucleic acid binding protein. PloS one **8:**e67629.

193. **Ohniwa RL, Ushijima Y, Saito S, Morikawa K.** 2011. Proteomic analyses of nucleoid-associated proteins in *Escherichia coli*, *Pseudomonas aeruginosa*, *Bacillus subtilis*, and *Staphylococcus aureus*. PloS one **6:**e19172.

194. **Shank EA, Kolter R.** 2011. Extracellular signaling and multicellularity in *Bacillus subtilis*. Curr Opin Microbiol **14:**741-747.

195. **Cheung GY, Wang R, Khan BA, Sturdevant DE, Otto M.** 2011. Role of the accessory gene regulator agr in community-associated methicillin-resistant *Staphylococcus aureus* pathogenesis. Infection and immunity **79:**1927-1935.

196. **Novick RP.** 2003. Autoinduction and signal transduction in the regulation of staphylococcal virulence. Molecular microbiology **48:**1429-1449.

197. **Smeltzer MS, Hart ME, Iandolo JJ.** 1993. Phenotypic characterization of xpr, a global regulator of extracellular virulence factors in *Staphylococcus aureus*. Infection and immunity **61:**919-925.

198. **Nygaard TK, Pallister KB, Ruzevich P, Griffith S, Vuong C, Voyich JM.** 2010. SaeR binds a consensus sequence within virulence gene promoters to advance USA300 pathogenesis. J Infect Dis **201:**241-254.

199. **Voyich JM, Vuong C, DeWald M, Nygaard TK, Kocianova S, Griffith S, Jones J, Iverson C, Sturdevant DE, Braughton KR, Whitney AR, Otto M, DeLeo FR.** 2009. The SaeR/S gene regulatory system is essential for innate immune evasion by *Staphylococcus aureus*. J Infect Dis **199:**1698-1706.

200. **Rogasch K, Ruhmling V, Pane-Farre J, Hoper D, Weinberg C, Fuchs S, Schmudde M, Broker BM, Wolz C, Hecker M, Engelmann S.** 2006. Influence of the two-component system SaeRS on global gene expression in two different *Staphylococcus aureus strains*. Journal of bacteriology **188:**7742-7758.

201. **Cassat JE, Hammer ND, Campbell JP, Benson MA, Perrien DS, Mrak LN, Smeltzer MS, Torres VJ, Skaar EP.** 2013. A secreted bacterial protease tailors the *Staphylococcus aureus* virulence repertoire to modulate bone remodeling during osteomyelitis. Cell host & microbe **13:**759-772.

202. **Mainiero M, Goerke C, Geiger T, Gonser C, Herbert S, Wolz C.** 2010. Differential target gene activation by the *Staphylococcus aureus* two-component system *saeRS*. Journal of bacteriology **192:**613-623.

203. **Jeong DW, Cho H, Jones MB, Shatzkes K, Sun F, Ji Q, Liu Q, Peterson SN, He C, Bae T.** 2012. The auxiliary protein complex SaePQ activates the

phosphatase activity of sensor kinase SaeS in the SaeRS two-component system of *Staphylococcus aureus*. Molecular microbiology **86:**331-348.

204. **Steinberg N, Kolodkin-Gal I.** 2015. The Matrix Reloaded: Probing the Extracellular Matrix Synchronizes Bacterial Communities. Journal of bacteriology.

205. **Grilo IR, Ludovice AM, Tomasz A, de Lencastre H, Sobral RG.** 2014. The glucosaminidase domain of Atl - the major Staphylococcus aureus autolysin - has DNA-binding activity. Microbiologyopen **3:**247-256.

206. **Seper A, Fengler VH, Roier S, Wolinski H, Kohlwein SD, Bishop AL, Camilli A, Reidl J, Schild S.** 2011. Extracellular nucleases and extracellular DNA play important roles in Vibrio cholerae biofilm formation. Molecular microbiology **82:**1015-1037.

207. **Morfeldt E, Taylor D, von Gabain A, Arvidson S.** 1995. Activation of alpha-toxin translation in Staphylococcus aureus by the trans-encoded antisense RNA, RNAIII. EMBO J **14:**4569-4577.

208. **Bose JL, Daly SM, Hall PR, Bayles KW.** 2014. Identification of the Staphylococcus aureus vfrAB operon, a novel virulence factor regulatory locus. Infection and immunity **82:**1813-1822.

209. **Fernandez Guerrero ML, Alvarez B, Manzarbeitia F, Renedo G.** 2012. Infective endocarditis at autopsy: a review of pathologic manifestations and clinical correlates. Medicine (Baltimore) **91:**152-164.

210. **Hentzer M, Teitzel GM, Balzer GJ, Heydorn A, Molin S, Givskov M, Parsek MR.** 2001. Alginate overproduction affects *Pseudomonas aeruginosa* biofilm structure and function. Journal of bacteriology **183:**5395-5401.

211. **Davies DG, Parsek MR, Pearson JP, Iglewski BH, Costerton JW, Greenberg EP.** 1998. The involvement of cell-to-cell signals in the development of a bacterial biofilm. Science **280:**295-298.

212. **Konovalova A, Petters T, Sogaard-Andersen L.** 2010. Extracellular biology of Myxococcus xanthus. FEMS Microbiol Rev **34:**89-106.

213. **Kroos L, Kuspa A, Kaiser D.** 1986. A global analysis of developmentally regulated genes in *Myxococcus xanthus*. Dev Biol **117:**252-266.

214. **Inouye M, Inouye S, Zusman DR.** 1979. Gene expression during development of Myxococcus xanthus: pattern of protein synthesis. Dev Biol **68:**579-591.

215. **Wireman JW, Dworkin M.** 1977. Developmentally induced autolysis during fruiting body formation by Myxococcus xanthus. Journal of bacteriology **129:**798-802.

216. **Nariya H, Inouye M.** 2008. MazF, an mRNA interferase, mediates programmed cell death during multicellular *Myxococcus* development. Cell **132:**55-66.

217. **Rice KC, Nelson JB, Patton TG, Yang SJ, Bayles KW.** 2005. Acetic acid induces expression of the Staphylococcus aureus cidABC and lrgAB murein hydrolase regulator operons. Journal of bacteriology **187:**813-821.

218. **Yang SJ, Rice KC, Brown RJ, Patton TG, Liou LE, Park YH, Bayles KW.** 2005. A LysR-type regulator, CidR, is required for induction of the Staphylococcus aureus cidABC operon. Journal of bacteriology **187:**5893-5900.

219. **Yang SJ, Dunman PM, Projan SJ, Bayles KW.** 2006. Characterization of the Staphylococcus aureus CidR regulon: elucidation of a novel role for acetoin metabolism in cell death and lysis. Molecular microbiology **60:**458-468.

220. **Seidl K, Muller S, Francois P, Kriebitzsch C, Schrenzel J, Engelmann S, Bischoff M, Berger-Bachi B.** 2009. Effect of a glucose impulse on the CcpA regulon in Staphylococcus aureus. BMC microbiology **9:**95.

221. **Collins FM, Lascelles J.** 1962. The effect of growth conditions on oxidative and dehydrogenase activity in Staphylococcus aureus. J Gen Microbiol **29:**531-535.

222. **Seidl K, Goerke C, Wolz C, Mack D, Berger-Bachi B, Bischoff M.** 2008. Staphylococcus aureus CcpA affects biofilm formation. Infection and immunity **76:**2044-2050.

223. **Sadykov MR, Hartmann T, Mattes TA, Hiatt M, Jann NJ, Zhu Y, Ledala N, Landmann R, Herrmann M, Rohde H, Bischoff M, Somerville GA.** 2011. CcpA coordinates central metabolism and biofilm formation in Staphylococcus epidermidis. Microbiology **157:**3458-3468.

224. **Strasters KC, Winkler KC.** 1963. Carbohydrate Metabolism of Staphylococcus Aureus. J Gen Microbiol **33:**213-229.

225. **Brunskill EW, Bayles KW.** 1996. Identification and molecular characterization of a putative regulatory locus that affects autolysis in *Staphylococcus aureus*. Journal of bacteriology **178:**611-618.

226. **Patton TG, Yang SJ, Bayles KW.** 2006. The role of proton motive force in expression of the Staphylococcus aureus cid and lrg operons. Molecular microbiology **59:**1395-1404.

227. **Lukat GS, McCleary WR, Stock AM, Stock JB.** 1992. Phosphorylation of bacterial response regulator proteins by low molecular weight phospho-donors. Proceedings of the National Academy of Sciences of the United States of America **89:**718-722.

228. **McCleary WR, Stock JB, Ninfa AJ.** 1993. Is acetyl phosphate a global signal in Escherichia coli? Journal of bacteriology **175:**2793-2798.

229. **Stock AM, Robinson VL, Goudreau PN.** 2000. Two-component signal transduction. Annu Rev Biochem **69:**183-215.

230. **Klein AH, Shulla A, Reimann SA, Keating DH, Wolfe AJ.** 2007. The intracellular concentration of acetyl phosphate in Escherichia coli is sufficient for

direct phosphorylation of two-component response regulators. Journal of bacteriology **189:**5574-5581.

231. **Sadykov MR, Bayles KW.** 2012. The control of death and lysis in staphylococcal biofilms: a coordination of physiological signals. Curr Opin Microbiol **15:**211-215.

232. **Brunskill EW, Bayles KW.** 1996. Identification of LytSR-regulated genes from *Staphylococcus aureus*. J. Bacteriol. **178:**5810-5812.

233. **Richardson AR, Libby SJ, Fang FC.** 2008. A nitric oxide-inducible lactate dehydrogenase enables Staphylococcus aureus to resist innate immunity. Science **319:**1672-1676.

234. **Stewart PS, Rani SA, Gjersing E, Codd SL, Zheng Z, Pitts B.** 2007. Observations of cell cluster hollowing in Staphylococcus epidermidis biofilms. Lett Appl Microbiol **44:**454-457.

235. **Wojtczak L.** 1996. The Crabtree effect: a new look at the old problem. Acta Biochim Pol **43:**361-368.

236. **Petrova OE, Schurr JR, Schurr MJ, Sauer K.** 2012. Microcolony formation by the opportunistic pathogen Pseudomonas aeruginosa requires pyruvate and pyruvate fermentation. Mol Microbiol.

237. **Anderl JN, Zahller J, Roe F, Stewart PS.** 2003. Role of nutrient limitation and stationary-phase existence in *Klebsiella pneumoniae* biofilm resistance to ampicillin and ciprofloxacin. Antimicrob. Agents Chemother. **47:**1251-1256.

238. **Borriello G, Werner E, Roe F, Kim AM, Ehrlich GD, Stewart PS.** 2004. Oxygen limitation contributes to antibiotic tolerance of Pseudomonas aeruginosa in biofilms. Antimicrobial agents and chemotherapy **48:**2659-2664.

239. **Irvin RT, Govan JW, Fyfe JA, Costerton JW.** 1981. Heterogeneity of antibiotic resistance in mucoid isolates of Pseudomonas aeruginosa obtained from cystic

fibrosis patients: role of outer membrane proteins. Antimicrobial agents and chemotherapy **19:**1056-1063.

240. **Stewart PS, Franklin MJ.** 2008. Physiological heterogeneity in biofilms. Nat. Rev. Microbiol. **6:**199-210.

241. **Chai Y, Chu F, Kolter R, Losick R.** 2008. Bistability and biofilm formation in Bacillus subtilis. Mol Microbiol **67:**254-263.

242. **Lopez D, Vlamakis H, Kolter R.** 2009. Generation of multiple cell types in Bacillus subtilis. FEMS Microbiol Rev **33:**152-163.

243. **Lopez D, Vlamakis H, Losick R, Kolter R.** 2009. Paracrine signaling in a bacterium. Genes & development **23:**1631-1638.

244. **Garrett JM, Young R.** 1982. Lethal action of bacteriophage lambda S gene. J. Virol. **44:**886-892.

245. **Strasser A, Cory S, Adams JM.** 2011. Deciphering the rules of programmed cell death to improve therapy of cancer and other diseases. Embo J **30:**3667-3683.

246. **Heydorn A, Nielsen AT, Hentzer M, Sternberg C, Givskov M, Ersboll BK, Molin S.** 2000. Quantification of biofilm structures by the novel computer program COMSTAT. Microbiology **146 (Pt 10):**2395-2407.

247. **Vlamakis H, Aguilar C, Losick R, Kolter R.** 2008. Control of cell fate by the formation of an architecturally complex bacterial community. Genes & development **22:**945-953.